THIN GLASS SANDWICH

a thermal study of regular and semiregular tessellations used in bi-directional sandwiches

MARC A.J. DEN HEIJER

Thin Glass Sandwich
a thermal study of regular and semiregular
tessellations used in bi-directional sandwiches

Marc A.J. den Heijer
4220153
5th July 2019

Dr. ir. Christian Louter
AE+T | Structural Design

Dr. ir. Martin Tenpierik
AE+T | Building Physics and Services

Dr. Michela Turrin
AE+T | Design Informatics

TU Delft
Delft University of Technology
Faculty of Architecture and the Built Environment
Master Track Building Technology

ACKNOWLEDGEMENT

I would like to thank my mentors which all contributed so much to this graduation. My first first mentor, Christian Louter, who shared his extensive knowledge about glass and glass connections. You assisted with the structural aspect of this research and ordered the necessary pieces of glass for physical testing. My second first mentor, Martin Tenpierik, for his knowledge on building physics. Which proved very useful and helpful when my research changed and got more focussed on the thermal aspects. You also helped setting up the physical testing of the panels. And last but not least my second mentor, Michela Turrin, you supported during the entire graduation project and provided a lot of information about different methodologies to achieve my goal. Especially without you three this research would not be at this level.

ABSTRACT

Since the oil crises during the 1970s, there has been a growing awareness of thermal losses through windows in buildings. Nowadays, double-glazing is a common product for moderate maritime climate. In the Netherlands two permit requirements are calculations regarding nearly zero energy and environmental performance of a building. In order to reach nearly zero energy buildings, triple glazing and even quadruple glazing is considered as possibility. This has negative affects on the environmental performance of a building, because glass does need a lot of resources for production.
A solution to that challenge could be the application of thin glass sandwiches, a structural sandwich with two ultra-thin faces (0.5mm) of glass. The structural sandwich is common in the aviation industry to stiffen and strengthen an element without adding significant weight. Downside is the increased conduction through the core material. Question is: to what extent can a thin glass sandwich panel, compared to regular insulated glass units, counterbalance its decreased thermal performance by reducing embodied energy during production?
This research focusses on the material choice, quantity and distribution in the core of a sandwich panel in order to maximize thermal performance for a moderate maritime climate. In order to do so, materials from the CES library are evaluated. Detailed analytical calculations are used to determine the thermal performance regarding different patterns. FEA simulation software is used to determine the thermal performance regarding the cross-section of the actual thermal bridge between the two faces. From this research, the best solution is picked and evaluated on energy consumption, order to identify the effects on a building scale.
General trends are identified and transformed into a design for a thin glass sandwich. Next to that, design guidelines are extracted for designers in order to design a thin glass sandwich without the need of calculating.

Keywords: Thin glass, structural sandwich, thermal performance

TABLE OF CONTENTS

FRAMEWORK I

1.1 HISTORY

It is still uncertain where the manufacture of glass originated. Glazed ceramics found in Mesopotamia could mark the beginning, but also the greenish glass beads from the Egyptians found in tombs of pharaohs. However it may be, from the middle of the 2nd century BC, rings and small figures began to appear. It lasted till the Roman age before glass was first used as part of the building envelope. Green drawn panes, which were not particularly transparent. The Roman tradition progressed in the middle ages, although glass production became primarily focussed on the stained glass, which can be found in churches and monasteries. Around the 17th century, glass was no longer sold solely for churches and monasteries but also to dealers in the cities for glazing palaces and houses. Resulting in new methods of production like the casting of glass. Despite this, window glass continued to be an expensive material, partly because both sides had to be polished. Glass was so precious at the end of the 18th century that English tenants removed the window glass when they moved house as it did not constitute part of the fixed furnishings. During the 19th century and early 20th century, glass became cheaper by patents of Siemens, Fourcault and Bicheroux, making the process less energy consumptive and more industrialised (Staib, 2012, pp. 10-12).

The real breakthrough in glass architecture did not arrive until after the Second World War. The invention of the float glass process by Alistair Pilkington revolutionized the manufacture of glass together with the development of better and innovative sealants (Schittich, 2012, p. 30).
During the 20th century glass curtain walls became a status symbol. Mies van der Rohe became one of the modernist architects, well known for the extensive use of glass in buildings. Resulting in a new level of simplicity and transparency. To Mies, glass was an expression of the current age of industrialism as he believed a building should be "a clear and true statement of its times". Fundamental to Mies's design philosophy and one of the driving forces behind his use of glass was the concept of fluid space. He believed that architecture should embody a continuous flow of space, blurring the lines between interior and exterior. The use of glass was essential in making this philosophy a physical reality and brought glass to prominence (Rawn, 2014).

During the oil crisis of the 1970s, people became aware of the thermal losses through windows. This reduced for a short term the demand for glass. However, the admiration for its positive benefits of glass like its aesthetic value, the possibility to see through and transmit light resulted in the need for new solutions. Therefore, insulated glass units, already patented in 1865, became the replacement for single pane glass. Instead of using one glass barrier, the US practice Hellmuth Obata & Kassabaum designed the first modern double-leaf facades. Extensive testing led to a construction consisting of double glazing for the outer leaf, single glazing for the inner. Between the leaves there are adjustable louvre blinds automatically controlled by solar cells. Other architects like Richard Rogers followed, but used a different approach. In the Lloyd's Building the double-leaf façade is designed as an exhaust-air system. In winter, warm air from the interior is extracted and circulates in the cavity of the two leaves improving the thermal insulation of the façade. Renzo Piano in its design for Debis headquarters made the inner leaf of insulating glass, the outer leaf of glass louvres. In winter these louvres are closed, trapping a layer of air which heats up by solar radiation. In summer these louvres open to ensure ventilation and sufficient night-time cooling. Architects and engineers did reduce the thermal losses by windows, but at the expense of using of more glass (Schittich, 2012, pp. 45-48).

1.2 PROBLEM STATEMENT

According to Sadeghi, Sani and Wang (2015), the invisible material has nowadays, in extend of the architects of the 20th century, become a material that is a symbol of openness, democracy and modernity. What used to be a very defined line or wall, is now blurred. Rooms now blend into the outdoors without worrying about a solid distinction.

By laminating glass into structural components, even fully glazed facades become possible. Prime examples are designed in cooperation with Eckersly O'callaghan, like the Steve Jobs Theater and a variety of apple stores around the world. Next to that also skyscrapers like the Shard and Burj Khalifa show nearly full glass facades.

Of the various applications of flat glass, the building & construction sector is anticipated to lead the global flat glass market in terms of revenue share, estimated to hold more than 70% value share in the global flat glass market throughout the forecast period till 2025. It will dominate but also remain steady in terms of market growth, with an expected compound annual growth rate of 5.5% (Persistence Market Research, 2017).

Although its demand grows and glass clearly has benefits in terms of light entrance and visual connection with the outside. Glass also has multiple disadvantages:

- Considering the thickness of an insulated glass unit and considering the fact that only the small cavity between the glass panes insulates, windows do transfer energy at a much higher rate compared to solid walls. Resulting in heat loss in winter and heat gaining in summer. In summer this is even intensified by solar radiation.
- Solar radiation and heat loss are both partially tackled by applying various coatings at the inside of the insulated glass unit. Compromising the light transmittance of the window.
- Silica sand, the main ingredient, is extracted from natural sand features such as dunes and beaches, which means there is potential for damage to local ecosystems. Approximately 95 million metric tonnes of silica sand is mined each year. This silica is mixed with lime and soda and heated to approximately 1500 °C using fossil fuels. Significant amounts of energy are required in glass manufacture. Manufacturing 1000 kg of glass can generate up to 200 kg of mining waste and 14 kg of air pollutants. Glass furnaces discharge dust, sulphur dioxide, chlorine and fluorine to the atmosphere (Branz, 2017).
- In terms of weight, glass is around 2500 kg per cubic meter. Due to prevent heat transfer, nearly all windows are double or even triple glazed. Although energy can be saved during its lifetime, it increases the amount of material needed. Resulting in heavy units which are increasingly harder to transport, and install on site. Although minor compared to the total load, it increases the loads on the primary structure.

These disadvantages do not match with the sustainability goals, reduce material and energy. Resulting in the following problem statement:

> *"The tendency of increasing the amount of transparency in architecture, therefore increasing the amount of glass, conflicts with the aim of sustainability to reduce materials and energy."*

Research Aim

Reduce material and energy during the 'lifecycle' of insulated glass units.

1.3 RELEVANCE

Nowadays, thin glass is produced mainly for electronic devices. Although some companies are exploring the possibilities of thin glass for the construction industry. However, a commercial insulated glass unit of thin glass does not exist yet. There are several reports from the TU Delft on thin glass, mainly based on a single layer. Including connections for the second skin of a double façade. Iris van der Weijde did study on an insulated glass unit of thin glass, but focussed mainly on structural aspects, briefly touching heat flow. The intent of this report is to deepen the research on heatflow through insulated thin glass units.

The 'environmental performance building' (in Dutch MilieuPrestatie Gebouwen MPG), is required for every planning permission or developmental approval above 100m^2 for permanent housing and office. This report values the environmental impact of materials used in the building. Since January 1st 2018 the maximum is 1,00 euro per m^2 BVO per year of shadow costs. To determine these costs, a qualified Life Cycle Assessment results in eleven aspects combined into shadow costs (RVO, n.d.).

Next to the material requirements, also energy regulation is active. Around 2020 all new buildings within the Netherlands need to be 'nearly energy neutral buildings' (in Dutch Bijna Energie-Neutrale Gebouwen BENG). These regulations are based on three factors:

-Maximum energy demand (kWh/m^2/year)
-Maximum primary use of fossil fuels (kWh/m^2/year)
-Minimum amount of renewable energy

One proposed solution to achieve the BENG norm is to apply triple or even quadruple glazing (Heide, Vreemann, & Haytink, 2016). As stated in the problem statement the production of glass for the building industry is still increasing, but glass is weak in terms of sustainability, it will heavily impact the MPG. This report wants to offer an alternative to regular insulated glass units in order to save material and therefore energy in the production process.

1.4 HYPOTHESIS

Thin glass will greatly reduce the amount of energy used in the production of glass. Due to its thickness, a sandwich construction is needed to make it stiff. This interlayer will however conduct heat at a greater rate than air, therefore thermal performance will decrease.

1.5 OBJECTIVES

Research objective

Find the potential of an insulated thin glass unit, which can replace regular insulated glass units.

Sub-objectives

- Provide an overview of material specification and theories regarding glass and sandwiches.
- Get an understanding on how to calculate thermal flow.
- Find the relationships between material distribution and thermal flow.
- Identify the effect of a changing U-value for windows on the energy demand for a building.
- Evaluating the design of a thin glass unit on material and energy reduction.
- Define the connections for sandwich structures in relation to other building components.

1.6 QUESTIONS

Research Question

To what extent can a thin glass sandwich panel, compared to regular insulated glass units, counter-balance its decreased thermal performance by reducing embodied energy during production?

Background

- What are the physical properties of thin glass?
- What are the characteristics of different structural sandwiches?
- How is thermal flow calculated in structural sandwiches?

Research

- How do macro and micro material distributions affect thermal flow?
- What are the thermal losses through windows on a building scale?
- To what extend can thin glass sandwiches reduce embodied energy?

Application

- How can criteria for regular windows be applied to thin glass sandwiches?

1.7 CONSTRAINT

Sustainability is a broad term for meeting the needs of the present, without compromising the ability of future generations to meet their needs. It is term related to economic, environmental and social aspects. The production of glass has most notably an impact on the environment due to the extraction of sand from dunes and beaches, and energy used for melting the raw materials. This research does only focus on energy as a measurement of sustainability in order to compare the production phase with the operational phase of windows.

1.8 METHODOLOGY

Literature review

The literature review is the basis for this research. The key ingredients, glass and sandwiches are discussed. The state of art is presented, but also what enhancement techniques do exist. These techniques are organized by three themes: structural behaviour, thermal insulation and solar control.

Calculation methodology

After identifying the key concepts regarding thermal flow in thin glass sandwiches, a digital prototype is made to deepen the understanding on how to apply these formulas on four specific panels. Three methodologies of calculating the thermal flow are evaluated on both speed and accuracy. These digital prototypes are physically recreated to compare theory and practice, because practice is dealing with physical limitations and properties which are not taken into account by the analytical models.

Parameter study

The third phase aims to expand the knowledge found during background research. The parameters affecting thermal performance of the thin glass sandwich are identified and studied in more detail. Material choice is evaluated by using the CES library. Several geometric patterns are digitally modelled and evaluated on thermal performance. A separate study is made regarding the actual thermal bridges from one face to another. For determining the psi-value of each thermal bridge, a large variety of cross-sections is digitally modelled and evaluated with finite element analysis. This phase explores the effects of different parameters on the thermal performance of the panel itself and extracts general guidelines for designers.

Evaluation

The parameter study delivers a direction on how to get a better thermal performance regarding the panel itself. The best pattern is chosen and applied on a building scale. This evaluation is on a fictional office building in the Netherlands. In the first place the effects of lower and higher U-value for windows are identified. The next step is to evaluate the best pattern from the parameter study to see how much material can be saved and how much energy is lost by a thin glass sandwich.

Digital design

Lastly, the lessons learned and design guidelines from earlier phases will come together in a design of an actual panel. This will also include the connection and details in relation to other building components. This phase broadens the perspective to technology and techniques which are used nowadays in the glazing industry.

LITERATURE REVIEW II

2.1 PERFORMANCE ASPECTS

2.1.1. Structural behaviour

Mechanical properties are very important in order to withstand multiple types of loads. Like dead loads, windloads and special loads. In case of special loads, the structural properties are related to safety and security. It is important to understand that safety and security are two different things. The word safety is used in cases of accidental impact like fire and fracture. Security on the other hand focusses on deliberate. In both cases the framing system plays a huge role as well (Pilkington, 2010, p. 134). This research does not focus on these special types of loads, but on dead loads and static/dynamic windloads.

In order to verify structural requirements, limit state design is used. Which can be separated into two types of limit states. The ultimate limit state and the serviceability limit state.

ULS

When checking the ULS, none of the stresses should be surpassing the stresses the material can handle. Tensile strength and compressive strength are two material properties that should not be surpassed during an ULS test. When they do a construction will fail, and will bring people in danger. For this test a safety factor is integrated within the equation. To ensure a construction will stand also under extreme loads.

SLS

The SLS gives us results during normal use. In case of this research, the construction will be checked for deflection for the whole construction. Young's modulus, compression modulus and shear modulus are all properties that describe the resistance of a material to respectively tensile, compressive and shear forces.

2.1.2. Thermal insulation

Thermal energy is transferred when there is a temperature difference between two elements. In that case, energy flows from the element with higher temperature to the element with a lower temperature. The heat flux is the total amount of energy flowing per unit of time, where heat flux density is the flow of energy per unit of area per unit of time. In a metric system it is often denoted as W/m^2.

$$Q = A \cdot q$$

Q the total amount of energy flowing in W
A the surface area in m^2
q the heat flux density in W/m^2

The heat flux density however is determined by three types of energy transmittance, which occur simultaneously. The heat flux density of convection, radiation and conduction together result in the total heat flux from one element to another (Zeegers, 2006, p. 2).

$$q = q_{convection} + q_{conduction} + q_{radiation}$$

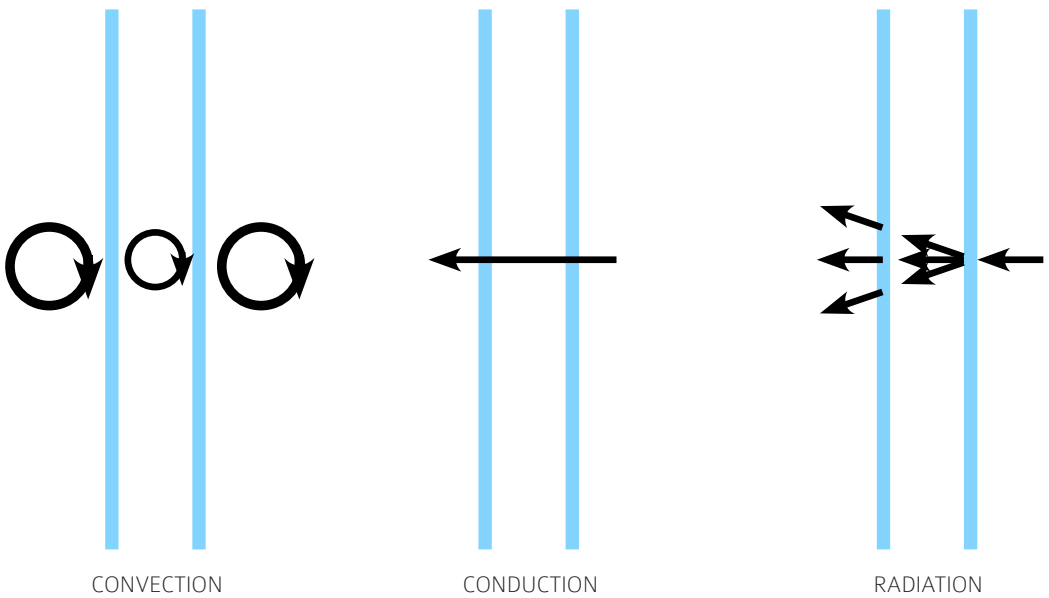

FIGURE 01 // Three different ways of heat transfer from high temperature to low temperature

Convection

Convection is the transfer of heat from one place to another by the movement of liquids or gases. For example, air taking heat from an object it is flowing past. This can either be natural, by temperature differences between surfaces, which cause air to move, or it can be forced with a fan. The amount of energy that is transported by convection depends on the speed of the fluid and the temperature difference between fluid and object (Zeegers, 2006, pp. 2-3).

$$q_{convection} = \alpha_{convection} \cdot \Delta T$$

q the heat flux density for convection in W/m^2
α the heat transfer coefficient in W/m^{2}K
ΔT the temperature difference in K or ^{o}C

Conduction

Conduction is the transfer of heat by atoms within an element. Where atoms vibrate against one another, transporting energy. Depending on the material or fluid atoms will do this at different rates. Another factor is the thickness of a material (Zeegers, 2006, pp. 2-3).

$$R = d / \lambda$$

R the thermal resistance in m^{2}K/W
d the thickness of the material in m
λ the thermal conductivity in W/mK

The thermal conductivity describes for a certain temperature difference, at what rate a material will conduct heat. Materials with a low conductivity do conduct less energy than materials with a high conductivity. Based on this equation, materials with a low conductivity require a bigger temperature difference in order to conduct the same amount of heat compared to materials with high conductivity (Granta, 2011).

Instead of using the resistance, 1/R gives us the ability of an element to transmit heat. Meaning that when insulating, the R-value should be high, resulting in a low U-value. When describing facades, an R-value or U-value is including a boundary resistance of 0.04 m^{2}K/W at the outside of the construction and a boundary resistance of 0.13 m^{2}K/W for the inside of the construction.

$$q_{conduction} = U \cdot \Delta T$$

q the heat flux density for conduction in W/m^2
U the thermal transmittance in W/m^{2}K
ΔT the temperature difference in K or ^{o}C

Radiation

Radiation is the transfer of heat by photons, which do not require solids, liquids or gases to transport. All bodies on earth do emit heat, except a body of 0K. The Stefan-Boltzmann equation describes the amount of heat radiated by a surface.

$$q_{radiation} = \epsilon \cdot \sigma \cdot T^4$$

q the heat flux density for radiation in W/m^2
ϵ the emissivity coefficient of the surface
σ the Stefan-Boltzmann constant
T the absolute surface temperature in K

Considering two parallel and infinite surfaces with a different temperature, they will send both heat radiation, absorb and reflect partly. Because they do this at different rates, the result is a flow from higher temperature to lower temperature (Zeegers, 2006, pp. 2-3).

$$q_{radiation} = \epsilon_{res} \cdot \sigma(T_1^4 - T_2^4)$$

q the heat flux density for radiation in W/m^2
ϵ_{res} the resultant emissivity coefficient
σ the Stefan-Boltzmann constant
T the absolute surface temperature in K

Cavity resistance

Convection, conduction and radiation are separate components, but can be combined into one thermal conductivity value. The thermal conductivity of air is 0.025 W/mK, but based on NPR 2068 this value drops to 0.094 W/mK when integrating radiation and convection component.

This value is suitable when using infinite wide cavities. NEN-EN-ISO 6946 however does also take into account the width of a cavity as well. Using these formulas, a more accurate number for thermal resistance of the cavity is obtained. The thermal resistance of an unventilated airspace wider than ten times its thickness is given by:

$$R_g = 1 / (h_a + h_r)$$

R_g the thermal resistance of the airspace in m^2K/W
h_a the conduction and convection heat transfer coefficient in W/m^2K
h_r the radiative heat transfer coefficient in W/m^2K

Determination of h_a for large airspaces

The conduction and convection component combined depends on the direction of the heat flow and the temperature difference over the cavity. Temperature difference for standardised tests is above 5 °C, for a façade the direction of the heat flow is horizontal. In that case the formula to obtain h_a is $0.73 \times \Delta T^{1/3}$ or, if larger, 0.025/d.

Determination of h_r for large airspaces

The radiation component is a multiplication between the radiative coefficient for a black-body surface and the intersurface emittance. Which are respectively depending on the average temperature within the cavity and the emissivity of the glass surfaces. An uncoated glass pane has an emissivity of around 0.9 while coated glass can obtain an emissivity down to 0.05

$$E = 1 / (1/\epsilon_1 + 1/\epsilon_2 - 1)$$

Determination of h_r for small airspaces

For small airspaces the combined conduction and convection heat transfer coefficient does not change. The radiative heat transfer coefficient will change depending on the width. The width is determined by the so-called hydraulic-diameter. Which is defined as four times the area of a cell divided by its perimeter.

$$h_r = h_r 0 / (1/\epsilon_1 + 1/\epsilon_2 - 2 + 2 / (1 + \sqrt{1 + d^2 / b^2} - d / b))$$

d the thickness of the airspace in m
b the width of the airspace in m
$\epsilon_{1,2}$ the hemispherical emissivity's of the surfaces

Noble gas

In order to improve the cavity resistance a coating will reduce the radiation through the glass panel, which only changes the emissivity of the surface. Reducing conduction can be done by filling the panel with a noble gas like argon or krypton. In that case, the Grashof number changes in comparison to air.

$$Gr = (g \cdot ß \cdot l^3 \cdot \Delta T) / v^2$$

g the gravity acceleration in m/s^2
$ß$ the volume expansion coefficient
v the kinematic viscosity in m^2/s
l the characteristic length in m
ΔT the temperature difference in K or ^{o}C

$$2 \cdot 10^4 < Gr < 2 \cdot 10^5 \ \& \ l > 3d$$
$$Nu = 0.18 \cdot Gr^{1/4} (l/d)^{-1/9}$$

$$2 \cdot 10^5 < Gr < 2 \cdot 10^7 \ \& \ l > 3d$$
$$Nu = 0.065 \cdot Gr^{1/3} (l/d)^{-1/9}$$

Depending on the size of the Grashof number, the formula to obtain the Nusselt number will change. This Nusselt number is the actual heat transfer coefficient in relation to that of still air over a given characteric length. In case of a vertical façade element, this characteristic length is the height of the cavity and needs to be larger than three times its depth. In order to calculate the heat transfer coefficient for convection and conduction the following formula is needed, this will replace the earlier obtained heat transfer coefficient for air (Johannesson, 2006).

$$h_c = (Nu \cdot \lambda) / l$$

Nu the Nusselt number
λ the thermal conductivity in W/mK
l the characteristic length in m

2.1.3. Solar control

Solar control is closely linked to topics like thermal insulation and light control. The sun emits electromagnetic waves both in the infrared and visible spectrum. Especially in hot climates, solar control is paramount in order to minimise the thermal loads and control glare.

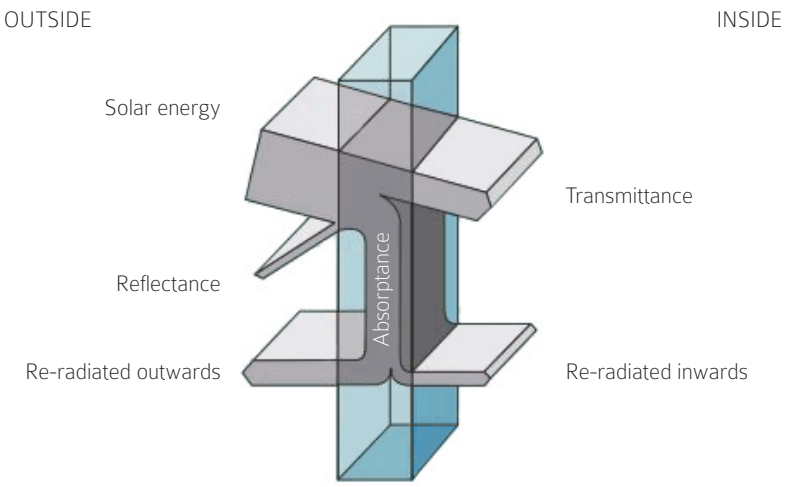

FIGURE 02 // Solar energy: reflectance, absorptance and transmittance (Pilkington, 2010)

Light transmission, reflection and absorption

Light transmission and reflection are the proportions of visible light, that are transmitted or reflected when light hits a surface at near normal incidence. Light can also be absorbed. Transparent materials like glass do consists of atoms, when a light wave with the same frequency as the atoms strikes the glass, those atoms will absorb the light and transform it into vibrational energy. When they also interact with a neighbouring atom, they will convert it into thermal energy (PhysicsClassroom, n.d.).

Solar energy transmission, reflection and absorption

Like light, also the waves of the invisible spectrum are divided into three components. Worth mentioning is the fact that energy absorbed by the glass, gets radiated inwards and outwards.

Solarfactor and selectivity index

In order to summerize the performance of a window, the so-called solar factor or g-factor represents the transmitted heat through the glass by all means. The selectivity index is a number that represents the ratio between light transmittance at one hand and the solar factor at the other hand (Pilkington, 2010, p. 11).

2.2 GLASS

2.2.1. Background

Glass is a solidified liquid, a solid produced by cooling molten material so that the internal arrangement of atoms remains in a random or disordered state, similar to the arrangement in a liquid. Contrary to crystalline materials, it does not form a crystal lattice. That is why glass is transparent. Another consequence is the fact that glass does not have a chemical formula. Glass also does not have a melting point but instead, upon applying heat, gradually changes from a solidified liquid state into a liquid state. The third result of the non-crystalline structure is its amorphous isotropy. This means that its properties are not dependent on direction (Balkow, 2012, p. 60).

To obtain glass, the raw materials among are heated to such a high temperature that the materials irreversible transform into a viscous state. This high viscosity coupled with the subsequent cooling leaves the ions and molecules no chance to arrange themselves, resulting in a non-crystalline glass structure.

Glass is composed of three types of elements: network formers, network modifiers and intermediates. Also called formers, fluxes and stabilizers. The glass network former is the key component of any glassy material, in most cases this is silica SiO_2. Due to the random order of atoms it gives room for other atoms to integrate within the structure. Pure silica is difficult to melt and uses a lot of energy, by adding fluxes the melting point decreases with a couple of 100 degrees. Stabilizers are very important. Glasses containing only a network former and fluxes have poor durability and in a lot of cases water-soluble. Stabilizers make the glasses stronger and more durable. Soda lime, the most common glass used in flat glass and bottles, is based on silica as the glass former, soda as the flux and lime as the stabilizer. By combining different atoms and molecules, glass can be produced in a large variety (Kolb, 2016).

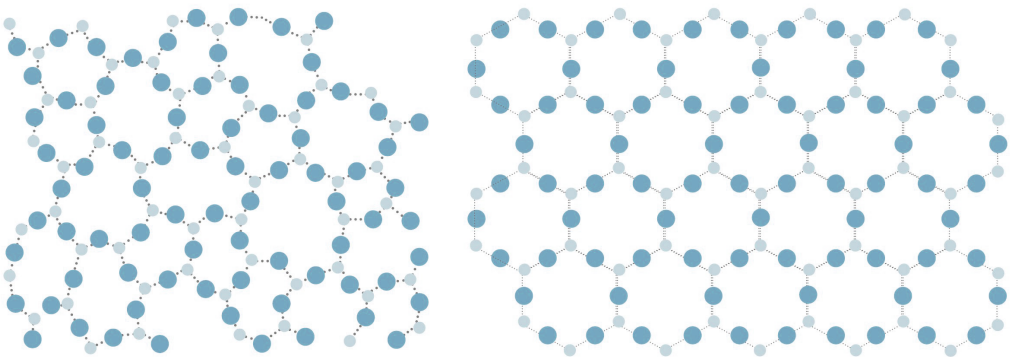

FIGURE 03 // Irregular atomic structure of glass and regular atomic structure of quartz (Weijde, 2017)

2.2.2. Types

High silica glass is nearly pure SiO_2, it resists temperature and thermal shock better than any other glass. However, it is glass with a high embodied energy. Soda-lime for example is cheaper to produce in large volumes, making it the most common used glass. Aluminosilicate combines the advantages of silica and soda-lime. More recently tough and scratch-resistant grades have been developed for use as cover glass for electronic devices, and this is the application for which they are probably most recognizable (CES, 2018). Most of the commercial thin glass types are made from aluminosilicate. Just like glass fibers, this type of glass is flexible. Nowadays, three large glass-manufacturing companies are producing thin glass sheets: AGC, Corning and Schott.

Glass type	Strengths	Limitations	Uses
Silica	High temperature resistance, very low coefficient of thermal expansion.	Difficult to process due to high melting temperature, leading to a higher cost.	Production processes of the semi-conductor industries, thermal barrier coatings.
Soda-lime	Reduced working temperature compared to other glasses. Easily recycled.	Reduced service temperatures, poor resistance to thermal shock.	Windows, bottles, containers.
Aluminosilicate	Able to withstand high temperatures and thermal shock.	Comparatively difficult to fabricate for a glass.	Combustion tubes, optical fibers, electronic components.

TABLE 01 // Comparison of glass properties (CES, 2018)

The embodied energy measured in MJ/kg are 30% more for aluminosilicate glass compared to soda-lime glass. Due to the thickness of thin glass, less weight is needed to produce one square meter of window. During the production, glass sheets can break or do not have the required quality. In these cases, the warm glass is melted again, saving energy.

In terms of durability, glass is an excellent product in facades, due to its resistance to many solvents including organic. It is non-flammable and does not degrade under UV radiation. Despite its recyclability, building glass at the end of its life, almost never is recycled into new glass products. The complete opposite of what we do with glass bottles and containers, which are recycled over and over. Due to a lack in properly organised collection, the building glass it is very often crushed together with the other building materials and put into landfills (GlassEurope, n.d.).

2.2.3. Production

Flat panes of glass can be created in a variety of ways. This chapter considers four of these methods: by floating, by rolling, by drawing and by fusion. Most of the flat glass, up to 83% of the total volume is produced for the building industry. (Business Wire, 2017). 90% of this flat glass is manufactured with a float glass production line (Wurm, 2007, p. 45).

Float

The float glass production is based on a process developed by Alastair Pilkington in 1959. Molten glass, at approximately 1200°C, is poured continuously from a furnace on to a large shallow bath of molten tin. It floats on the tin, spreads out and forms a level surface. Thickness is controlled by the speed at which the solidifying glass ribbon is drawn off the tin bath (Pilkington, 2007, p. 3).

Rolled

Rolled, cast or plate glass is produced using the "overflowing tub" principle: A pair of forming rollers with patterned surfaces continuously pull a glass ribbon out of the melt, after which the ribbon is cooled and cut. Rolled glass is also known as ornamental glass because of the ornamentation on one or both of its sides. Wired glass is produced in the rolling process by feeding wire mesh into the liquid glass. Out of these three, float glass is the most precise and flat way to produce glass for the construction industry. The irregular thickness of rolled glass means that it is only about half as strong as float or drawn glass (Wurm, 2007, pp. 46-47).

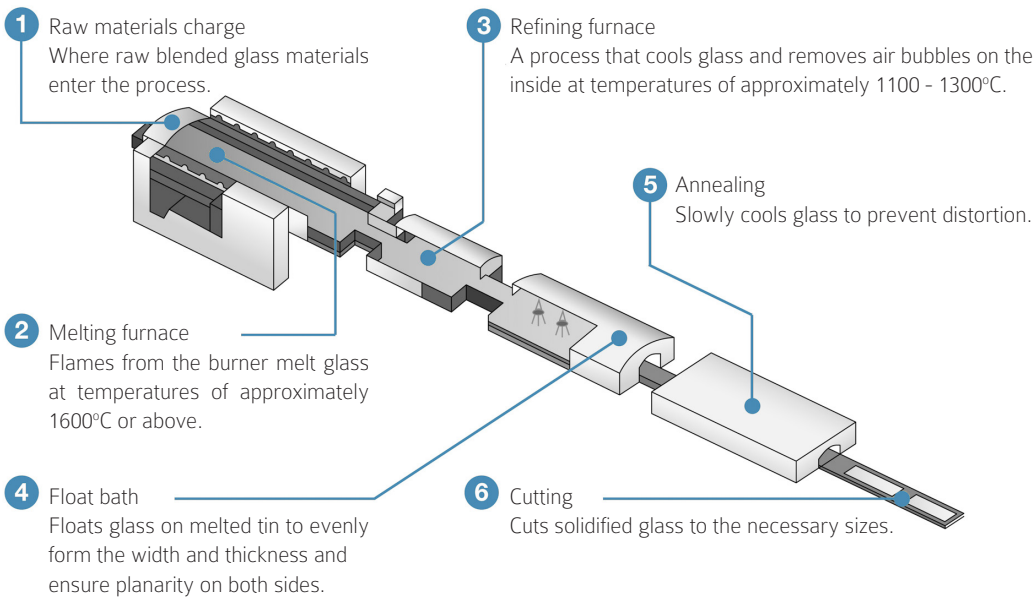

FIGURE 04 // Production process for float glass (Mansour, n.d.)

Drawn

Drawn glass is based on techniques of Fourcault. In the drawing method, a ribbon of glass is drawn vertically from the glass furnace up an annealing tower by rollers which grip the ribbon as soon as it has cooled enough, a few feet above the furnace. During which time it is annealed by cooling slowly to avoid in-built stresses. Schott alters this concept by reversing the direction of the material by down drawing it. Minimizing the thickness of glass to a 25 micrometer (Schott, n.d.).

Fusion

Corning developed their own techniques during the 1960s. The base materials for the alumino silicate glass are heated well above 1000 degrees Celsius. The molten glass is homogenized and conditioned before it is released into a large collection trough with a V-shaped bottom, known as an isopipe. The isopipe is carefully heated to manage the viscosity of the mixture and ensure uniform flow. Molten glass flows evenly over the top edges of the isopipe, forming two thin, sheet-like streams along the outer surfaces. The two sheets meet at the V-shaped bottom point of the isopipe and fuse into a single sheet. The main advantage of using this production method compared to the float method is avoiding post-production steps like polishing (Corning, n.d.a).

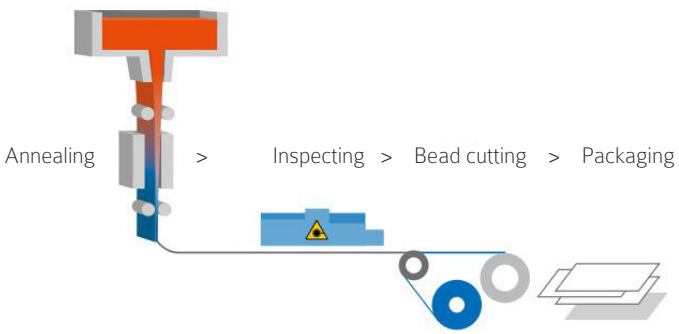

FIGURE 05 // Production of thin glass by down-drawn process (Schott, 2014)

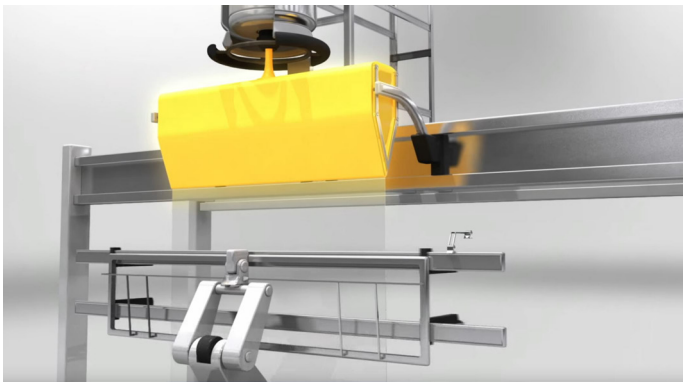

FIGURE 06 // Production of thin glass by fusion process (Corning, n.d.a)

2.2.4. Enhancement techniques

Structural behaviour

Annealing

Annealing of glass is a process of slowly cooling hot glass objects after the initial forming in a special machine known as lehr, to relieve residual internal stresses introduced during manufacture. At this point, the glass is too firm to distort or bend but remains soft enough for any built up stresses to relax. Holding the piece of glass at this temperature helps to even out the temperature throughout the piece of glass. Annealing of glass is critical to its durability. When not properly annealed, residual stresses are still within the product, decreasing the strength and reliability. In extreme cases, it may fail spontaneously (Abrisa, 2015).

After annealing, glass is ten times stronger in compression than in tension (CES, 2018). When a sheet of glass is subjected to bending, it will therefore fail due to tension rather than compression. Pre-stressing of the glass introduces possibilities to compensate tensile stresses at the glass surface, bringing compression at the glass surface.

Thermal pre-stressing

In case of thermal pre-stressing, glass is heated above the transition temperature. By force-cooling it, cooling it at a faster rate than annealed glass, surface and edge compression of the glass occurs. This procedure can be done at different rates, resulting in two types of glass: heat-strengthened and heat-tempered glass. Allthough tempered glass is twice as strong compared to heat-strengthened and four times stronger than annealed glass. It is prone to spontaneous breakage due to impurities of the glass. It can't be cut after tempering and its surface is warped by the rollers in the tempering oven. Thermal pre-stressing in general is only possible when glass is thicker than 2 or 3 millimeters (Abrisa, 2016).

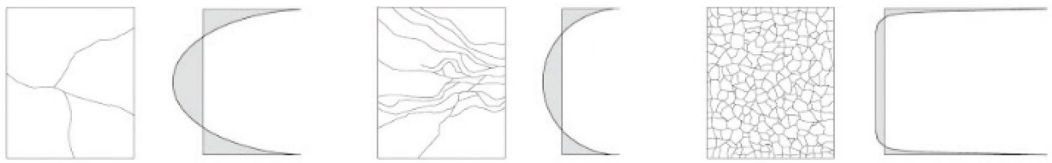

FIGURE 07 // Breakage pattern and stress distribution after different heat treatments (Weller et al., 2009)

Chemical pre-stressing

Chemical strenghtening is a method, also suitable for glass sheets under 3 millimeters. Although the principle of creating surface tension is the same. Its execution relies on chemicals, altering the chemical composition of the glass surface. In case of soda-lime glass, sheets are placed in a heated bath containing KNO_3. By ion exchange the smaller sodium ions are replaced by potassium ions. Potassium ions are bigger in volume and therefore create a compressive stress layer. The same principe works for alumino silicate glass, although now lithium ions are exchanged (Corning, n.d.b).

The DOL, depth of layer, MOR, modulus of rupture and CS, compressive strength of the glass sheet depend on time of ion exchange, temperature of the bath, the composition of the glass and the composition of the bath. But after this process, the glass can be subjected by larger forces and it is more scratch resistant. The breakage pattern and stress distribution is similar to tempered glass (Gomez et al., 2011).

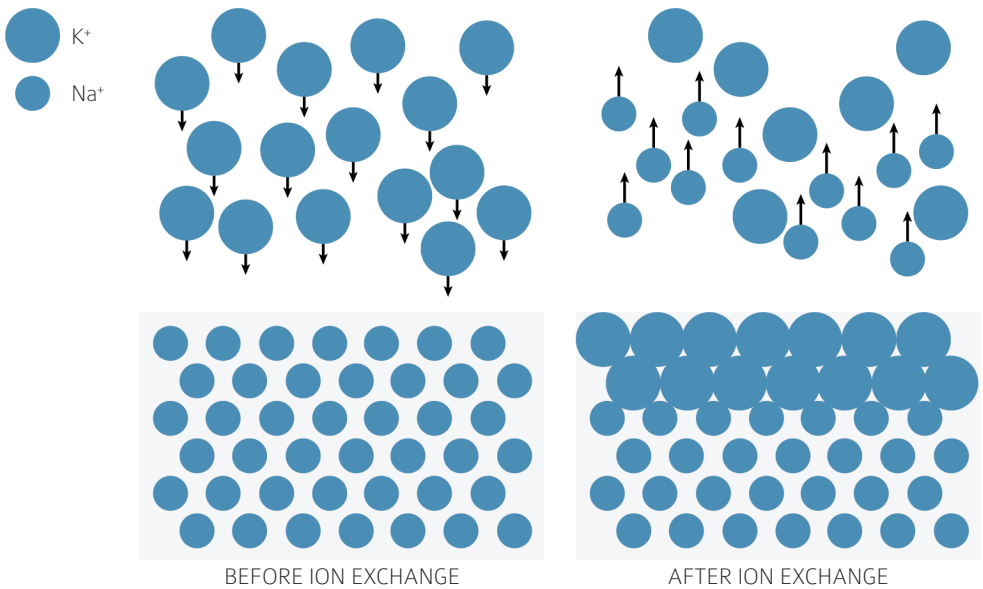

FIGURE 08 // Altering of glass surface by chemical toughening process (Trendmarine, n.d.)

Thermal insulation

Thermal conductivity of glass lies around 1 and 1.25 W/mK this is a material property and can not be altered in post-production of the glass. Radiation, or preventing radiation coming through glass can be done by applying a low-e coating. Effectively, low-emissivity glass will reflect energy back into a building, to achieve much lower heat loss than ordinary float glass. Normal emissivity coefficient of glass lies around 0.85 for the long-wave portion of the spectrum, but with a coating it can be as low as 0.04 (EfficientWindows, n.d.).

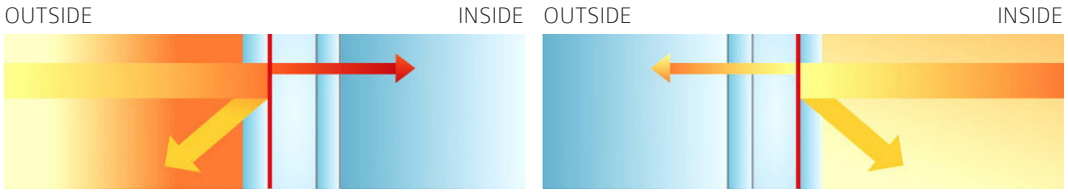

Coating on position 2 for solar control in warm climate

Coating on position 3 for thermal insulation in cold climate

FIGURE 09 // Balance between thermal insulation and solar control, regarding coating position (Jingglass, n.d.)

Solar control

Solar energy enters the building mainly as shortwave radiation but, once inside, it is reflected back by objects towards the glass as longwave radiation. Low-emissivity glass has a coating that allows the transmission of the sun's shortwave radiation at a higher rate than longwave radiation from heaters and occupants in de room. This provides an effective barrier to heat loss (Pilkington, 2010, pp. 78-79).

Depending on the climate, solar control is preferred instead of solar gain. While the tint of these coatings lowers also the transmittance of waves from the visible spectrum, it controls both heat gain from the sun as well as glare. Each manufacturer has its own range of products to find the coating that is most suitable for a certain climate. In order to apply the coating to the glass, two methods are commonly used. Pyrolysis, which is applied during the production phase. Sputtering, which is applied after the production phase.

- A typical pyrolytic coating is tin oxide, which is bonded tot the glass while it is in a semi-molten state. This process is called chemical vapour deposition and results in a low-e layer which is baked into the glass. Therefore it is called a hard-coating, which means that this type of coating can be applied to the air exposed side of a window. It is hard to damage these kind of coatings (EfficientWindows, n.d.).
- Sputtering, is a soft coating. In a vacuum chamber, several metals, metal oxides and metal nitrides are deposited on the glass. Although these coatings can consist of over ten layers, the total thickness is only one ten thousandth the thickness of a human hair. Due to the relative softness of this coating, it needs to be applied at the cavity side of a window (EfficientWindows, n.d.).

2.3 SANDWICHES

2.3.1. Background

A sandwich structure in its simplest form consists of three types of components: two outer layers, a core and a connection between the outer layers and the core. Main reason to make a sandwich structure is to create a lightweight but structurally very stiff structure.

Essentially a sandwich is an I-beam converted into a plate. The flanges of an I-beam or the outer layers of a sandwich carry the compressive, tensile and bending stresses. While on the other hand the web of an I-beam or the core of a sandwich resists the shear loads and holds the flanges apart. The connection of a sandwich has to be strong so it acts as one unit (Hexcel, 2000, p. 3).

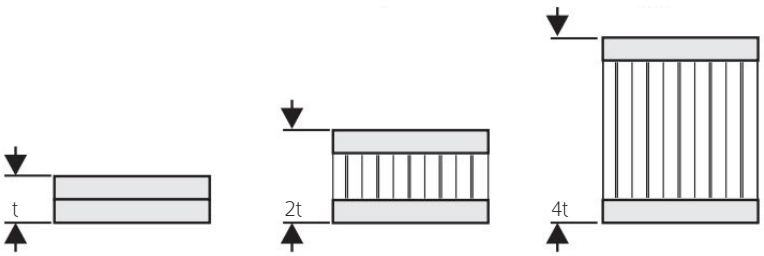

Stiffness	1.0	7.0	37.0
Flexural Strength	1.0	3.5	9.2
Weight	1.0	1.03	1.06

FIGURE 10 // Relative stiffness and weight of sandwich panels compared to solid panels (Hexcel, 2000)

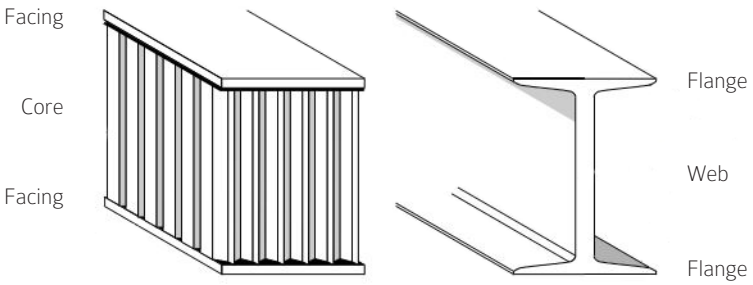

FIGURE 11 // Construction of a sandwich panel compared to an I-beam (Hexcel, 2000)

2.3.2. Types

The core of a sandwich can differ both in shape and material resulting in an unlimited variety of panel configurations. These two aspects determine the structural and thermal behaviour.

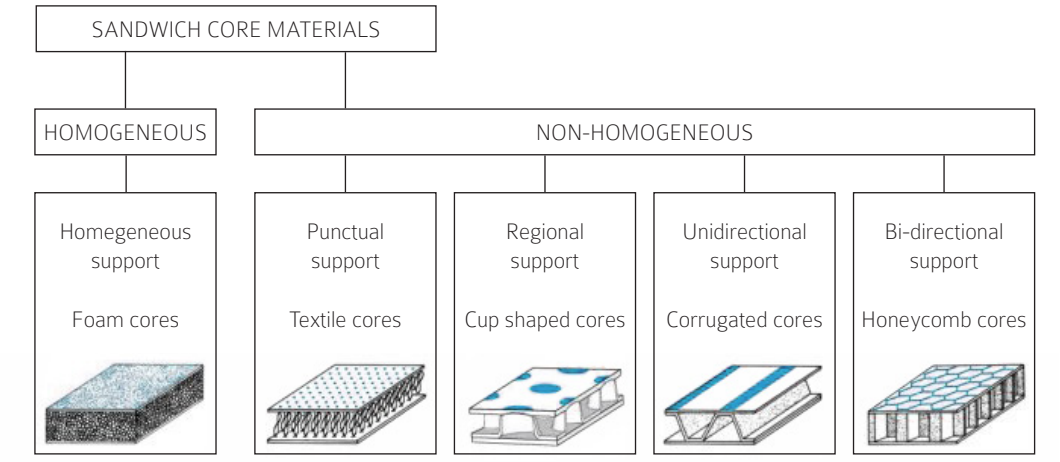

FIGURE 12 // Classification of sandwich cores (Econcore, n.d.)

Homogenous cores

When low-cost is a requirement, homogenous cores are used most frequently. In a lot of cases, foam is the main material to create the sandwich construction. For example polyurethane, polystyrene or phenolic foams. The density of these foams is closely related to its structural stiffness and its ability to handle shear stresses. Balsa wood can also be considered as a material for homogenous cores. In case of glass, laminating with materials like PVB or SG can be seen as a way to create a sandwich. It does however not exploit the principle of sandwiches because the core is very thin (Econcore, n.d.).

Punctual support

This type of support can be subdivided into textile structures and truss based structures. Which do create a sandwich with moderate mechanical properties, but they do allow for low density and maximum of flow through the panel itself (Vitalis, 2017).

Regional support

Is a variant on pin like punctual support, spreading loads on a bigger surface. Due to this fact, heat will flow much easier from one side to the other. Structurally they enhance shear transfer.

Unidirectional support

For this type of sandwich panels, the support of the panel itself plays a huge role. The corrugated core in cardboard is an example. Strong in the direction of the ribs, but weak in transverse direction. The big contact surface between outer layer and sandwich is a disadvantage regarding thermal performance (Econcore, n.d.).

Bi-directional support

These are also known as honeycomb sandwiches, which can offer weight and cost savings thanks to their excellent performance per weight. The term "honeycomb" is not only used to describe the hexagonal pattern, but is also used for square and triangular grids. Because of their excellent performance, there is extensive literature covering this specific type of sandwich for a variety of materials. When strength-weight ratio is most important, metals like aluminium and stainless steel are used a lot. Other possibilities are composites of aramid and glass fiber combined with different kinds of resins. The latter do conduct less heat than their metal counterparts. When taking 3D-printing into consideration, plastics like PETG, which do have good thermal properties are also transparent, making them especially suitable for windows (Econcore, n.d.).

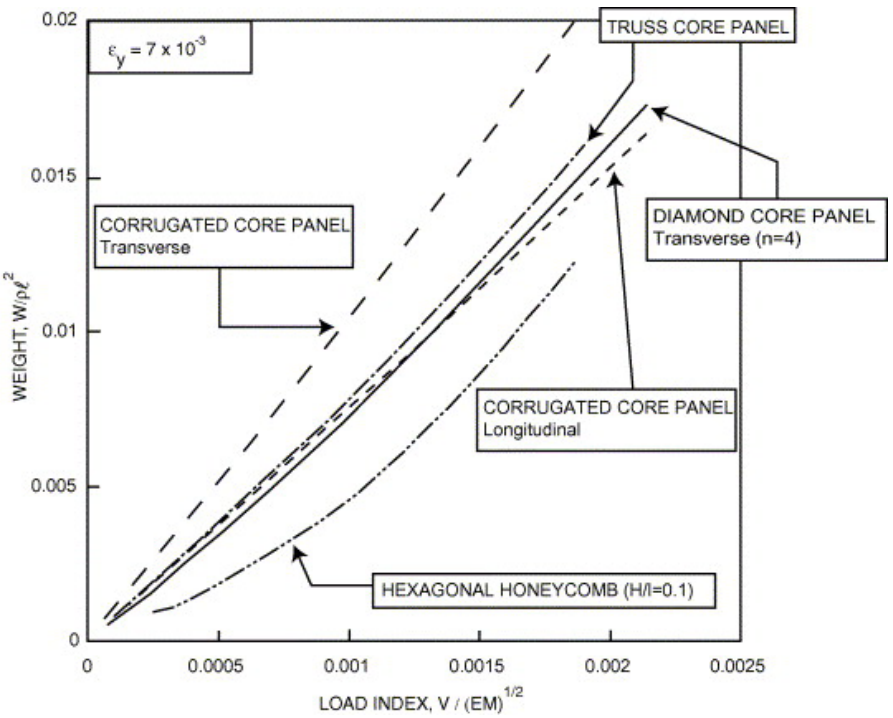

FIGURE 13 // Weight to load ratio of sandwich topologies (Valdevit, Hutchinson, & Evans, 2004)

Several researches in the past show the difference between different topologies. Among them are Valdevit, Hutchinson, & Evans (2004) and Campbell (2011). Both find that sandwich panels, especially the panels with bi-directional support like honeycombs, show significant better weight-to-load ratios. When honeycombs are applied in flat panels and subjected by bending, they are the benchmark if one is designing for low weight and high strength and stiffness (Evans, 2001).

Each typology has its advantages and disadvantages. For a thin glass sandwich, the core material should not block all the light, therefore the unidirectional and homogeneous are found unsuitable. Other criteria are weight to load ratio, the attachment of glue and thermal performance. Less weight for the same load-index, means less material used to obtain the desired stiffness and strength. Because every bit of material that is put between the two glass layers, will probably conduct more energy compared to air, it is paramount to reduce the amount of material.
Because sandwich and glass need to be connected, for either glue or welding a line-based contact is preferred above point-based contact, this makes the connection more secure. Regarding thermal performance, convection can be limited by creating small enclosed cavities and radiation can be blocked by the material of the core.

A bi-directional typology compared to punctual and regional typologies, does score better on all these criteria, therefore this typology is chosen to elaborate on. The three basic types of honeycomb structures are hexagonal, square and triangular. These are all regular tessellations, tessellations with only one kind of polygon. Therefore, the properties throughout the honeycomb are consistent and easy to produce.

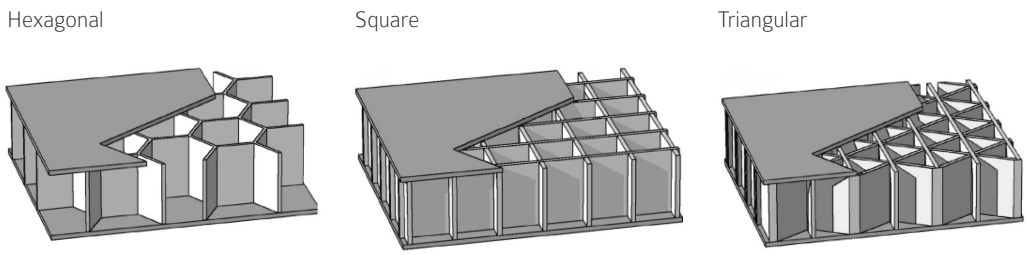

FIGURE 14 // Regular honeycomb structures (Pingle et al., 2011)

2.3.3. Production

Nowadays two production methods of the core are most used in commercial products. Expansion and corrugation. Both methods are suitable for metallic and non-metallic cores, but corrugation is mainly used when manufacturing high-density grids.

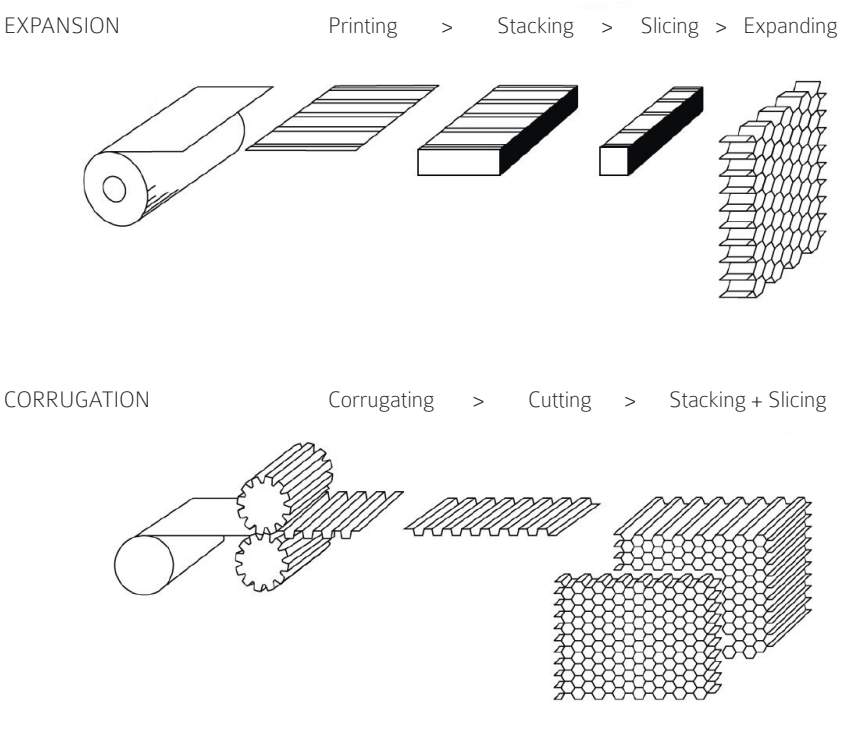

FIGURE 15 // Production of honeycomb cores (Hexcel, 2016)

The expansion process begins by stacking sheets of the core material. On selective locations an adhesive strip is printed. The sheets are therefore connected but not over the full length. This block, also called a HOBE (Honeycomb Before Expansion) is cut at desired distances. These slices can than be expanded to different shapes of honeycombs. Note that the strength depends on the directions of the honeycomb. The direction of parallel to the strips is stronger than perpendicular where glue connects the strips. Main difference between the expansion and corrugation method is that the corrugation process pre-shapes the strips before bonding them together (Hexcel, 2016).

One of the key issues for production is the joining method regarding glass sandwiches. Among the different options are bolting, welding and gluing. Disadvantage of bolting is the fact that holes need to be drilled, in combination with pre-stressed glass, these holes need to be there direct after the main production. The brittleness of glass also implies that these holes are prone to stress concentrations, especially when the bolts touch the glass. Welding of glass is an expensive operation and needs craftsmanship to execute it, mistakes are easily made. According to Veer, Janssen, & Nägele (2005) adhesives like epoxy, acrylate, polyurethane or silicone are the best way to join glass, although also that method has some disadvantages. Glue is hard to apply evenly, has a low water resistance and it will creep under sustained load. In case of a two-component adhesive, also the curing process is a factor regarding the reliability of the joint.

There are multiple ways to manufacture a sandwich panel. If the panel is curved or complex, vacuum bag processing or matched mould processing is often used. When creating a flat panel, the heated press is one of the well-established methods. Pre-impregnated facing skins are bonded are pressed together, ensuring a tight and secure connection between skin and core (Hexcel, 2000, p. 21).

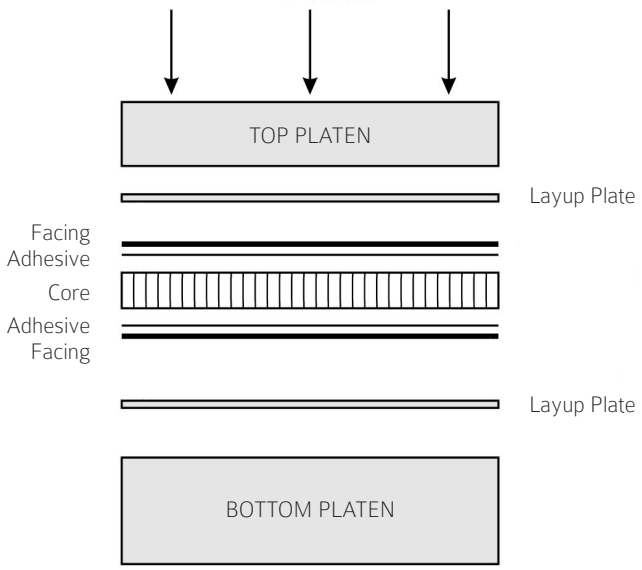

FIGURE 16 // Heated press production method for flat panels (Hexcel, 2000)

2.3.4. Enhancement techniques

Structural behaviour

A few aspects are already identified in this research. The thickness of the core, the material choice for the core and skin layers and the glue for connecting core and skin layer. These aspects are also closely linked together. For example, choosing a better shear resistant core material does only make sense when the glue can transfer these loads, otherwise the total panel will fail.

Thermal insulation

It is important to understand that these materials, leave space for gases. These gases do not contribute to a better structural behaviour, but will influence the thermal behaviour of the total panel. Air does have low conductivity of around 0.024 W/mK but argon has a conductivity of around 0.016 W/mK, reducing even more conductivity. Next to that, it is slightly heavier than air. Meaning that there is less risk on convection when applying a larger cavity. Krypton gas has an even better performance, but is also more expensive. Window cavities are not perfectly sealed. The partial pressure differentials between the air outside and the gas inside cause both argon and krypton to naturally escape over time. A perfectly constructed insulated glass unit still loses 1% per year (Wallender, 2019; EcolineWindows, n.d.).

Solar control

The core material, but especially the shape of the material determines how it will control both sun and glare. A homogeneous filled sandwich will block light and radiation, but would also influence the transparency of the panel. A low density punctual support on the other hand will be highly transparent but does not block radiation. Bi-directional extrusions could block radiation, but when standing perpendicular to the panel it might be still transparent like louvre systems.

2.4 CONCLUSION

Thin glass brings new opportunities to redesign façade elements which are made stronger by chemical strengthening and lighter in weight. Due to its thickness and flexibility it is not stiff enough to use as a single sheet.

Sandwiches are well known in the aircraft industry for providing stiffness, but they come with the disadvantage of conducting energy from one side to another. Multiple possibilities for improvements both on structural and thermal performance bring a façade sandwich element within reach.

Out of five base typologies for sandwich cores, homogeneous and unidirectional cores are found unsuitable, because these will block all light. The bi-directional typology is chosen for further research, considering the following advantages:

- Most efficient regarding weight to load ratio, therefore minimizing conduction
- Line-based contact between core and sheet, ensuring a secure connection
- Limits convection by creating smaller cavities within the total cavity
- Limits radiation by blocking sunlight

CALCULATION METHODOLOGY III

3.1 SETUP

The primary aim of this chapter is to evaluate different analytical calculations on both speed and accuracy. The most suitable calculation is selected as calculation methodology during research. Secondary aim is to show the difference between the digital and physical model. First step is to show how to assemble a thin glass panel and its visual appearance, second step is to compare the analytical calculations to physical measurements.

The size of the panels is determined by the physical size of the test sheets of AGC Falcon glass (appendix 9.1). The available sheets are rectangles of 250x150mm and a thickness of 0.5mm. From the literature review, paragraph 2.3.2, bi-directional sandwiches do have high potential. Three types are most common in commercial applications and scientific research: hexagonal, square and triangular. These are all tessellations consisting of only one type of polygon, ensuring a consistent performance throughout the whole panel. Therefore, this rectangle is populated by a 'regular' tessellation of polygons.

In order to prevent cut-off patterns, the polygons are squeezed in one or the other direction in order to fit in the rectangle 250x150mm. However, it is implemented to be as regular as possible, that means, with the least amount of deforming the grid. Edges of the cells are all approximately the same length. Although due to the amount of cells, the square one is more of a rectangle. The cavity thickness of 16mm, and therefore the depth of the sandwich extrusion, is derived from commercially available insulating glass units. This thickness ensures that there is little to no convection from air in the cavity. Having a commercial insulating glass unit as a reference makes it also possible to make a fair comparison later on. For the digital workflow, each panel consists of a volume representing a core and one or several volumes of air.

Following four prototypes are created for research. Hexagonal grid, square grid, triangular grid, no grid. Each panel including the one with no grid does have a brim around the edge of 2mm thickness, the same thickness as the ribs creating the grid for the first three prototypes.

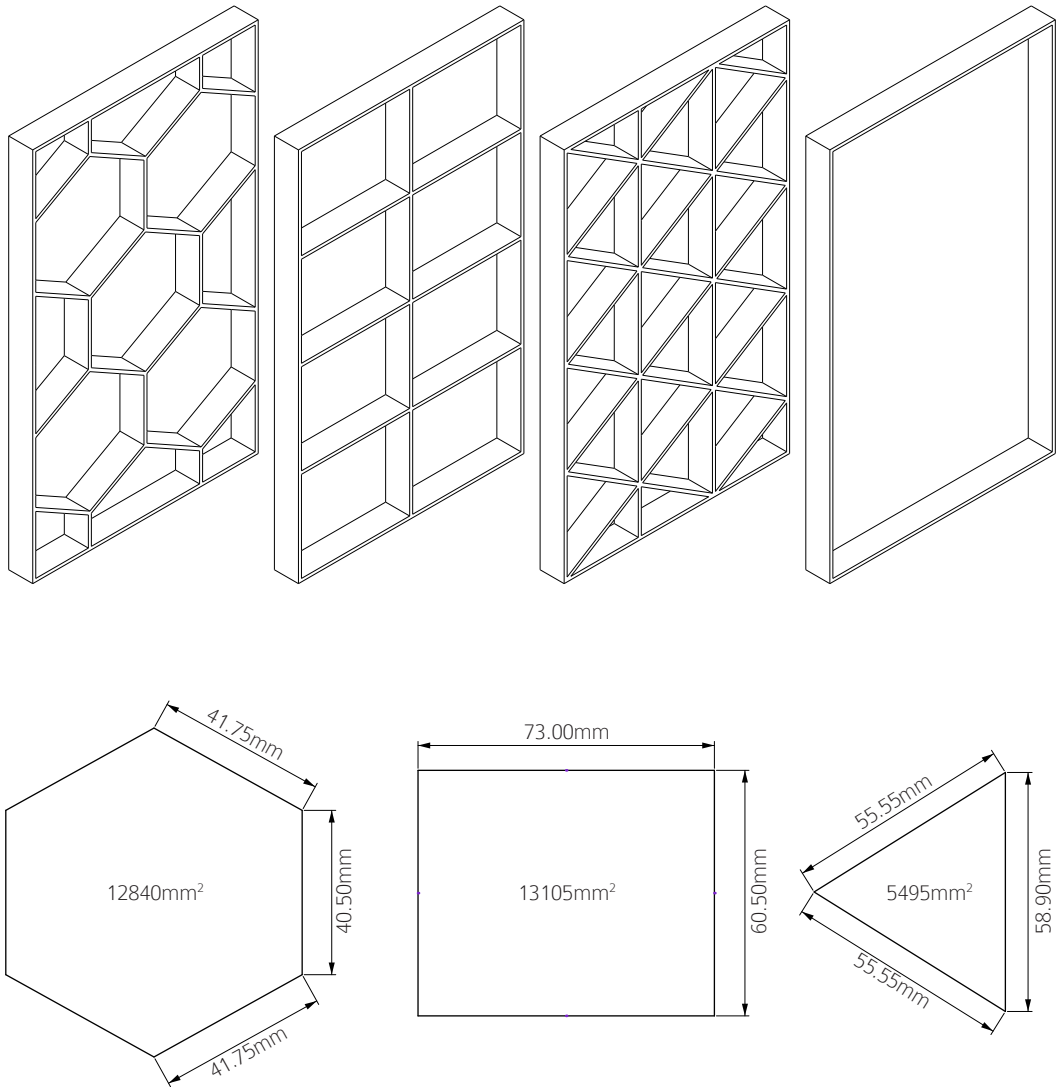

FIGURE 17 // Layout of the protoypes

3.2 ANALYTICAL CALCULATIONS

The thermal conductivity of PETG is 0.29 W/mK (CES, 2018), this value remains constant throughout all experiments. For all these analytical calculations, the cavity of 0.016 m is filled with air and glass is uncoated with an emissivity of 0.875

During the physical test, the horizontal temperature difference over the cavity is around 10 °C with a average temperature of 30 °C. Therefore the formula to obtain the conductive/convective coefficient is 0.73 x $\Delta T^{1/3}$ and the radiative coefficient for a black-body surface ($h_r 0$) is 6.3 W/m²K.

The convective/conductive component is in all cases the same, but the placement and amount of extrusions block more or less radiation, leading to differences in the radiative component. The width however is determined as an average for the panel itself, not for all the individual cells.

	R_g (m²K/W)	h_a (W/m²K)	h_r (W/m²K)	b (m)
Hexagon	0.166	1.573	4.447	0.060
Square	0.164	1.573	4.528	0.075
Triangle	0.174	1.573	4.163	0.033
Empty	0.154	1.573	4.900	0.150

TABLE 02 // Cavity resistance calculation

3.2.1. Simple analytical calculation

The resistance of an element depends on the thickness and its material property for thermal conductivity. When a homogeneous façade element consists of different layers, the individual resistances can be summed in order to obtain the total resistance.

$$R = d / \lambda$$

$$R_c = R_1 + R_2 + R_3 + R_n$$

R the thermal resistance in m²K/W
d the thickness of the material in m
λ the thermal conductivity in W/mK

In outdoor applications, the heat boundary resistance to the outside is 0.04 m²K/W. In order to match the indoor environment of the physical test a heat boundary resistance of 0.13 m²K/W is added to both sides.

	t (m)	λ (W/mK)	R (m^2K/W)	U (W/m^2K)
Boundary 'outside'			0.13	
Glass	0.0005	1.25	0.0004	
PETG	0.016	0.29	0.0552	
Glass	0.0005	1.25	0.0004	
Boundary inside			0.13	
Total			0.3160	3.1648

TABLE 03 // Resistance through PETG rib

	t (m)	λ (W/mK)	R (m^2K/W)	U (W/m^2K)
Boundary 'outside'			0.13	
Glass	0.0005	1.25	0.0004	
AIR	0.016	0.104	0.1545	
Glass	0.0005	1.25	0.0004	
Boundary inside			0.13	
Total			0.4153	2.4079

TABLE 04 // Resistance through AIR cavity

In this case, heat flow in one direction is considered, going from high temperature to low temperature, without heat flowing sideways. Note that when heat is flowing through the airy part, the heat boundary resistances are more than half of the total resistance. Regarding the PETG part it is even 80% of the total resistance.

When introducing the pattern, the conduction through PETG parts is different from the air volumes. This causes heat to flow where resistance is lower, so it will also flow sideways. Which makes the equation much more complicated. One way of dealing with this situation, is calculating the average of the absolute maximum resistance of the panel and the absolute minimum of the panel.

Regarding the maximum calculation, the heat flow is considered to be still only in one direction through the panel. Disregarding the heat flow in horizontal and vertical direction around the thermal bridge. The minimum calculation assumes an infinite thin layer of infinite conducting material between the glass and air layers.

Maximum

Based on the ratio between PETG and air, the total heat flow and heat resistance is calculated.

$$Q_{total} = (A_{PETG} / R_{PETG}) + (A_{AIR} / R_{AIR})$$

$$R_{total} = (A_{PETG} + A_{AIR}) / (Q_{PETG} + Q_{AIR})$$

	Ratio (%)		Area (m^2)	
	PETG	AIR	PETG	AIR
Hexagon	9.04	90.96	0.00339	0.03411
Square	7.84	92.16	0.00294	0.03456
Triangle	13.95	86.05	0.00523	0.03227
Empty	4.22	95.78	0.00158	0.03592

TABLE 05 // Ratio between PETG and AIR

	Q (W)	
	PETG	AIR
Hexagon	0.01073	0.07990
Square	0.00930	0.08137
Triangle	0.01655	0.07416
Empty	0.00501	0.08648

TABLE 06 // Heat flow when sideways flow is excluded

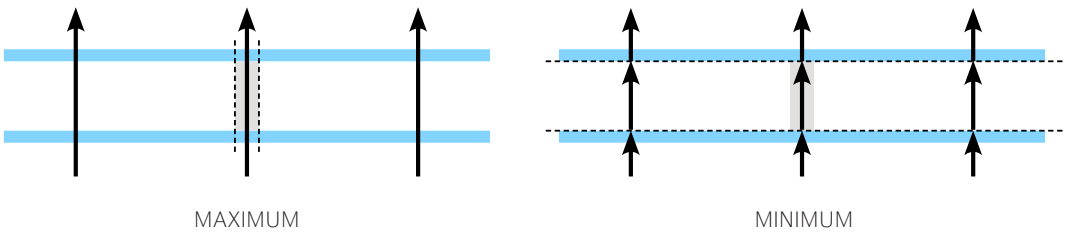

FIGURE 18 // Disregarding sideways flow and maximizing sideways flow

Minimum

Based on the ratio between PETG and air, the combined heat conductivity PETGAIR is calculated.

$$\lambda_{PETGAIR} = (\lambda_{PETG} \cdot A_{PETG} + \lambda_{AIR} \cdot A_{AIR}) / (A_{PETG} + A_{AIR})$$

This combined heat conductivity can then be used as a value representing the conductivity of the complete core. Therefore, maximizing the sideways flow.

	λ (W/mK)		
	PETG	AIR	PETGAIR
Hexagon	0.00098	0.00329	0.11382
Square	0.00085	0.00333	0.11150
Triangle	0.00152	0.00311	0.12332
Empty	0.00046	0.00372	0.11144

TABLE 07 // Combined heat conductivity

Results

There are no big differences between the optimum and the minimum variant, this is because the heat boundary resistance is a large part of the total resistance. The empty panel performs slightly worse than the square and hexagon, because the edge around the empty panel conducts heat but does not block much radiation. The resistance of the cavity is bigger for the panels with pattern, because the radiative heat transfer component is lower. This can be explained by the fact that these ribs do block radiation.

	U (W/m^{2}K)		
	Maximum	Minimum	Average
Hexagon	2.417	2.491	2.453
Square	2.418	2.473	2.445
Triangle	2.419	2.561	2.488
Empty	2.440	2.473	2.456

TABLE 08 // Results simple analytical calculation

3.2.2. Detailed analytical calculation

This second method, is one described by Tenpierik, Spoel and Cauberg (2007). This formula takes also the psi-value of the edge into consideration. Making it a more flexible when the section or composition of the edge changes.

$$U_{eff} \approx (U_{cop} \cdot S_{cop} + \psi^{c}{}_{edge} \cdot l_{p}) / (S_{cop} + S_{edge})$$

U the thermal transmittance in W/m^{2}K
S the surface area in m^2
ψ^c the linear thermal transmittance in W/mK
l the length of the edge in m

All cells are separately calculated, but the U-value for 'center of panel' is obtained by taking the average cavity resistance as calculated in table 03. Each cell has an edge of one millimeter, this is also the case for cells which are connected to the outer edge of the panel. The edge is calculated separately and added in the end to the calculation.

FIGURE 19 // Demarcation for each cell is halfway its thermal bridges

Indoor condition

Determination of the psi-value is based on a calculation model of Tenpierik (2007) delivered with the research by Tenpierik, Spoel and Cauberg (2007). Inputs for this model are identical to the information for the simple analytical model.

Facings		Edge		Boundary conditions	
λ (W/mK)	thickness (m)	λ (W/mK)	width (m)	U (W/m^{2}K)	U (W/m^{2}K)
1.25	0.0005	0.29	0.001	7.7	7.7

TABLE 09 // Input for psi-factor calculation

The differences between the different patterns lie in the different thermal conductivities of the core. These are derived from the calculated resistances of the core.

	λ cavity (W/mk)	ψ edge (W/mk)
Hexagon	0.09631	0.0039
Square	0.09762	0.0039
Triangle	0.09177	0.0040
Empty	0.10356	0.0038

TABLE 10 // Derived psi-values

	U (W/m^{2}K)	
	Simple	Detailed
Hexagon	2.453	2.473
Square	2.445	2.463
Triangle	2.488	2.533
Empty	2.456	2.454

TABLE 11 // Comparison between simple and detailed analytical calculation

Noticeable differences between the simple and more detailed analytical calculation. Especially regarding the dense triangular pattern. Probably due to the influence of the edges which is overlapping and not calculated correct within such a confined space and tight angles.

Till now, each calculation is performed for a complete panel, but it is only 250x150mm. The edge therefore is affecting the total score because it is over 2% of the total panel. Another disadvantage of calculating such a small panel is the interruption of the cells at the edges. This is especially true for the hexagon where only five full cells are found. Therefore, this calculation is performed again but on cell level. The empty panel is now calculated without any PETG material.

	U (W/m^{2}K)	
	Panel	Cell
Hexagon	2.473	2.422
Square	2.463	2.446
Triangle	2.533	2.472
Empty	2.454	2.408

TABLE 12 // Comparison between performance of the panel and one isolated cell

The U value for a panel without pattern is considerably lower, because the edge and therefore all the PETG is removed. Still a comparison with a commercial regular glass unit is not possible. Another major factor is the heat resistance boundary, because we assumed two times an indoor value of 0.13 m^2K/W this will not be comparable to industry standards.

Outdoor condition

Therefore, a separate U-value is calculated with different heat boundary resistances. Meaning a value of 0.13 m^2K/W at the inside and a value of 0.04 m^2K/W. This will change also the cavity resistance and therefore also the psi values.

	R_g (m^2K/W)	h_a (W/m^2K)	h_r (W/m^2K)	b (m)
Hexagon	0.195	1.573	3.558	0.060
Square	0.191	1.573	3.655	0.075
Triangle	0.210	1.573	3.189	0.033
Empty	0.181	1.573	3.967	0.150

TABLE 13 // Cavity resistance calculation

In comparison to the input for table 09, only cavity resistance will change together with the heat exchange coefficients. At the inside 7.7 W/m^2K, at the outside 25 W/m^2K.

	λ cavity (W/mk)	ψ edge (W/mk)
Hexagon	0.08209	0.0058
Square	0.08364	0.0058
Triangle	0.07619	0.0060

TABLE 14 // Derived psi-values

	U (W/m^2K)	
	Panel	Cell
Hexagon	2.473	2.422
Square	2.463	2.446
Triangle	2.533	2.472
Empty	2.454	2.408

TABLE 15 // Comparison between performance of the panel and one isolated cell

Again, the values change noticeably. It is however not a linear change. For example the triangle variant is affected more than the empty one.

Reference

To place this into perspective Planibel Clearlite from AGC is taken as a reference. Which consists of two times 6mm glass and has a U-value of 2.7 W/m^{2}K according to the datasheet (appendix 9.1). To make a comparable situation, this value is verified by a manual calculation.

	t (m)	λ (W/mK)	R (m^{2}K/W)	U (W/m^{2}K)
Boundary 'outside'			0.04	
Glass	0.006	1	0.006	
AIR	0.016	0.088	0.1809	
Glass	0.006	1	0.006	
Boundary inside			0.13	
Total			0.3629	2.7559

TABLE 16 // Resistance through Planibel Clearlite

The differences are very marginal considering the dense pattern. Main reason is the lower radiation through the panel. At the other hand the difference between the reference and best performing pattern is still 0.21 W/m^{2}K so when a building has 1000 m^2 of glass, it will lose 210 J/sK

3.2.3. Numerical analysis

Numerical analysis is performed in DIANA, a finite element analysis program. The input values for this experiment are identical to the simple analytical calculation. Meshsize is set to 2mm to match the thickness of the ribs, creating cubical mesh elements. Meshtype is hexa/quad with linear interpolation.

For a FEA cubical elements give the most reliable data, therefore the glass parts are not modelled due to the thickness of that layer. When trying, the mesh creates a redundant amount of mesh elements not understanding what to connect. Instead, the resistance of the glass is incorporated in the heat exchange coefficient of the boundary condition.

Conductivity through glass is thickness divided by thermal conductivity, which results in a resistance of 0.0004 m^{2}K/W, this resistance is added by the heat boundary resistance resulting in a total heat boundary resistance of 0.1304 m^{2}K/W for both sides of the digital prototypes. The average resistance of the cavities as calculated in table 02 is converted into a conductivity value by dividing the thickness of the cavity by the resistance.

Inside temperature is 48°C, outside temperature 23°C, matching generally the temperatures of the physical test. The edge around each prototype is adiabatic, energy can only transfer between two heat boundary interfaces. These surfaces are exactly matching the glass panels of 250x150mm, the front and back.

	U (W/m²K)		
	Simple	Detailed	Numerical
Hexagon	2.453	2.473	2.472
Square	2.445	2.463	2.452
Triangle	2.488	2.533	2.481
Empty	2.456	2.454	2.454

TABLE 17 // Comparison between all three calculations with indoor conditions

Result of this test is the average heat flow of the mesh elements on the inside of the mesh. Divided by the temperature difference leading to the total resistance of the panel. The U-value for the hexagon and empty panel compared to the detailed analytical calculation are very close. The simple analytical calculation however does estimate the cells in a very confined area better.

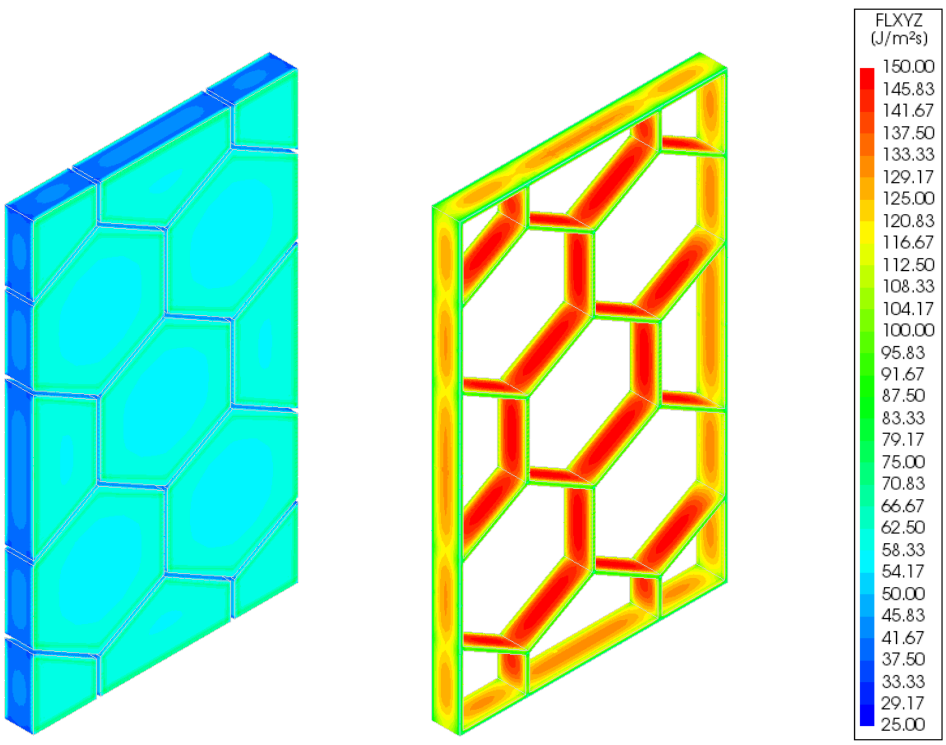

FIGURE 20 // Heatflow through prototype with hexagonal grid

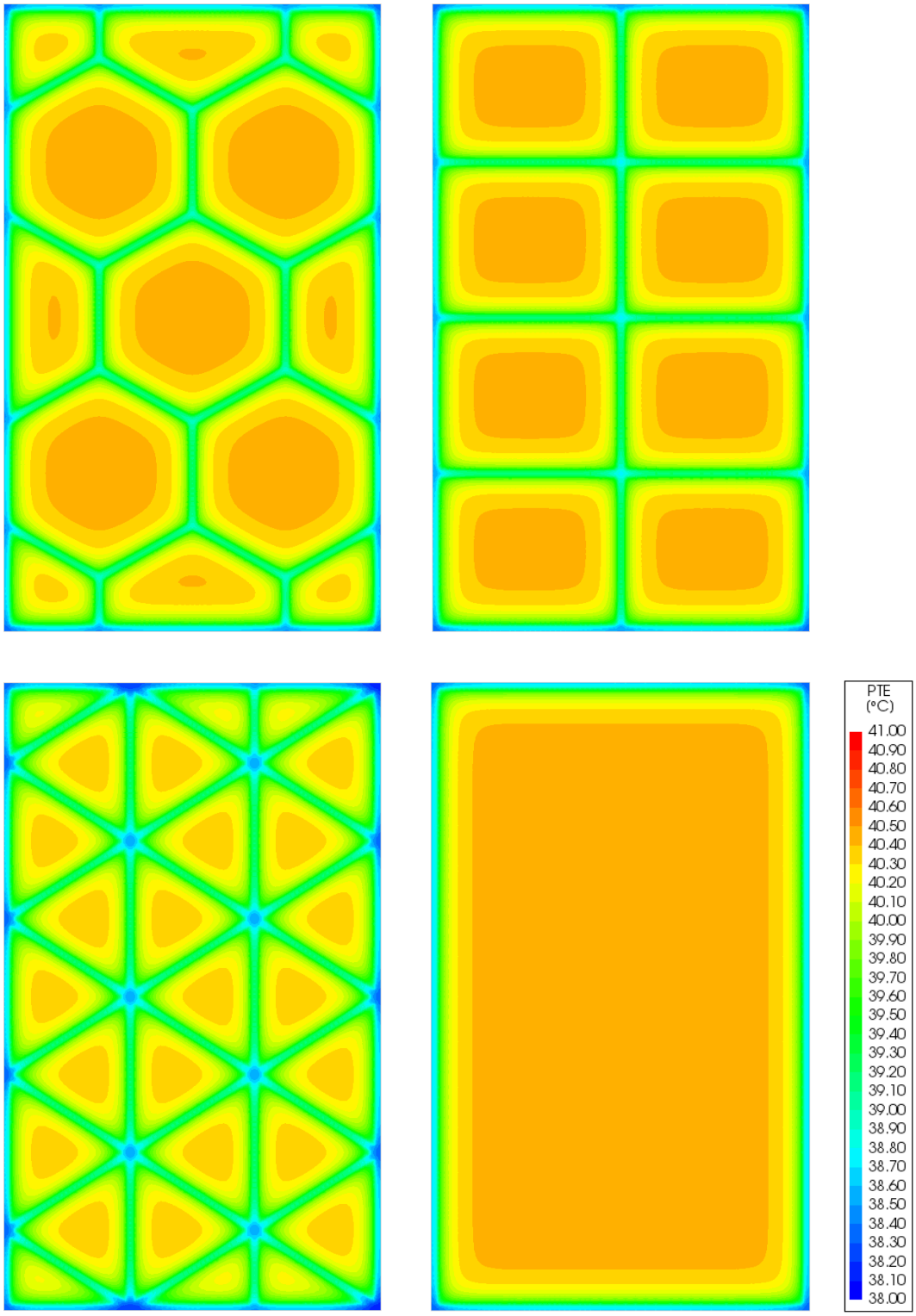

FIGURE 21 // Temperature distribution at the inside

3.3 PHYSICAL MODEL

Due to practical reasons, 3D printing with PETG is chosen as the rapid prototyping technique. This requires only a few hours to obtain a low conductivity, translucent core. The core for these panels is PETG (appendix 9.1) from Innofil 3D and printed with a Leapfrog Creatr 3D printing machine with a following inputs. Due to the size of the nozzle in relation to the 2mm ribs, no infills were used for this prototype.

Printing temperature	240 °C
Printing speed	30 mm/s
Nozzle size	0.8 mm
Layer height	0.5 mm
Fan speed	35 %
Heatbed temperature	50 °C

TABLE 18 // Printing settings for rapid prototyping

Assembling is best to be done on a PE table, preventing the glue to stick on the table. First step is to clean the sheets of glass and the PETG core with isopropyl alcohol to remove all grease and dust. This assures a tight bond between the two elements. Make sure the room is well ventilated.

The glue used for these physical models is DELO photobond 4494 (appendix 9.1), a transparent glue with a medium viscosity. It is a UV-curing acrylate adhesive and especially designed for glass bonding. Apply glue to one side of the core and place one sheet of glass exactly on top of it. Prevent any lateral movements when placing this sheet.

Next step is curing the glue with the Delolux 80 UV lamp. General rule is that the longer the curing time is, the better they joint. Within three seconds, the two parts are fixed together. In order to create a very stiff bonding, the glue is exposed for 120 seconds to the UV light. Flip the panel and repeat the applying of glue and placing the sheet for this side. Note that the glue should be applied as lines and not as dots ensuring structural stiffness. This means that top and bottom of each rib is covered with glue and implicates that the complete core will transfer heat and forces from one side to another. The prototype is now ready to use for the physical experiment.

In case of this research, the nozzle used for printing is not an official one from Leapfrog but manually drilled by TOI TUDelft from a 0.5mm nozzle. This results in a sometimes jagged print. Second inaccuracy happened during the assembling process of the triangular grid, lateral movement was introduced when placing the second sheet. This led to glue smearing sideways. The glass sheet is removed and cleaned again with the isopropyl alcohol. Some traces of glue are still visible on the prototype.

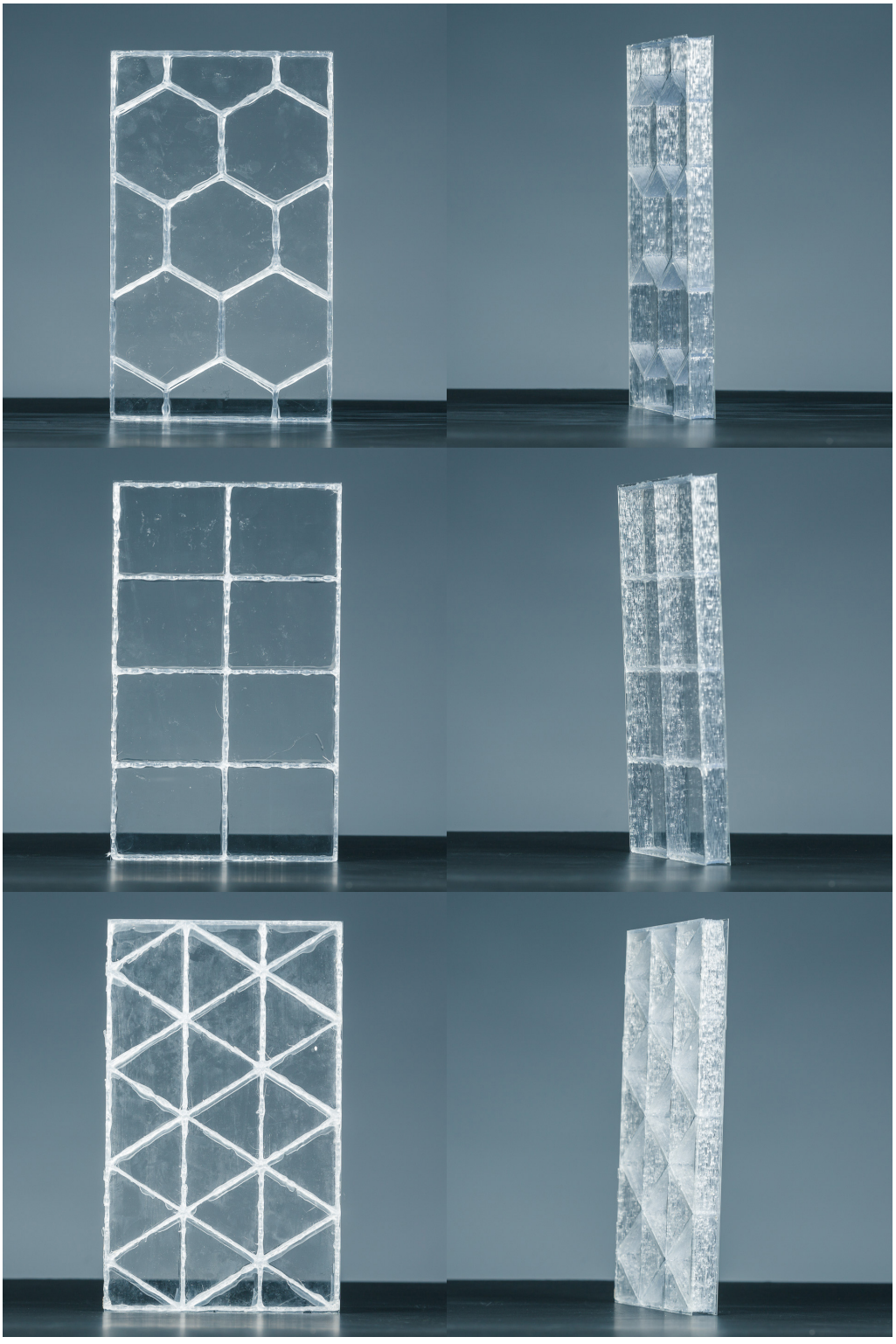

IMAGE 01 // Printed samples

In front view, the ribs appear as white, not particularly transparent or translucent. The excess amount of glue however does appear as transparent. When looking from an angle to the core, sometimes it shows translucent and even transparent in some places. At certain angles the core is reflected in the back glass sheet, which results in an overlay for the objects behind the glass. Note that this core is printed, it is created by stacking layers of material. This results in reflection and refraction in all directions. Another production method like extruded beams would result in a much clearer core with less refraction and an even reflection.

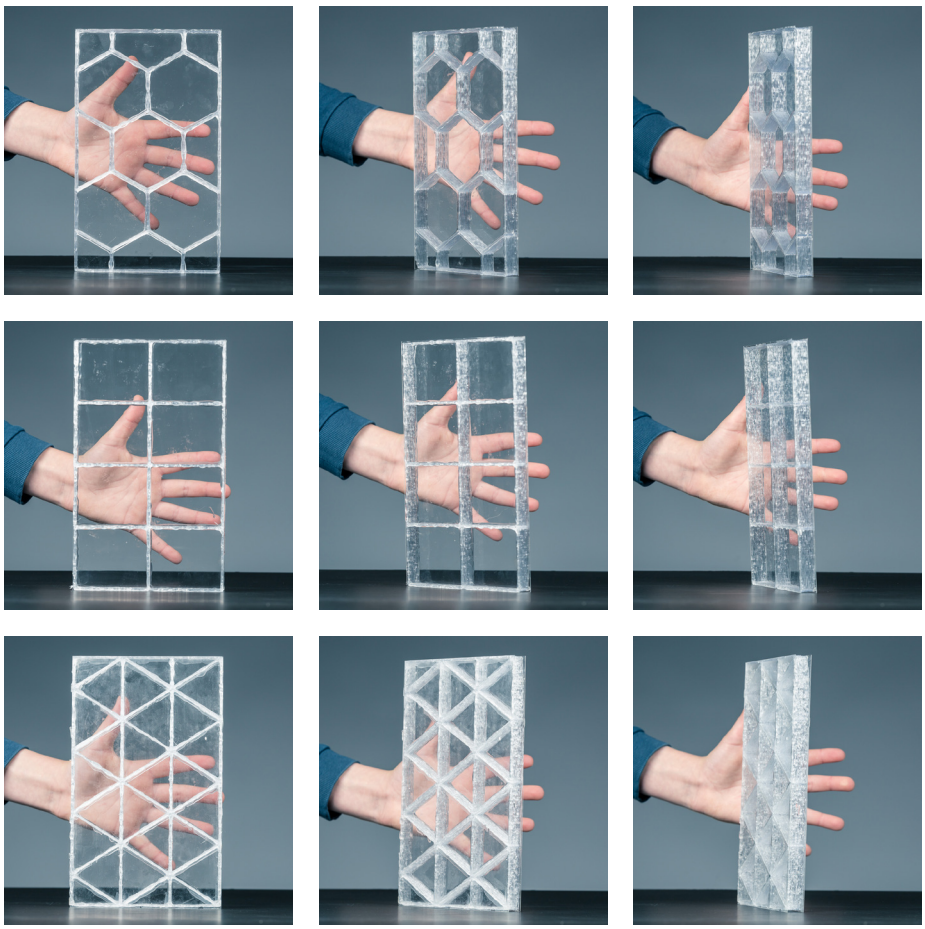

IMAGE 02 // Visual effect of the grids when viewing at an angle

Dense patterns make it impossible to look through from an angle. The overlapping ribs result in too much reflection and refraction. The blocked view from an angle might seem as a drawback, at the other hand it results in a playful interaction between sun and pattern. Thoughtful design can lead to a particular quality of steering or scattering light, which opens new opportunities for designers.

3.4 PHYSICAL MEASUREMENTS

The idea behind the physical test is to create a comparison between theory and practice. Some elements, like the glue are not modelled. Due to the amount of glue applied, the contact surface might be larger than in the analytical models. Other elements like the ribs are 3D-printed in lines, but are represented as volumes in the analytical model.

Materials

1x Tempex box 1x1x1 m^3
1x Lightbulb 60W
1x Laptop
1x Eltek squirrel datalogger 1000 series
1x Eltek darca software
2x Wireless transmitters
2x Hukseflux heat flux sensor HFP01 model
4x Thermo couplers type T

4x Prototypes

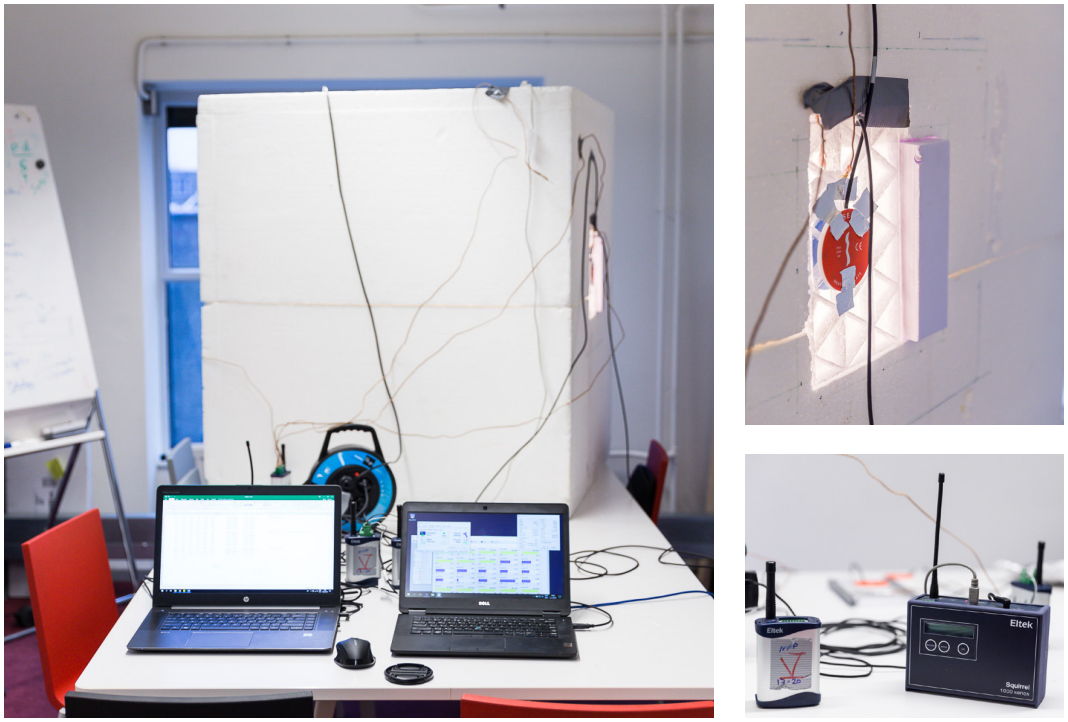

IMAGE 03 // Setup during physical measurements

Execution

When starting at room temperature, close all holes of the box and heat it with the lightbulb. This will take around one hour before temperature will be stable. In de mean time connect all sensors with the transmitters. Connect the transmitters wireless with the datalogger and make sure the laptop gets updates of the changing values from the sensors.

- Place one thermocouple in the room
- Place one thermocouple in the box
- Place one thermocouple and heat flux sensor at inside prototype
- Place one thermocouple and heat flux sensor at outside prototype

When the temperature in the box reaches a stable temperature, remove the cover from the prototype holder. Place the prototype and seal it in place. Ideally, no air should leak around the prototype. During this process the temperature inside the box will drop. It takes between 15 and 30 minutes before it reaches again a stable temperature. Measure for half an hour the readings from all sensors. Execute measurements for three times per grid. One measurement at the centre of the cell. One measurement at the intersection of the ribs and a measurement halfway a rib.

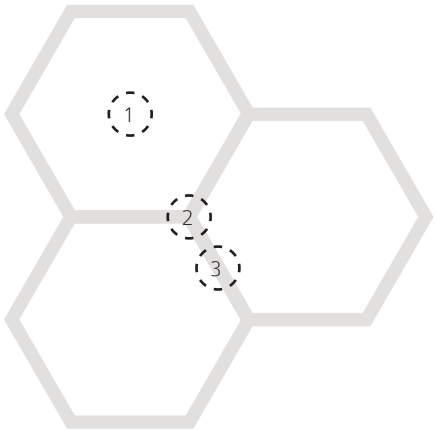

FIGURE 22 // Three positions for measurements

Results

The air within the box and room is moving slow, therefore an indoor heat boundary resistance of 0.13 m^2K/W is applied to both sides, in order to obtain the correct U-value.

	Q (W/m^2)		
	Cell	Knot	Element
Hexagon	59.86	67.08	64.03
Square	62.65	62.60	62.00
Triangle	61.52	66.24	67.87
Empty	63.64		

TABLE 19 // Heat flux derived from appendix 9.2

	U (W/m^2K)		
	Cell	Knot	Element
Hexagon	2.46	2.37	2.54
Square	2.55	2.45	2.61
Triangle	2.39	2.50	2.53
Empty	2.54		

TABLE 20 // Thermal transmittance including heat boundary resistance

Reflection

For this kind of experiments, around 15% variation between results is expected. All values are relatively close to each other and within the range of variation. Therefore, the accuracy of the results is low. On the other hand, it gives a direction for all prototypes to expect U-values somewhere between 2.37 and 2.61 W/m^2K. Especially the fact that knots have a lower U-value than the parts with an air cavity gives an indication that these results are not accurate. Multiple factors can influence the results, like:

- Air leaking from sample: When placing the sample, there is no tight seal preventing warm air leaking from the box. Influencing both the thermal and heat flow sensors on the outside.
- Placing thermocouple at a 'similar' spot: It is impossible to place a thermal sensor and a heat flux sensor at the exact same spot, therefore the thermal sensor is placed on a similar spot of the pattern, causing a small fluctuation.
- Placing sensors at the exact spot: Thermal sensors and heat flux sensors need to be perfectly opposite to each other. Because the panel is not homogeneous filled, every movement of a millimetre will cause inaccuracies.

- Radiation on heat flux sensor outside: At the inside, a piece of aluminium foil is preventing light from the lightbulb to directly radiate on the heat flux sensor at the inside. The heat flux sensor at the outside however is not protected. There is a possibility that it also measured also radiation from the lighting in the room.
- Placing thermal sensors: In contrast to the heat flux sensors, the thermal sensors do consist of two thin but stiff metal wires. These are difficult to attach to the glass, which makes it hard to ensure that they really measure the temperature of the glass.

3.5 CONCLUSION

Regarding the prototype panels, following values are retrieved. Although the physical test does not entirely reflects the results from the other calculations, its values are around the same order.

	U (W/m^2K)			
	Physical	Simple	Detailed	Numerical
Hexagon	2.37-2.54	2.453	2.473	2.472
Square	2.45-2.61	2.445	2.463	2.452
Triangle	2.39-2.53	2.488	2.533	2.481
Empty	2.54	2.456	2.454	2.454

TABLE 21 // Comparison between physical measurements and analytical calculations

Each of the calculation methods has its pros and cons. The simple analytical calculation is quite accurate when comparing it to the numerical analysis. It is also a very fast arithmetic method, which makes it suitable for optimization strategies. The downside is that it only depends on the amount of material and its conductivity value. Which makes it unreliable when the cross-section changes to a different shape, which is not symmetric or constant in thickness.

The numerical method is very accurate, certainly when the mesh size is small. At the other hand it would require more time to calculate in comparison with arithmetic methods. This becomes even more important when the panel would be 2100x1200mm instead of 250x150mm.

The detailed analytical calculation is the golden mean. Providing a more elaborate formula, which includes the psi-factor of a cross-section, so it could even be a multi-material section. It still is arithmetic solvable, which means it is fast and can also easily implemented in a program as Grasshopper. It is however less accurate when calculating small cells. Probably because the influence of each edge overlaps with the influence of another edge within the same cell, something that is not taken into account. For further analysis, this method is used to calculate U-values.

CORE MATERIAL DISTRIBUTION IV

4.1 MATERIAL SELECTION

Before heading over to different tessellations, it is important to identify the material which is best suitable for this sandwich. Based on CES (2018), fiber reinforced polymers and metals like stainless steel and aluminium are widely used. Stainless steel and aluminium are not an option because of their high thermal conductivity of respectively 16 and 140 W/mK. Thinner ribs cannot compensate this, because they would not be stiff enough for structural application.

To avoid the optical effect of subdividing, and being able to print or extrude the sandwich layer, opaque fiber reinforced polymers are impossible. Therefore, a selection of transparent and widely available polymers is made.

	PETG	PA	PLA
Density (kg/m^3)	1260 - 1280	1090 - 1100	1240 - 1270
Young's modulus (GPa)	2.01 - 2.11	1.60 - 1.68	3.30 - 3.60
Tensile strength (MPa)	60 - 66	40 - 47	47 - 70
Compressive strength (MPa)	57.5 - 63.5	55.0 - 46.7	66.0 - 86.4
Thermal conductivity (W/mK)	0.29	0.24	0.15
Resistance UV radiation	Fair	Fair	Good
Recycleble	True	True	True
Embodied energy (MJ/kg)	89 - 98	210 - 232	52 - 58

TABLE 22 // Material properties of selected transparent polymers (CES, 2018)

All of them are recyclable, do have more or less the same density and a tensile/compressive strength comparable to each other. There are also differences between these three polymers.

When applied in a transparent façade panel, two properties are paramount. Thermal conductivity and resistance to UV. This immediately makes PLA an outstanding option. It has nearly half the thermal conductivity compared to PA and PETG. Also its good resistance against UV, makes it a better option over the other two polymers. In addition to that, it does have a higher Young's modulus which resist against bending. PLA stands for polylactide, which is a biodegradable thermoplastic, derived from corn or sugarcane. This also shows in its embodied energy, which is the lowest of all three. Based on the properties above PLA, is the material to use in the sandwich.

When using rectangular cross-sections, polymers can be easily extruded in strips and glued together, much like the corrugation manufacturing method. When using more intricate sections like I-beams, extrusion of the separate elements is preferred, thermal welding could be used to weld all separate elements and form the sandwich core.

4.2 MACRO SCALE

4.2.1. Setup

Time to scale up, during the physical measurements the size was determined by the size of the provided sheets of glass. A commercial insulating glass unit can be much bigger than that. The following analysis assumes therefore an infinite panel of glass. This avoids a cut-off pattern to the edge, but also disregards the effect of the spacer. This way the calculated U-value is comparable with industry products, which are also measured at the centre of the glass.

There is an infinite amount of ways to tessellate a surface. In this research the focus lies on regular and semiregular tessellations. What and how does that affect the effective U-value. To place this into perspective Planibel Clearlite from AGC is again taken as a reference. Which consists of two times 6mm glass and has a calculated U-value of 2.756 W/m^2K

Cavity resistance is calculated according to the method described and elaborated in table 13. Effective U-value for a cell or collection of cells is calculated according to the detailed analytical calculations as described in paragraph 3.2.2

Cavity thickness is 16mm
Thickness of ribs is 2mm
Thickness of the thin glass is 0.5mm

Thermal conductivity of the thin glass is 1.25 W/mK
Thermal conductivity of the PLA ribs is 0.15 W/mK

Heat exchange boundary for inside is 0.13 m^2k/W and 0^oC
Heat exchange boundary for outside is 0.04 m^2k/W and 20^oC

4.2.2. Regular tessellation

The prototypes made use of nearly regular polygons. Because they were squeezed a little bit they were technically no regular tessellation. Regular tessellations are composed of regular polygons of one kind. Meaning that all sides have the same length.

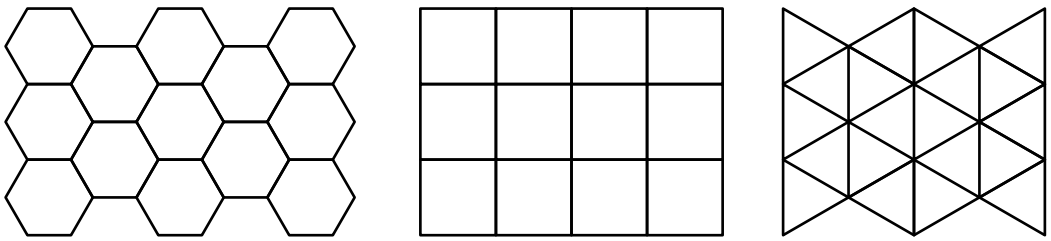

FIGURE 23 // Regular tessellations

Where the lines meet in one point is called a vertex. A tessellation can be described by the amount of polygons meeting at such a vertex and the kind of polygons which make up the tessellation. For example these three regular tessellations are described as 6.6.6 for hexagonal, 4.4.4. for the square grid and 3.3.3.3.3.3 for the triangular division. They are the only mathematically possible regular tesselations. Regular pentagons for example, can not create a closed pattern.

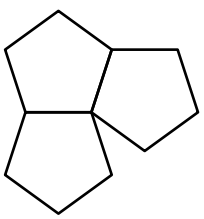

FIGURE 24 // Regular pentagons leaving open spaces

According to the formula in paragraph 3.1.2 the size of each cell determines for a major part its U-value. The width necessary to calculate the radiative heat transfer component is determined by the so-called hydraulic-diameter. Which is defined as four times the area of a cell divided by its perimeter. First step is to compare five different regular polygons. Three, four and six-sided polygons can be used to form regular tessellations. While eight and twelve-sided polygons can be used to form semiregular tessellations. These semiregular tessellations will be investigated next.

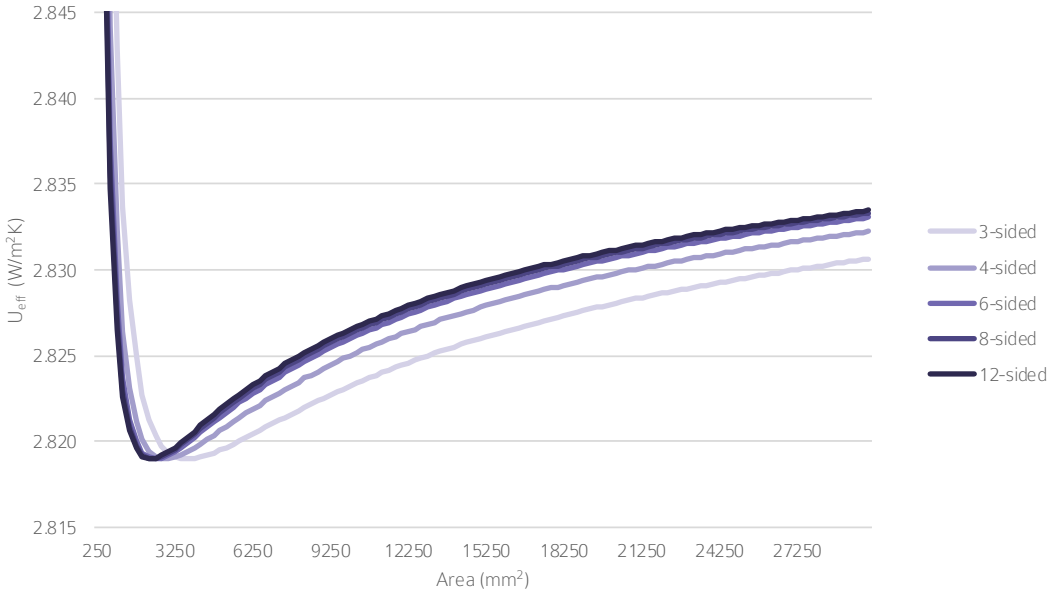

FIGURE 25 // Relation between size of polygon and U-value

Polygon	3-sided	4-sided	6-sided	8-sided	12-sided
Area (mm²)	3750	3000	2500	2500	2250

TABLE 23 // Optimum area for polygon regarding U-value

Each polygon does reaches the same bottom at 2.8190 W/m²K. What is different is where they do have their bottom. The more a polygon resembles the shape of a circle, the earlier it will reach its bottom limit. In the long run they will climb at a faster rate compared to triangles.

The more sides a polygon has, the less thermal bridging is needed to cover the same area. So, a triangle uses relatively more material compared to a octagon to cover the same area. This results in a high thermal conduction for a triangle when its size is small. In the long run it will block a certain amount of radiation, because it simply has more material to block radiation. The bottom or dip in this chart shows where the radiative component through the cells takes over from the conduction through the PLA.

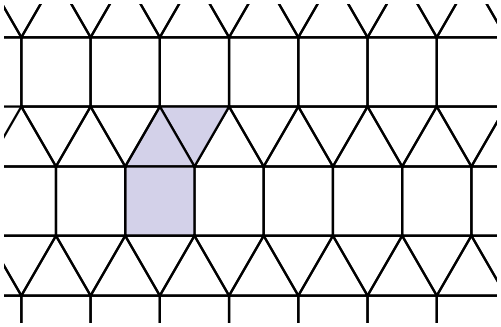

Pattern A 3.3.3.4.4

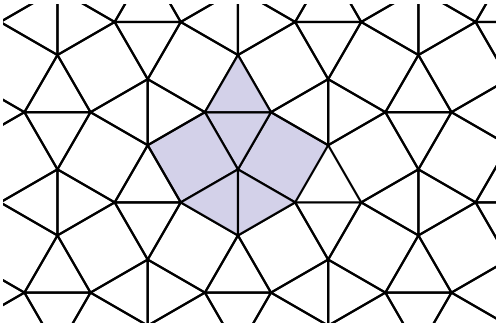

Pattern B 3.3.4.3.4

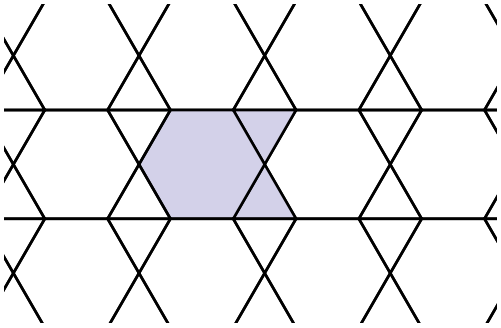

Pattern C 3.6.3.6

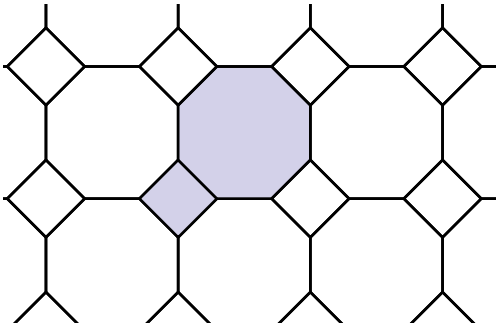

Pattern D 4.8.8

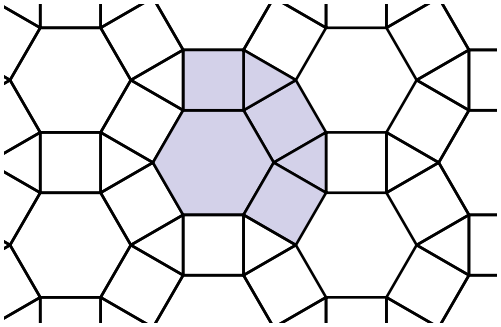

Pattern E 3.4.6.4

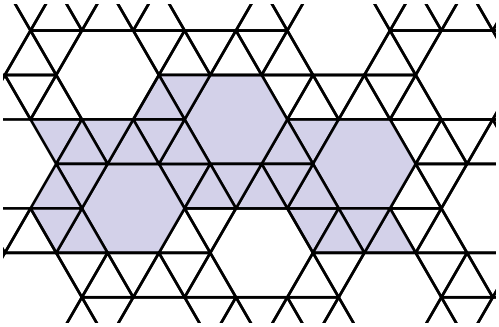

Pattern F 3.3.3.3.6

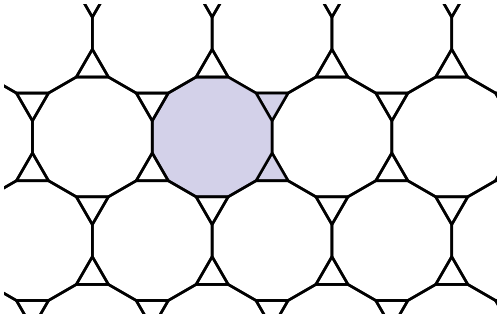

Pattern G 3.12.12

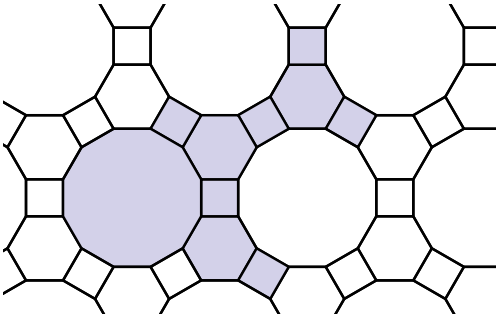

Pattern H 4.6.12

FIGURE 26 // Semiregular tessellations

4.2.3. Semiregular tessellation

In order to bring more variation in cell sizes also semiregular tessellations are studied. Semi-regular tessellations are composed of regular polygons of different kinds. At each vertex in the tessellation the configuration of adjacent polygons is exactly the same. Therefore, there are only eight semiregular tessellations possible. The purple part indicates the repeating pattern. This pattern will be scaled uniform to identify the optimum for each pattern.

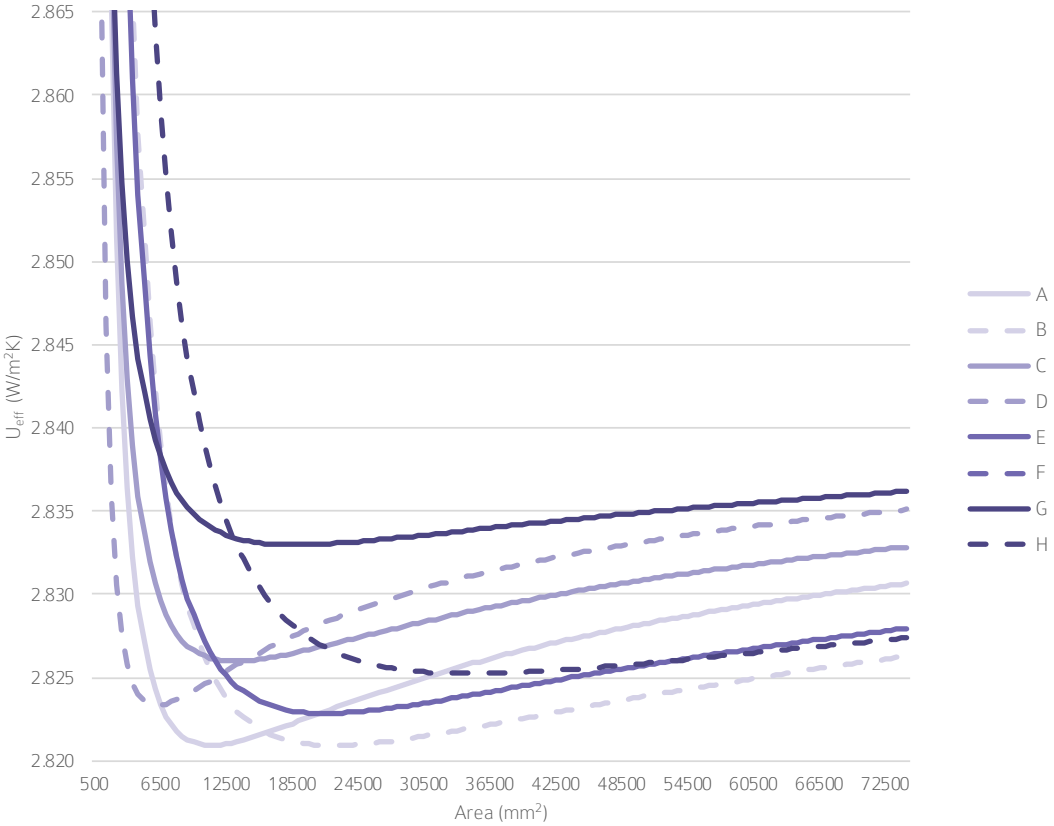

FIGURE 27 // Relation between size of repeating pattern and U-value

Polygon	A	B	C	D	E	F	G	H
Elements	3	6	3	2	6	27	3	10
Area (mm²)	11000	22000	13250	6000	21500	-	18750	35000
U (W/m²K)	2.8209	2.8209	2.8260	2.8233	2.8228	2.8411	2.8330	2.8252

TABLE 24 // Optimum area for repeating pattern regarding U-value

When scaling the repeatable pattern from 500mm² to 75.000mm², pattern A and B do have the lowest bottom, best U-value. Both pattern consist of triangles and squares. Pattern B has double the amount of triangles and squares so its optimum lies double the amount of area for pattern A.

Pattern F has 27 elements as a repeating pattern, lots of triangles and a few hexagons. It does not reach an optimum but converges to a U-value significant higher than the other patterns. When it reaches this 'optimum', the pattern already covers 2.000.000 mm^2 and stretches more than 1.5 meter. This increases the risk that the pattern will be interrupted and therefore perform even less.

Pattern H does have his optimum at a relatively large area. Still when considering that area as a square, it would be a square with sides of 187mm. This is perfectly applicable in larger windows without too much intterrupting of the panel.

Generally speaking cells with a large variation in cell sizes should be avoided, these do thermally perform weak, because the optimum of each cell individually is not reached at the same time. This is the case for pattern G, at a small scaling the 12-sided polygon will perform optimal, while the triangles will conduct at high rate. Scaling this pattern will improve the performance of the triangles but weaken the performance of the 12-sided polygons.

4.2.4. Rectangular tessellation

Till now only regular shapes are analysed, but changing the ratio into elongated cells creates a new perspective. That way blocking radiation is increased while conduction through the material is minimalised. The horizontal rectangle should be the ideal pattern, because convection would be limited by the horizontal louvres.

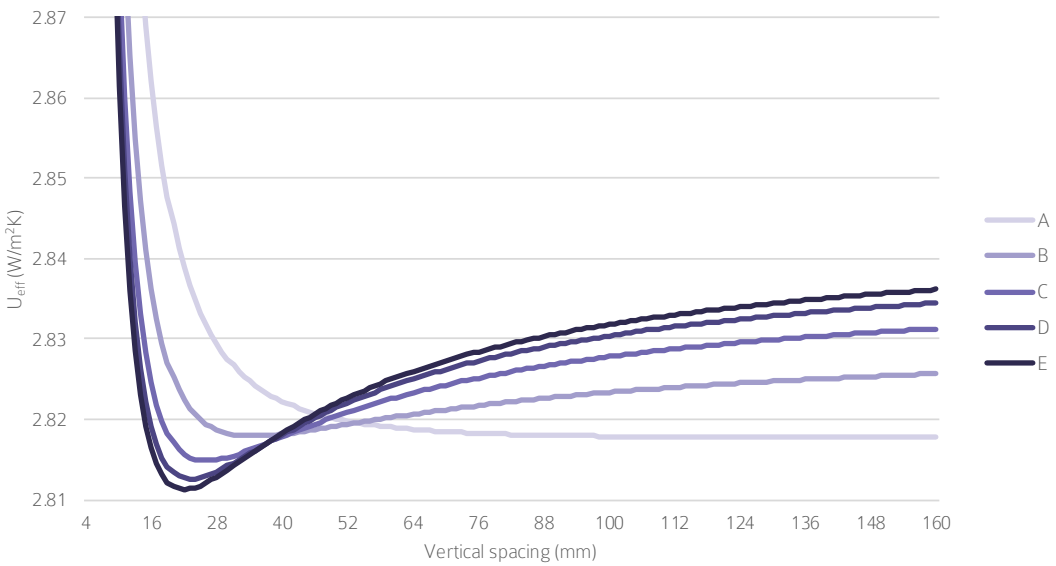

FIGURE 28 // Relation between ratio of rectangle and U-value

Rectangle	A	B	C	D	E
Width (mm)	40	80	160	320	640
Height (mm)	132	34	26	23	22
U (W/m^{2}K)	2.818	2.818	2.815	2.813	2.811

TABLE 25 // Optimum ratio for rectangle regarding U-value

Based on the graph and table, a louvre within the window to prevent radiation is effective. Even bigger ratio's are tried, but these result also in a vertical spacing of 22mm and a U-value of 2.811 W/m^{2}K. Horizontal louvres are chosen over vertical louvres based on the reduction of convection.

4.3 MICRO SCALE

4.3.1. Setup

Till now the cross-section was during the entire research assumed as a rib of 2x16mm. Which is the limit from a structural standpoint. Making the rib even narrower than a ratio of 1:8 would introduce a too small surface to attach for the glass sheets and makes the section very unstable.

If more stiffness is needed, or from the beam standpoint, more resistance to bending. The second moment of area needs to be enlarged. This has also consequences for the thermal performance of the beam, because generally more material is used. What is the best geometric distribution of this material?

A cross-section over the panel is modelled to define the psi-factor of different thermal bridge designs. Basically, the psi-value is the difference in heat flux between a cavity with and without thermal bridge. This can be described as:

$$\psi = (q_2 * l_2 - q_1 * l_1) / \Delta T$$

Heat flux in Y direction at the boundary interface is calculated over 150mm, because preliminary calculations show that the influence of the thermal bridge is around 50mm to both sides.

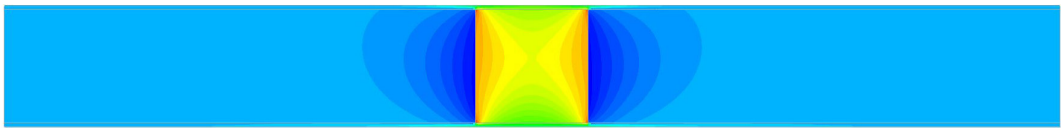

FIGURE 29 // Heatflow in Y direction, 48.01-91.73 J/m^{2}s

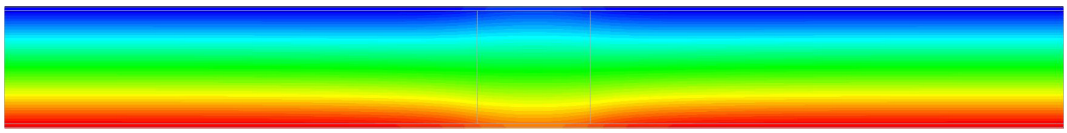

FIGURE 30 // Temperature, 2.24-12.67 °C

This experiment is executed in Diana FEA, this time the glass pieces are modelled as actual geometry. Meshsize is set to 0.5mm which is the thickness of the glass, creating square mesh elements. Meshtype is hexa/quad with linear interpolation.

Cavity thickness is 16mm
Thickness of the thin glass is 0.5mm

Thermal conductivity of the thin glass is 1.25 W/mK
Thermal conductivity of the PLA ribs is 0.15 W/mK
Thermal conductivity of air is 0.088 W/mK

Heat exchange boundary for inside is 0.13 m^{2}k/W and 0°C
Heat exchange boundary for outside is 0.04 m^{2}k/W and 20°C

The thermal conductivity of air includes the convective and radiative component through the cavity. This value is also used for the hollow sections, which will give a slight distorted view, they will perform worse than reality.

4.3.2. Cross-section thermal bridge

All the following sections are analysed. Regarding the hollow and beam sections, the thickness is 2mm. Except the bottom two rows where a section of 2x16mm is rotated around its centerpoint. Each section results in a certain amount of material, a psi-value and a second moment of area. Most interesting is the ratio between material and psi-value, material and second moment of area, and ratio between psi-value and second moment of area. Results for each section profile can be found in appendix 9.3

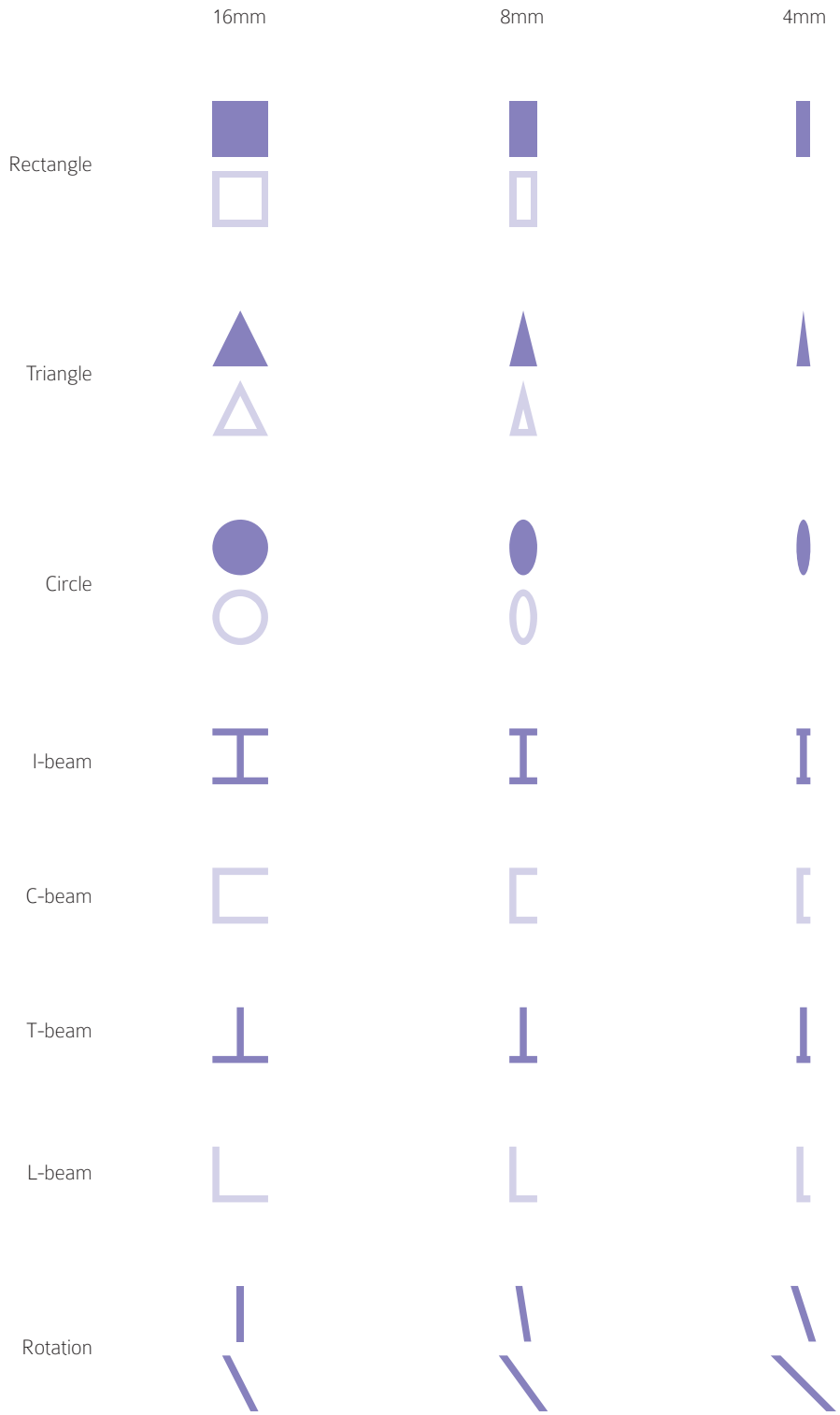

FIGURE 31 // Selection of cross-section profiles

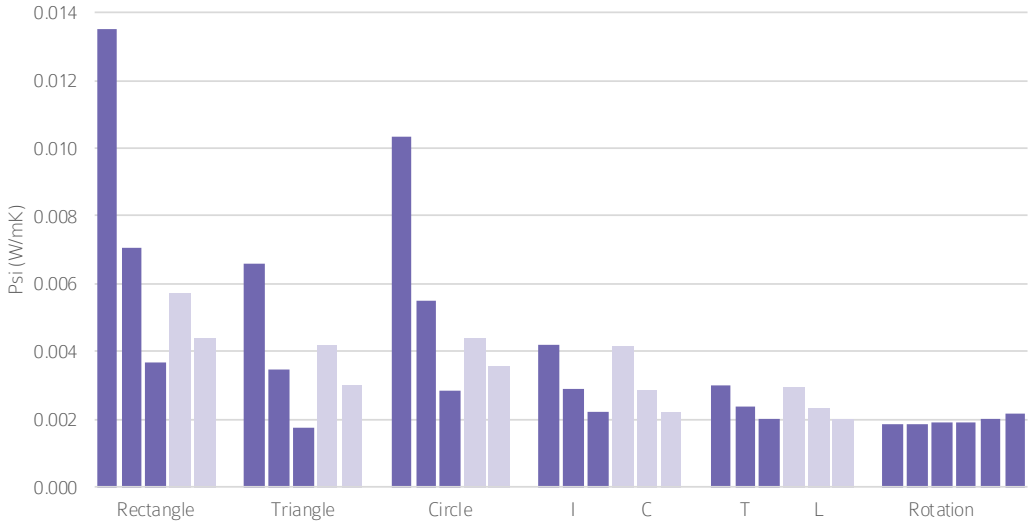

FIGURE 32 // Section profiles evaluated on psi-value

When looking at the psi-values for each of the sections, obviously the 16x16mm rectangle has the biggest psi-value. It has the most contact surface and most material use.

The triangle section has a large contact surface at one side, and virtually none at the other side. This decreases the psi-value by a factor two. The circle section however has very small contact surfaces but still has a high psi value. This means that the amount of material used in the section is more important than the contact surface. The strong decreased psi-values of the hollow rectangular, triangular and circle sections support this conclusion.

The I-beam in comparison with the C-beam do show very marginal differences. They do have the same amount of area. Shifting the most conductive path to the left or right, does not have a significant effect. This is also demonstrated by the marginal difference between T and L-beams.

What does have a significant effect is removing material from the I and C-beam. When converting these to respectively a T and L-beam the psi-value drops immediately. But as concluded before, this is a matter of removing material, not because the contact surface is smaller.

Rotation of a beam does has not much effect. One might expect that a rotated beam has a longer conductive path and therefore a lower psi-value. This test rejects that idea, this is due to the fact that a rotated beam requires more material to span diagonally.

These absolute values lead to the conclusion that more material leads to more conduction, no matter how long the path of conduction is. Which is expected because the conductivity through PLA is nearly two times higher.

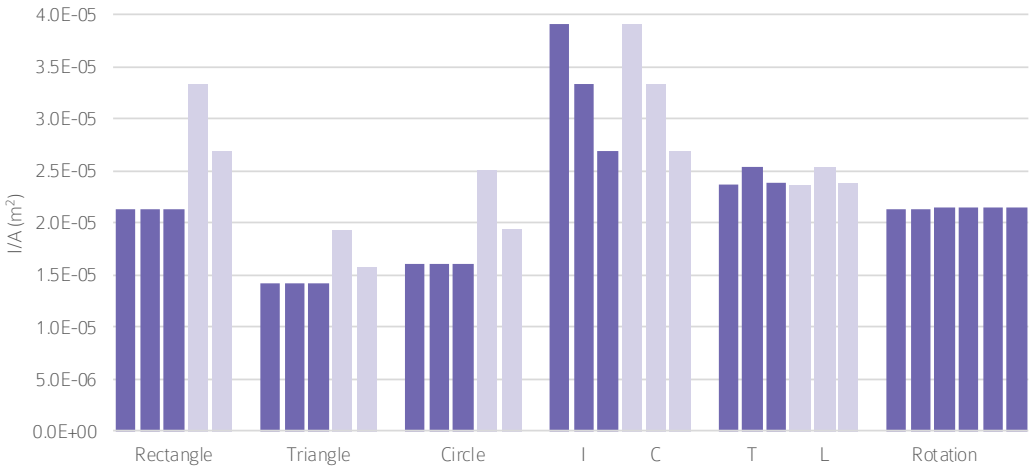

FIGURE 33 // Section profiles evaluated on ratio between second moment of area and area

As expected, the second moment of area for the solid rectangular, triangular and circular sections, does not change because shrinking the section in width will linear decrease the second moment of area. The hollow sections are performing better, because material around the neutral axis is removed. Material far from the neutral axis will contribute more to the second moment of area.

This effect is demonstrated by the I-beams and C-beams, which are essentially rectangular hollow sections but with one vertical element removed. Especially the variants with large flanges are performing best. Removing one of the flanges results in T-beams and L-beams which are structurally performing worse.

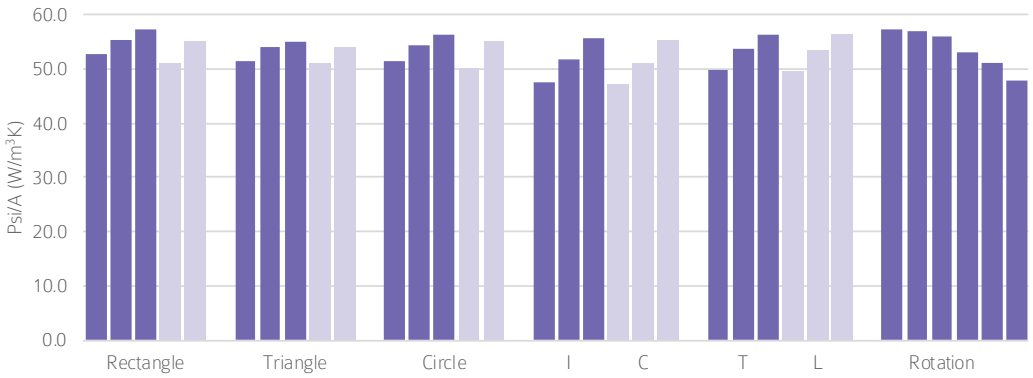

FIGURE 34 // Section profiles evaluated on ratio between psi-value and area

A low bar is a thermally better performing section. Apparently, a very slim section like 2x16mm as used during previous analysis, does perform relatively bad. This means that a 4x16mm profile does conduct less than two times the energy. Making it relatively better. In this case, the rotation of the beam does have a positive effect on its psi-value. The longer path of conduction leads to a better psi-value/area ratio.

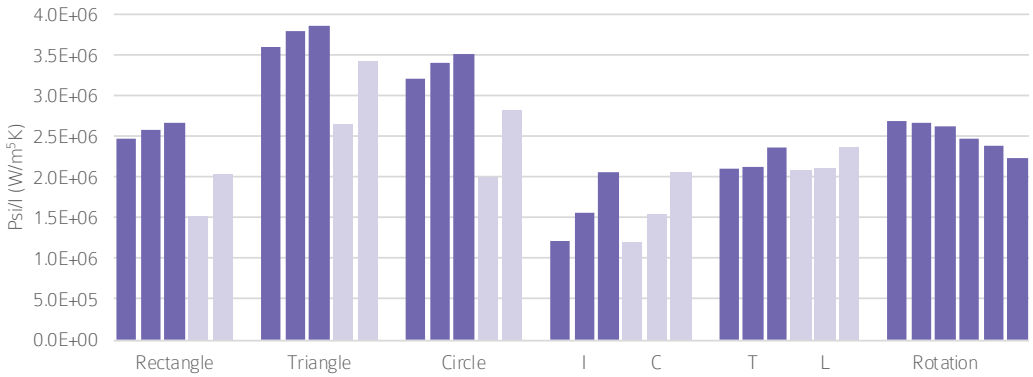

FIGURE 35 // Section profiles evaluated on ratio between psi-value and second moment of area

In the end it comes down to the most efficient use of material. The graph above shows the ratio between psi-value/second moment of area. Which looks in shape very similar to the psi-value/area ratio. The height of the bars is however inversely proportional to the second moment of area/area. Sections that do score well on this ratio are also efficient regarding psi-value/second moment of area. This can be explained by the fact that when optimizing the second moment of area, material will be pushed as far from the neutral axis as possible. For an I-beam, the amount of material around the neutral axis is minimalized, leading to less conduction through the web.

4.4 CAVITY RESISTANCE IMPROVEMENTS

Until now, each configuration is calculated based on a cavity filled with air and uncoated glass. In paragraph 4.2.2, regular tessellations show a certain balance between radiation blocked and heat conducted by the ribs. Nowadays, commercial insulating glass units are commonly coated and filled with a noble gas to improve thermal performance. In order to identify the effect of noble gasses and coated glass, the experiment described in paragraph 4.2.2 is repeated while changing the cavity resistance according to the formulas described in paragraph 2.1.2.

When applying a coating, only the emissivity of one of the glass panes will drop from 0.875 to 0.05 leading to a lower resultant emissivity of 0.0496 instead of 0.778 when no coating is applied.

Earlier calculations used the simplified formula from NEN-EN-ISO 6946 to determine the heat transfer coefficient for both conduction and convection. In order to calculate the heat transfer coefficient for argon, the Grasshof and Nusselt number are determined first. The characteristic length required for Grasshof and Nusselt number, in order to calculate the heat transfer coefficient, is set to be the maximum height of a cavity. This results in a slight inaccurate value which is higher than the true value, because convection increases with the height of a cavity.

g (m/s²)	ß	v (m²/s)	d (m)	ΔT (K)	λ (W/mK)
9.81	0.0035	1.43e-5	0.016	10	0.017

TABLE 26 // Input values to calculate Grasshof and Nusselt numbers

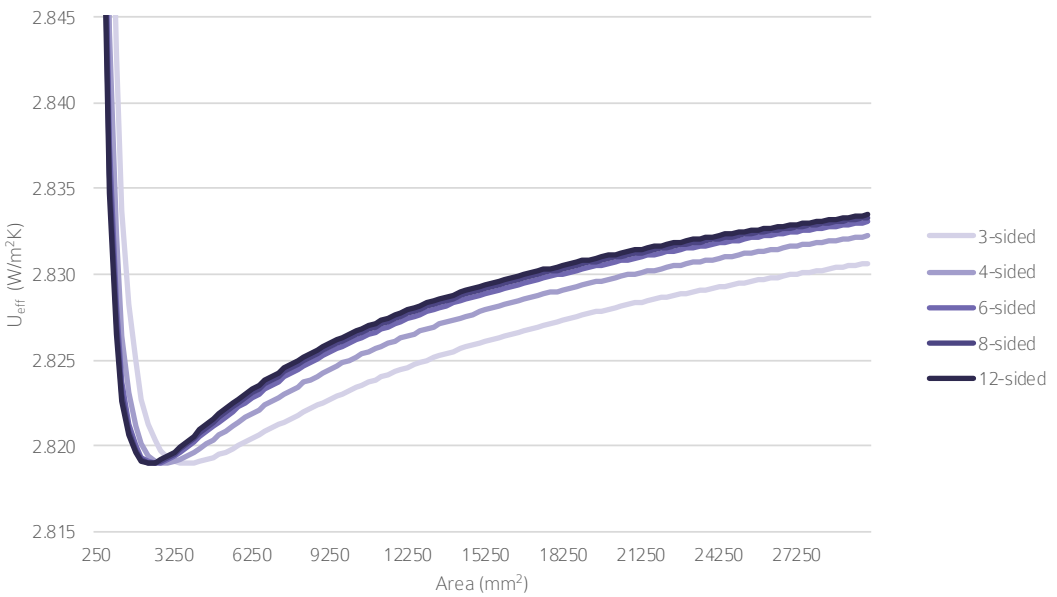

FIGURE 36 // Air-filled and uncoated, sizes of polygons in relation to U-value

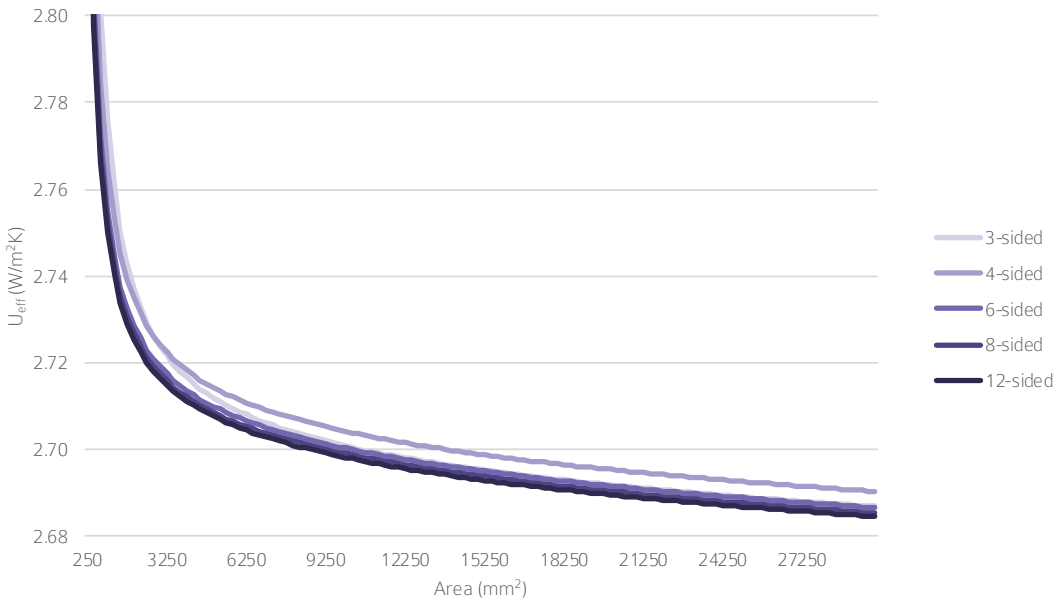

FIGURE 37 // Argon-filled and uncoated, sizes of polygons in relation to U-value

The combined convective and conductive heat transfer coefficient of argon is around a third less of that of air. This means the cavity resistance is improved and the difference in thermal conductivity of the cavity in comparison to the ribs is improved. Around 3000 mm^2 there is still a noticeable change in effective U-value, but in case of argon this value keeps decreasing due to the increased resistance of the cavity. Meaning that for this panel cell sizes should be maximized regarding thermal performance. Structural performance would become the limiting factor.

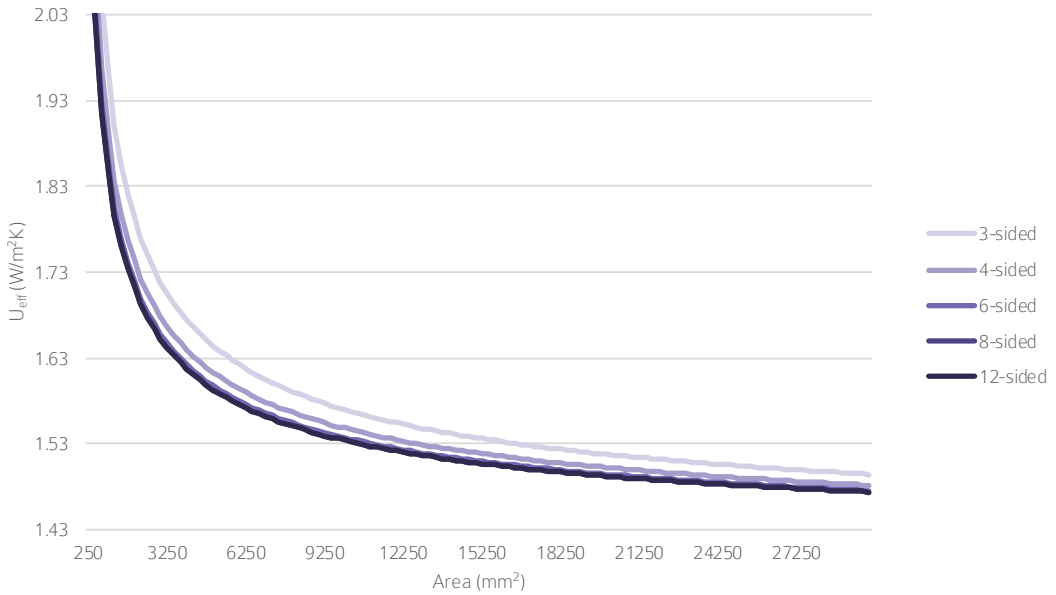

FIGURE 38 // Air-filled and coated, sizes of polygons in relation to U-value

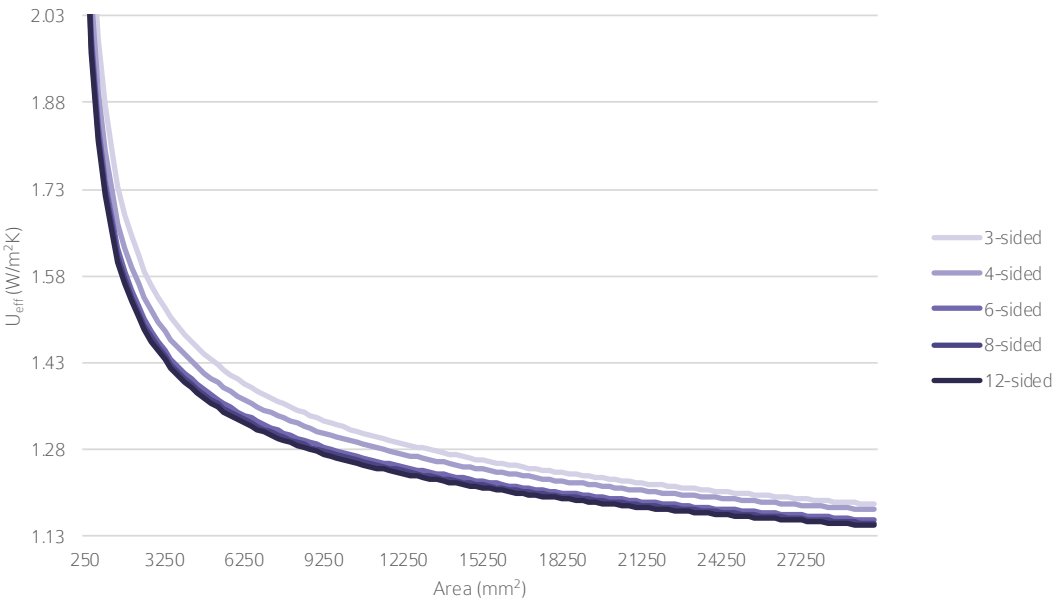

FIGURE 39 // Argon-filled and coated, sizes of polygons in relation to U-value

A coating reduces the effective U-value nearly by 50% compared to uncoated and air-filled. When choosing between coating and noble gas filling. Reducing radiation should be first priority, because this has a bigger effect on the cavity resistance.

Filling the cavity with argon reduces the conductivity even more. When applying a coating, the radiation blocked by the ribs is not important, conductivity through the ribs is far more prominent. That is the reason that when applying a coating, the perimeter-area ratio of a cell is much more important. Therefore, the U-values correlate to the amount of sides of the polygon.

In order to reach an average U-value of 1.65 W/m^{2}K regarding all doors, windows and frames (Bouwbesluit 2015) an argon filling is insufficient, but a coating only would be sufficient to reach that goal. In order to reach 1.2 W/m^{2}K, a coated and argon-filled unit requires a square pattern with sides of only 160mm. The advantage of a square or rectangular pattern is that there are no or very limited cut-off cells at the edges. Note that in the calculations a coating with emissivity 0.05 is used, which is a high performance coating.

4.5 CONCLUSION

Material

Although commercial structural sandwiches are often made from aluminium, stainless steel or fibre reinforced polymers. The conductivity values of the first two are above 16 W/mK, which is undesired for a façade. It probably will result in a very cold inside glass sheet during winter, which could result to condensation of the thin glass sandwich. Fibre reinforced polymers are aesthetically not an option and are non-extrudable. PETG, PA and PLA are all three extrudable, recyclable and transparent polymers. PLA is the final choice, because it has a lower thermal conductivity, better resistance against UV and has the lowest embodied energy of all three.

Macro

Regular and semiregular tessellations are investigated. Size is the most important factor affecting the radiative component through the cavity and the conduction through the ribs. There are virtually no differences between regarding the U-value. U-value for all patterns reaches 2.8190 W/m^{2}K. What does make a difference is the amount of sides. Polygons with more sides reach their optimum earlier, but in the long run will perform less than their counterparts with less sides.

Semiregular tessellations are less effective than regular tessellations. The tessellations with cells around the same size do perform better than tessellations with large variations in cell sizes. This ensures that the individual cells are performing at its best at the same time. With large size differences in cells, the optima of the individual cells are not happening at the same time and therefore losing efficiency. The best performing semiregular tessellations are the 3.3.3.4.4 pattern and 4.4.3.3.4 pattern. Which both reach a U-value of 2.8209 W/m^{2}K

Both tessellations come close to the Planibel Clearlite with a U-Value of 2.756 W/m^{2}K. But because elongation will change the radiative component different than the conductivity component, a third experiment is carried out featuring an elongated rectangle. This is the most pragmatic way of picking the best vertical spacing while minimizing the conduction by removing horizontal dividers. This method proved very successful regarding thermal performance, the optimum vertical spacing converges to 22mm. Wider than 640mm will not increase thermal performance, the optimum converges to a U-value of 2.811 W/m^{2}K.

When applying a coating and filling the cavity with a noble gas the U-value drops significant. It even drops below the value of 1.65 W/m^{2}K required for a Dutch building permit. The ribs are not necessary to block radiation in this case, but the conduction through them becomes the most important factor affecting the U-value.

Design rule
Regarding structural performance, designers tend to put more material at regions with high stresses than at regions with low stresses. Regarding thermal performance, it is advised to take also the shape of these cells in consideration. Horizontal elongated cells with a height between 35mm and 22mm do increase thermal performance.

When the cavity is filled with argon and glass is coated, the vertical spacing does not matter as much. In that case, conduction through the ribs is the most important factor affecting the U-value. Therefore, cell sizes should be maximized and structural performance would be the limiting factor. Horizontal elongated cells are still beneficial, they are not necessary to block radiation but they limit the convection within the cavity.

Micro

The actual bridge to one side to the other will influence directly how much energy will be flowing. Based on the absolute numbers, the amount of material used for the bridge is more important than the contact surface at both sides of the bridge.

A thermal bridge with a good ratio of second moment of area/area will likely also be well performing regarding thermal insulation. I-beams and C-beam of 16mm in width proved to be the best performing sections regarding psi-value/second moment of area while solid triangles and circles (although they do have less contact surface) are among the worst performing.

Design rule
Regarding the selection of beams for thermal bridges, it is important to choose in the first place for beams with the best matching second moment of inertia. Second step is to choose a beam which has an optimal second moment of area/area ratio, like I-beams.

ENERGY CONSUMPTION EVALUATION V

5.1 SETUP

The parameter study delivers a direction on how to get a better thermal performance regarding the panel only. This energy model is a fictional office building in the Netherlands. First experiment identifies the effects of lower and higher U-values of windows in buildings and to what extent parameters as glazing percentage, R-value of walls, internal heat load and heat capacity do change the energy demand. Second experiment evaluates the elongated rectangles with vertical spacing of 22mm from previous chapter against a regular glass unit. In order to answer the research question, energy use during production is compared to energy use during lifetime.

For both experiments, grasshopper ladybug and honeybee are used for an energy calculation. A weather file of Amsterdam (062400_IWEC) is used to simulate a moderate maritime climate.

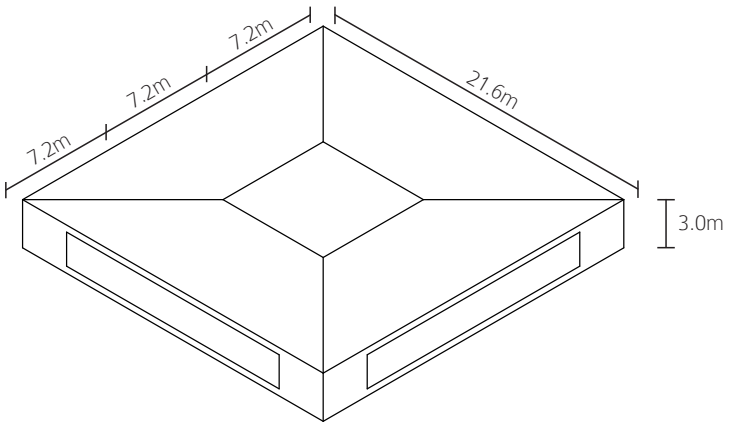

FIGURE 40 // Energy model dimensions

Partition walls are placed diagonally to the core in order to calculate the effects per façade and the floorplan behind it. These partition walls consist of three layers.

	Gypsum	Mineral wool	Gypsum
Thickness (mm)	25	100	25
Density (kg/m^3)	800	20	800
Conductivity (W/mK)	0.17	0.035	0.17
Specific heat (J/kgK)	1090	1000	1090

TABLE 27 // Settings for partition walls

Top and bottom faces, are modelled as adiabatic faces. Which means that no energy is lost through the top and bottom. Energy can only escape to the outside by flowing through the façade.

The occupancy of the building is between 9am and 5pm from Monday to Friday. At these times a internal load of 30 W/m^2 is applied for people, lighting and equipment. During occupancy the set points for HVAC are determined according to EN15251 (2007) which dictates a setpoint of 20^{o}C during winter as the limit for the heating to switch on. During summer, 26^{o}C is the limit for the cooling to switch on. The HVAC is purely theoretical, the result is calculated as an ideal air load. Meaning that the efficiency of the HVAC is not taken into account, but only the heating and cooling demand in kWh. Therefore, absolute values are most certainly off.

ASHRAE Standard 62.1-2007 prescribes a default occupancy of 1 person per 20 m^2 and a ventilation rate of 0.36 l/s/m^2 when the actual occupancy is not known. No natural ventilation is applied.

Different configurations are taken into consideration to create an overview of what affects the heat loss of the building. Each of these configurations is measured with a window of 2 W/m^{2}K and of 4 W/m^{2}K. Four parameters are introduced to create several configurations.

- The percentage of glass in the façade, 25% of glazing is a very closed façade while 75% of glazing represents a modern office with large glass surfaces. No sun shading is applied.
- The R-value of the closed façade, which will affect also the heat flow through windows, because heat will always choose the way with the least resistance. A value of 3.5 m^{2}K/W was the R-value required under the old building code in the Netherlands. A value of 10.5 m^{2}K/W is representing an energy neutral office building.
- The internal heat load, which will change the heating and cooling demand. 15 W/m^2 is an office building with a low occupancy, led lighting and people working on laptops. 45 W/m^2 represents an office building with high occupancy, fluorescent lighting and people working on advanced desktops with multiple screens.
- The heat capacity of closed facades, floor and ceiling. 5cm represents a lightweight structure like a wooden and gypsum structure. 15cm represents a heavy structure. The values for the concrete are a density of 2000 kg/m^3 and 750 J/kgK for specific heat.

5.2 OPERATIONAL ENERGY

5.2.1. Benchmark energy model

The dashed line indicates the average kWh per month. Annually 22.1 kWh/m^2 for windows with U-value of 2 W/m^{2}K and 38.4 kWh/m^2 for windows with a U-Value of 4 W/m^{2}K. Although the U-value doubles, the energy demand raises roughly 1.75 times. This is expected because thermal losses and gains are not only dictated by the windows only. Typical numbers for offices are more around 75-100 kWh/m2 for heating and cooling combined (Enerdata, 2012;MonumentPlace, 2014). Which means this number is around three times off.

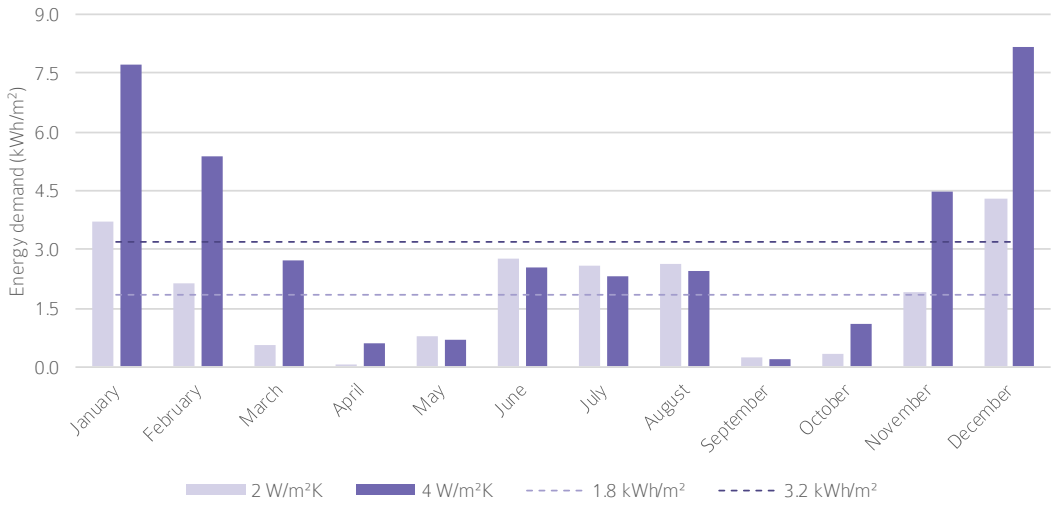

Glazing (%)	R-value (m²K/W)	Heat load (W/m²)	Heat capacity (cm)
50	7.0	30	10

FIGURE 41 // Monthly energy demand for benchmark energy model

A building with windows with a U-value of 4 W/m²K do loses his energy faster, therefore the energy demand in winter situation is much higher, because during occupancy the building needs to be at least 20°C. Especially around March this results in an energy demand of over three times more. In summer this is an advantage because heat which is build up throughout the day is released during night. Which causes the cooling demand to be a little lower during May till August.

5.2.2. Alternative energy models

When looking at the annual results, in each and every case, a window with U-value 4 W/m²K does significantly contribute to a higher thermal load. The first row of percentages does indicate this difference. When the glazing percentage is 75%, the difference between a U-value of 4 W/m²K and a U-value of 2 W/m²K increases to 84%

Glazing percentages do have the biggest impact, secondly the internal load is a major factor. Based on this information, heating demand is more important than cooling demand. The total thermal load throughout the year is decreased when internal load is higher.

Added thermal capacity and insulation do affect the thermal demand, but not as much as the two other factors. The glazing percentage gives the biggest range in differences between 4 W/m²K and 2 W/m²K. Therefore, it is the most interesting one to use for further research. The next step will show, if a lower production energy can counterbalance the decreased thermal performance.

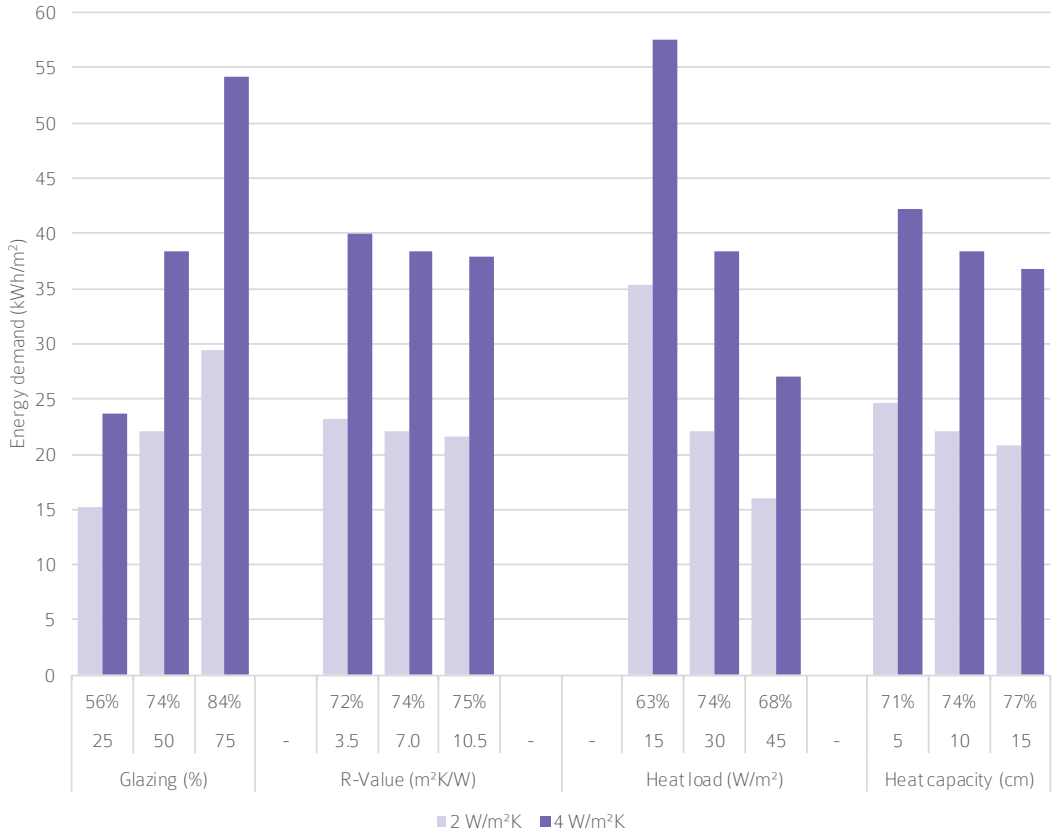

Glazing (%)	R-value (m²K/W)	Heat load (W/m²)	Heat capacity (cm)
25	7.0	30	10
50	7.0	30	10
75	7.0	30	10
50	3.5	30	10
50	7.0	30	10
50	10.5	30	10
50	7.0	15	10
50	7.0	30	10
50	7.0	45	10
50	7.0	30	5
50	7.0	30	10
50	7.0	30	15

FIGURE 42 // Annual energy demand for alternative energy models, elaboration in appendix 9.4

5.3 EMBODIED ENERGY

This part is dedicated to formulate an answer to the research question. Can a thin glass sandwich panel, reduce more energy during production then it will increase during use, compared to regular insulated glass units?

As a reference is taken the Planibel Clearlite with a U-value of 2.756 W/m^{2}K. The best performing thin sandwich is filled with a PLA tessellation consisting of horizontal louvres with a vertical spacing of 22mm. Resulting in an U-value of 2.811 W/m^{2}K. Because these values are close together, only embodied energy needs to be determined.

	Insulating Glass Unit	Thin Glass Sandwich
Glass total thickness (mm)	12	1
Glass type density (kg/m^3)	2500	2430
Glass type embodied energy (MJ/kg)	10.6	13.9
Window embodied energy (MJ/kg)	318.0	33.8

TABLE 28 // Comparison embodied energy of glass per square meter window

For the glass production of a square meter thin glass sandwich only 11% of the energy is needed compared to an insulating glass unit. This makes sense, because the most energy is required for heating the raw materials to its melting temperature. With the same volume of glass, a much larger can be covered with thin glass.

Not only does the PLA contribute to the conductivity of the panel, it also requires energy to produce. The vertical spacing of the ribs is 22mm, thickness 2mm and depth 16mm.
-Density of PLA is 1255 kg/m^3
-Embodied energy of PLA is 55.4 MJ/kg
-Extruding energy for PLA is 5.9 MJ/kg

PLA (%)	8.90
PLA (m^3/m^2)	1.14e-3
Embodied energy PLA (MJ/m^2)	98.99
Embodied energy extruding (MJ/m^2)	10.54
Embodied energy sandwich (MJ/m^2)	143.3

TABLE 29 // Embodied energy for PLA infill

Production energy is only 45% for a thin glass sandwich, compared to a regular insulating glass unit. It is the amount of PLA which contributes most to the embodied energy of a thin glass sandwich. Still, the total amount of embodied energy is lower than for regular glass units.

Regarding thermal performance, a comparison with a commercial regular glass unit of U-value 1.1 W/m^{2}K is made. For this comparison, the glazing percentage is chosen to evaluate because a glazing percentage of 25% will give the smallest difference between high and low U-value. A glazing percentage of 75% will give the biggest difference between high and low U-value.

Glazing percentage (%)	25	50	75
Energy demand IGU (kWh/m^2/year)	19.06	26.88	35.85
Energy demand TGS (kWh/m^2/year)	27.59	44.48	62.95
Δ Energy demand (kWh/m^2/year)	8.53	17.60	27.11
Δ Energy demand (MJ/m^2/year)	30.72	63.37	97.58

TABLE 30 // Differences in energy demand for insulating glass units and thin glass sandwiches

The savings per square meter of window need to be converted to square meters of floor area.

Glazing percentage (%)	25	50	75
Glazing area (m^2)	64.8	129.6	194.4
Δ Embodied energy (MJ/m^2)	24.25	48.52	72.78

TABLE 31 // Savings for embodied energy per square meter floor area

This makes clear that an uncoated thin glass sandwich filled with air cannot compete with a modern glass unit with U-value 1.1 W/m^{2}K. Already in one year the amount of embodied saved by the thin glass sandwich is lost through the window. Note that this is a very conservative calculation, in practice this difference is probably higher. Because the expected lifetime of an insulated glass unit is around 20 years, U-value is more important than saving energy in the production process.

5.4 CONCLUSION

The energy model does give an indication but regarding accuracy, a few aspects need to be mentioned. Only thermal loads are calculated. Efficiency of the HVAC is a major factor in order to meet de heat and cold demands. By excluding this, operational energy lacks accuracy. The energy model also lacks accuracy for the glazed parts. Glass sheets cannot be produced in the sizes which are now used in the energy model. In real world the glazed parts would be subdivided by window frames. Spacers would be put around the edges. These factors are not taken into account by this energy model.

Regarding the embodied energy, spacers are also not taken into account. It also is restricted to primary production only. Assembling the windows into commercial units and transporting them to the building site is excluded. Assembling the windows would cost more energy for the thin glass sandwiches because more types of materials are used in that configuration. Transport would require more energy for heavy regular insulating glass units compared to thin glass sandwiches.

Compared to an uncoated and air filled insulating glass unit, a thin glass sandwich does save more than half of the embodied energy and is therefore a viable solution. When comparing to a coated and krypton filled glass unit, the savings in embodied energy are already lost during the first year by the extra demand in heating and cooling.

The material of the structure within the cavity will likely conduct more energy than the cavity itself. The conductive component through the ribs will be even more important when cavity resistance is increased. Therefore, thin glass sandwiches should not be considered for saving energy. They do however save twelve times the amount of raw materials for glass, which means less environmental damage is done. It does use PLA, but that is only 8.9% of the cavity, volumetric seen less material is used. Furthermore, the panels are significantly lighter to transport and install on the building site.

DIGITAL DESIGN VI

6.1 CONTEXT

After the fire of May 2008, which destroyed the Faculty of Architecture, architecture firm Braaksma & Roos designed a new masterplan for the old main building of the TU Delft. In order to create a creative and lively atmosphere for the architecture students, they came up with the concept of a street. This street connects all building wings, to a coherent 'city' with closed rooms like studios and open functions like the library and restaurant. Additionally to this concept, two large 'conservatories' are placed over the courtyards.

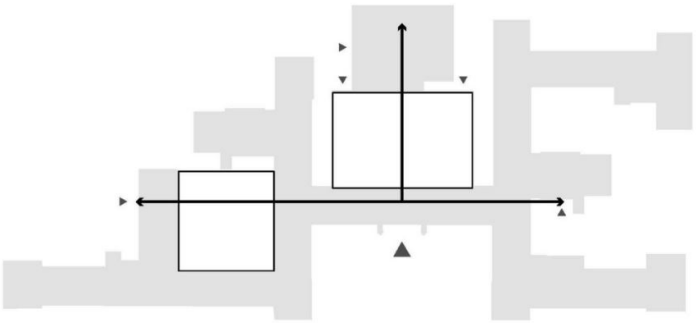

FIGURE 43 // Floorplan of TU Delft (BraaksmaRoos, n.d.)

In this diagram left, is called the orange hall. A space of 2500m^2 covered by a large spaceframe. Light is coming in by rooflights and a full glazed southeast façade. Due to the large vertical span, a vertical truss provides the necessary strength and stiffness. A secondary steel structure in horizontal direction carries load from the curtain wall to the trusses.

IMAGE 04 // View on the curtain wall (BraaksmaRoos, n.d.)

6.2 DESIGN CRITERIA

The aim of this design is to see how thin glass units can be applied in the built environment. Minimum requirements are based on Dutch regulations regarding glass in facades. Like regular glass units, the cavity itself should be air and water tight, as well the façade in total.

Size

The insulated glass units of this curtain wall measure 1250x1250mm and are foursided supported. The cavity within the glass is restricted to 16mm, avoiding convection. To reach the optimum thermal performance a horizontal louvre system is chosen with a vertical spacing of 22mm.

Structural

Stresses should not exceed the limits of PLA and the glass. According to design code NEN2608, the centre of a glazing element should not deflect more than its span diagonally divided by 65. The edge of a glazing element should not deflect more than its span divided by 200.

$$Deflection\ centre = \sqrt{1250^2+1250^2} / 65 = 27mm$$
$$Deflection\ edge = 1250 / 200 = 6.25mm$$

	PLA	Glass
Tensile strength (MPa)	47	41.9
Compressive strength (MPa)	66	850

TABLE 32 // Structural limits of PLA and aluminosilicate glass (CES, 2018)

Thermal insulation

Minimum requirement for thermal insulation is an average U-value of 1.65 W/m^{2}K regarding all doors, windows and frames. (Bouwbesluit, 2015). Based on this research, it is already known this requirement will not be met with a regular glass unit or thin glass sandwich.

Aesthetics

Because this panel is significantly lighter than the original glazing, the concept is to create also a curtain wall system which is very transparent and visual lightweight. The original structure of the curtain wall is removed and a new system is made on top of the primary steel structure.

In detail, the spacer at the edge of the glass which makes the cavity air and water tight also has a structural function. 'Wings' of the curtain wall do hold these panels invisible. This results in small mullions between the glass panels. Only the rubber elements making the façade elements water tight are visible from the outside. Inside these rubber elements the draining is applied. Big rubber elements at the inside, hiding behind the spacer ensure air thightness.

6.3 INTEGRATED DESIGN

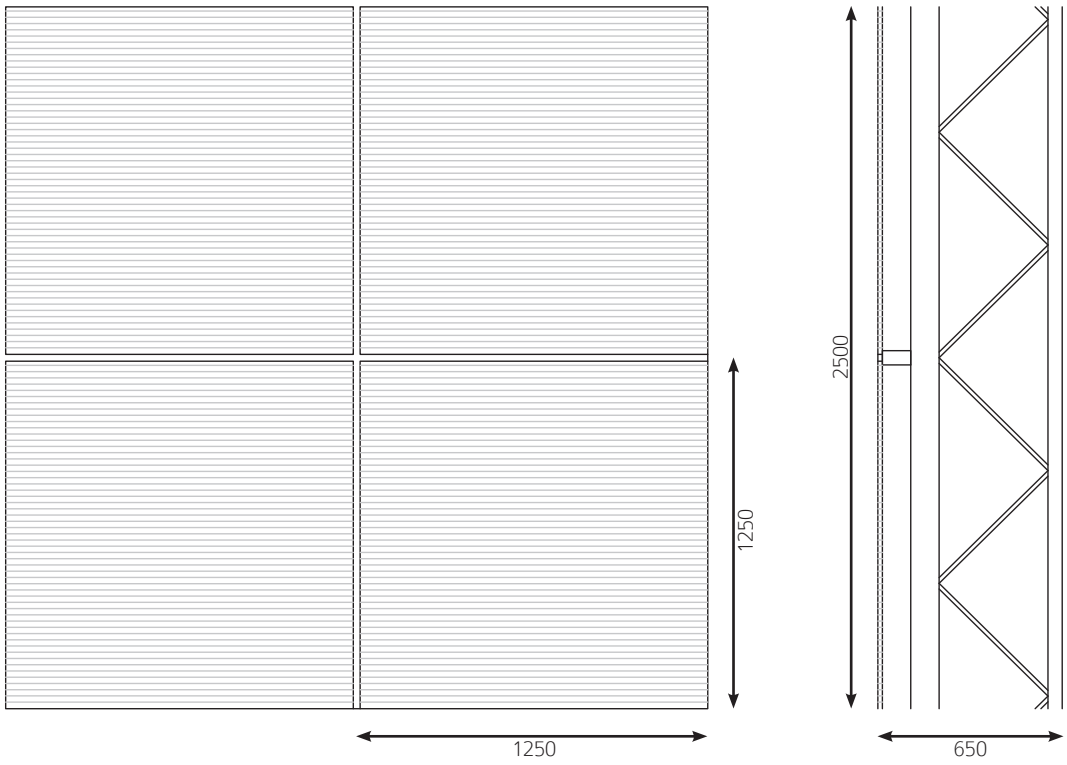

FIGURE 44 // Façade fragment 1:20 and detail 1:5

IMAGE 05 // Interaction between sun and louvre pattern (BraaksmaRoos, n.d.)

6.4 STRUCTURAL VERIFICATION

A simulation in Diana FEA verifies the structural aspects of this new designed panel. It focusses on the panel itself and considers the edges of the inner glass sheet as supports which are fixed for a translation in XYZ direction. Meshtype is hexa/quad with linear interpolation, mesh size 8mm.

	PLA	Glass
Shell thickness (mm)	2	0.5
Dimensions (mm)	16x1250	1250x1250
Young's modulus (GPa)	3.5	77
Poisson ratio	0.39	0.23
Density (kg/m^3)	1255	2500

TABLE 33 // Material settings regarding finite element analysis (CES, 2018)

Structural verification is done two times, one time for the service limit state (SLS) and another for verifying the ultimate limit state (ULS). Regarding SLS, based on NEN-EN 1991-1-4+A1+C2:2011 a wind load of 800 N/m^2 is equally distributed over the front face. Gravity force is also applied. Regarding ULS both gravity and wind load are multiplied by 1.3 as a safety factor. Both edge and centre displacement do not exceed their maximum. Also stresses are within the boundaries of the materials used. Therefore both ULS and SLS are successful verified.

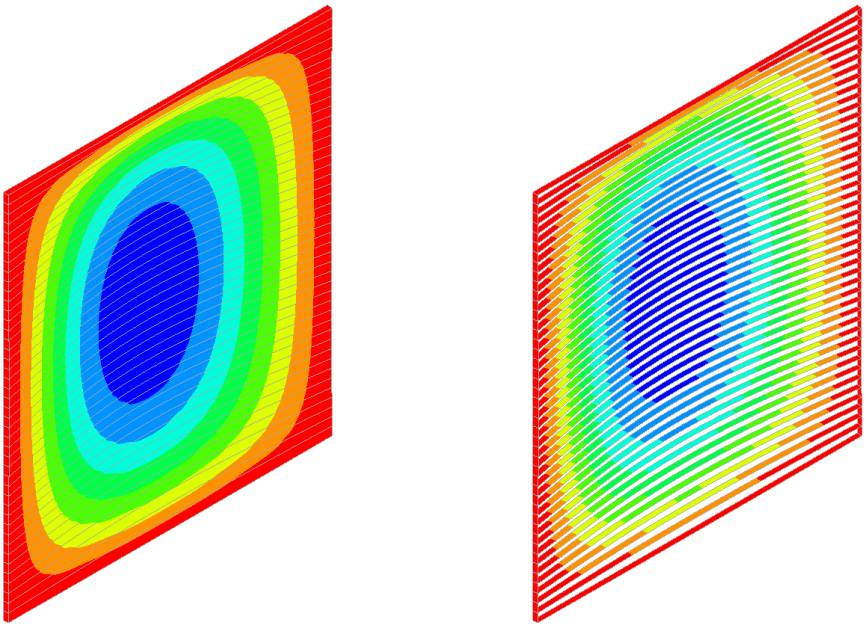

FIGURE 45 // Maximum displacement of 5.67mm for both glass and ribs

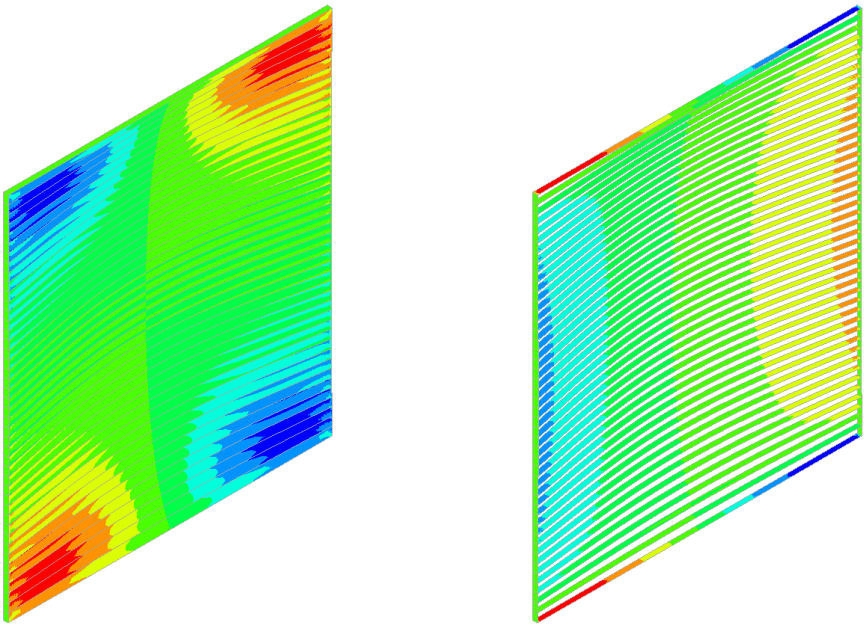

FIGURE 46 // Principal stresses glass range -10.7 to 10.7 MPa, principal stresses ribs range -1.73 to 1.73 MPa

6.5 EVALUATION

Multiple companies do investigate possibilities to bring windows to the next level. A few trends are: filling the cavity with solid material, limiting energy use by removing gas from the cavity, limiting material use by selectively replacing thick glass by thin glass.

Core

Nowadays noble gas fillings are common in the building industry. Okalux is a company that has multiple products which incorporates materials and structures within the cavity. Some of them are pure aesthetic like stone inserts. Others like capillary inserts which add to the thermal insulation, but also disperse daylight deep into the room while offering sun and glare-protection. Metal and wood inserts do not add thermal insulation but block radiation and protect against glaring. OKA-freeD is their new invention, where they try to commercialize 3D printed inserts (Okalux, 2018).

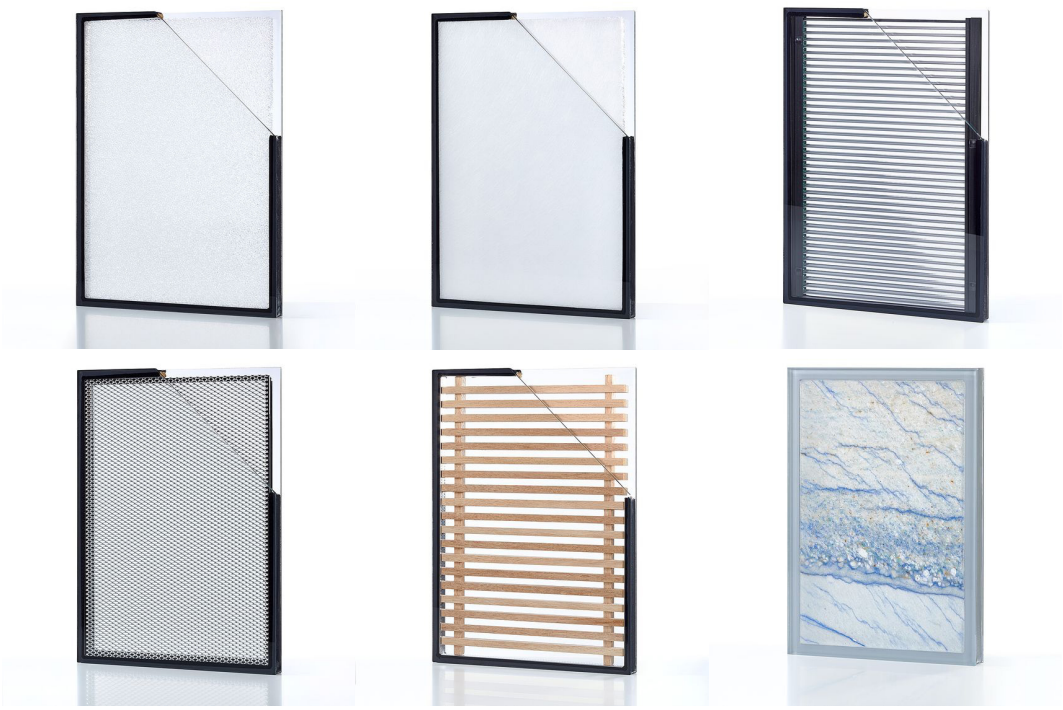

IMAGE 06 // Various glass units with cavity inserts (Okalux, 2018)

Vacuum

Recently AGC (2018) presented Fineo, a new type of vacuum units. Their claim is to have excellent thermal and acoustic insulation properties as good, or even better than triple glazing. By having only two panes of glass, it also has a very high light transmission. Due to the cavity of only 0.1 mm the total thickness of this unit is less than 7mm.

IMAGE 07 // AGC Fineo with U-value 0.7 W/m^{2}K (AGC, 2018)

When comparing Fineo with the thin glass sandwich, the thickness of only 7mm is remarkable; considering the researched thin glass sandwich is already 17mm. However, vacuuming thin glass is not possible, because it is very flexible. This would result in imploding panels where the two sheets of glass will touch each other. A similarity between vacuum glass and the thin glass sandwich is the use of spacers. Due to the conduction of the spacers, the glass sheets do have spots where temperature is significantly different. Therefore, condensation can occur as a pattern.

Quadruple glazing

Adding multiple layers of regular glass does have a few challenges. A significant increase in weight, which is more difficult to install on site. The increase in weight is also a challenge for mechanical properties of the spacers, how to ensure mechanical stability? The addition of a fourth layer results in a lower light transmission. MEM4WIN (2012) is an organisation which invented a quadruple glazing unit with six thin glass panes. The outer panes consist of two laminated thin glass panes, where the cavities are also separated by thin glass. The laminated panes avoid the need of an additional structure to ensure wind load can be handled. The three cavities filled with argon result in an impressive U-value of only 0,3 W/m^{2}K which is an R-value of 3.3 m^{2}K/W

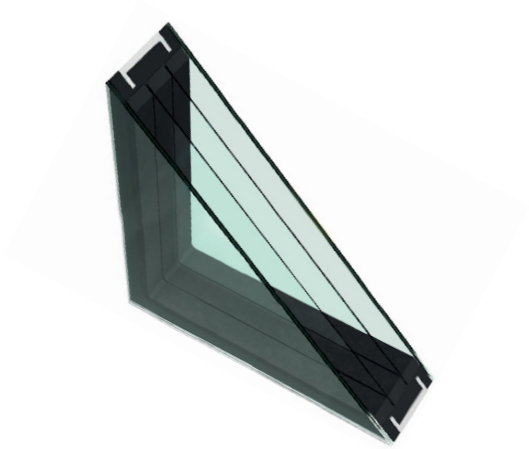

IMAGE 08 // Quadruple thin glass (MEM4WIN, 2012)

CONCLUSIONS & RECOMMENDATIONS VII

7.1 CONCLUSIONS

What are the physical properties of thin glass?

Thin glass brings new opportunities to redesign façade elements which are made stronger by chemical strengthening and lighter in weight. Due to its thickness and flexibility it is not stiff enough to use as a single sheet.

What are the characteristics of different structural sandwiches?

Sandwiches are well known in the aircraft industry for providing stiffness, but they come with the disadvantage of conducting energy from one side to another. Multiple possibilities for enhancements both on structural and thermal performance bring a façade sandwich element within reach. According to the literature review, hexagonal honeycomb cores are most efficient regarding weight-load ratio. Because sandwich and glass need to be connected, for either glue or welding a line-based contact is preferred above point-based contact, this makes the connection more secure. Regarding thermal performance, the bi-directional grid encloses cavities of air. This could reduce convection even more. Regarding solar control, it might be possible to block radiation.

How is thermal flow calculated in structural sandwiches?

Each of the evaluated calculation methods has its pros and cons. The simple analytical calculation is fast and accurate, but does not include the psi-value of a section. This makes it unreliable when the cross-section changes to a different shape, which is not symmetric or constant in thickness. The numerical method is very accurate, certainly when the mesh size is small. At the other hand it requires more time to calculate in comparison with arithmetic methods. The detailed analytical calculation is the golden mean. This formula includes the psi-value of a cross-section, but is still fast and arithmetic solvable. It is however less accurate when calculating small cells. Probably because the influence of each edge overlaps with the influence of another edge within the same cell, something that is not taken into account.

How do macro and micro geometric distributions affect thermal flow?

Regular and semiregular tessellations are investigated. Size is the most important factor affecting the radiative component through the cavity and the conduction through the ribs. Polygons with more sides reach their optimum earlier, but in the long run will perform less than their counterparts with less sides. Semiregular tessellations are less effective than regular tessellations. The tessellations with cells around the same size do perform better than tessellations with large variations in cell sizes. This ensures that the individual cells are performing at its best at the same time. With large size differences in cells, the optima of the individual cells are not happening at the same time and therefore losing efficiency. Horizontal elongated cells are providing even better thermal performance by blocking a large part of the radiation, preventing convection and minimizing edges and therefore conduction.

When applying a coating and filling the cavity with a noble gas the U-value drops significant. It even drops below the value of 1.65 W/m^{2}K required for a Dutch building permit. The ribs are not necessary to block radiation in this case, but the conduction through them becomes the most important factor affecting the U-value.

The actual bridge from one side to the other will influence directly how much energy will be flowing. Based on the absolute numbers, the amount of material used for the bridge is more important than the contact surface at both sides of the bridge. A bridge with a good ratio of second moment of area/area will likely also be a well performing bridge regarding thermal optimization. I-beams and C-beams of 16mm in width proved to be the best performing sections regarding the psi-value/second moment of area ratio, while solid triangles and circles (although they do have less contact surface with the glass) are among the worst performing.

To what extent can a thin glass sandwich, compared to regular glass units, counterbalance its decreased thermal performance by reducing energy consumption during production?
The energy model is a very simplified model and should be interpreted as a preliminary study. But with that restriction, compared to an uncoated and air filled insulating glass unit, a thin glass sandwich does save more than half of the embodied energy and is therefore a realistic alternative.

When comparing to a coated and krypton filled glass unit. The savings in embodied energy are already lost during the first year by the extra demand in heating and cooling. Coating and filling the thin glass sandwich with krypton will not compensate for that.

The material of the structure within the cavity will likely conduct more energy than the cavity itself. The conductive component through the ribs will be even more important when cavity resistance is increased. Therefore, thin glass sandwiches should not be considered for saving energy. They do however save twelve times the amount of raw materials for glass, which means less environmental damage is done. It does use PLA, but that is only 8.9% of the cavity, volumetric seen less material is used. Furthermore, the panels are significantly lighter to transport and install on the building site.

7.2 RECOMMENDATIONS

Using coatings and noble gasses

This research focusses on uncoated glass an air-filled cavity. This lead to a balance between radiation and conduction through a thin glass sandwich. This is possible because radiation is a relatively large factor in the total equation. The use of noble gasses and coatings is briefly described, but but further research should investigate more in depth how coatings will affect the radiation. Not only that but also the production process of glass sandwiches will change when coatings are applied. Bonding methods need to be discussed. The air filled cavities do already have a larger resistance when coatings are applied. This could be enlarged by filling the cavity with noble gasses like argon or krypton. In that case the sealing around the edges should be improved to prevent noble gasses leaking and therefore reduce the thermal performance. Both options, coatings and noble gasses, combined will improve the total thermal performance but limiting the conduction through the ribs will be even more important.

Material distribution in elevation

This research discusses only the cross-section of the thermal bridges or ribs. When coatings and noble gasses are applied further optimization of the ribs is necessary. One direction could be to also remove material from the web. Castellated beams for example would limit conduction even further without decreasing structural performance much. Material should be removed around the neutral axis to be most effective. It is important to understand that modifying the ribs in elevation will also have an effect on the amount of radiation blocked by the ribs. When there is no coating applied to the glass, this will have a bigger impact in comparison to coated glass sheets. This will also affect the cavity resistance as described in paragraph 2.1.2

Aspects for commercial product

Before a thin glass sandwich can be applied on a commercial scale, several subjects like durability, acoustics, safety and security would be necessary to research. How does PLA behave under elevated temperatures or even fire? Sound or acoustics is relevant because by limiting the amount of glass, a lot of the original weight is removed. Because mass will dampen sound, the assumption is that thin glass sandwiches will perform worse. Additional research is needed to find ways how even with low mass these kind of windows can still provide acoustic comfort.

Accurate energy model and embodied energy

As pointed out in the conclusion, the energy model and calculations for embodied energy lack accuracy and should therefore be used and interpreted as preliminary model. In order to better understand what can be saved regarding energy a more detailed model is required.

REFERENCES IIX

Abrisa. (2015). Annealing vs. tempering - Glass strengthening. Retrieved 22 May 2019, from: https://abrisatechnologies.com/2015/04/annealing-vs-tempering-glass-strengthening/

Abrisa. (2016). Technical note: Heat tempering vs. heat strengthening. Retrieved 22 May 2019, from: https://abrisatechnologies.com/2016/04/Heat-Temper-vs-Heat-Strengthening.pdf

Balkow, D. (2012). Glass as a building material. In C. Schittich (Ed.), Glass Construction Manual (pp. 60-89). Berlin: Walter de Gruyter.

BraaksmaRoos. (n.d.) BK city, Delft: een bruisende onderwijsomgeving, Retrieved 22 May 2019, from: http://www.braaksma-roos.nl/project/bk-city/

Branz. (2017). Extraction and manufacture of glass. Retrieved 22 May 2019, from: http://www.level.org.nz/fileadmin/downloads/Materials/LevelMGlass.pdf

BusinessWire. (2017). Flat glass market- Forecasts and analysis by Technavio. Retrieved 22 May 2019, from: https://www.businesswire.com/news/home/20170907006557/en/Flat-Glass-Market---Forecasts-Analysis-Technavio

Campbell, F.C. (2006). Manufacturing Technology for Aerospace Structural Materials. Amsterdam: Elsevier.

CES (2018). Granta Design Limited.

Corning. (n.d.a). How it works: Corning's glass fusion process. Retrieved 22 May 2019, from: https://www.corning.com/worldwide/en/innovation/the-glass-age/science-of-glass/how-it-works-cornings-fusion-process.html

Corning. (n.d.b). The secret of tough glass: ion exchange. Retrieved 22 May 2019, from: https://www.corning.com/worldwide/en/innovation/the-glass-age/science-of-glass/the-secret-of-tough-glass-ion-exchange.html

EcolineWindows. (n.d.). How modern windows benefit from noble gas. Retrieved 22 May 2019, from: https://www.ecolinewindows.ca/gas-fill-important-feature-in-modern-windows/

Econcore. (n.d.). Classification of sandwich core materials. Retrieved 22 May 2019, from: http://www.econcore.com/en/classification

EfficientWindows. (n.d.). Window technologies: Low-E coatings. Retrieved 22 May 2019, from: https://www.efficientwindows.org/lowe.php

Enerdata. (2012). Energy efficiency trends in buildings. Lessons from the odyssee mure project.

Evans, A.G. (2001). Lightweight Materials and Structures. MRS bulletin, 26(10), 790-797.

GlassEurope. (n.d.). Recycling of end-of-life building glass. Retrieved 22 May 2019, from: https://glassforeurope.com/recycling-of-end-of-life-building-glass/

Gomez, S., Dejneka, M.J., Ellsion, A.J., & Rossington, K.R. (2011). A look at the chemical strengthening process: Alkali Aluminosilicate Glasses vs. Soda-Lime Glass. In C.H. Drummond (Ed.), 71st conference on glass problems: ceramic engineering and science proceedings (pp. 61-66). New York: John Wiley & Sons

Granta. (2011). Thermal properties. Retrieved 22 May 2019, from: http://inventor.grantadesign.com/en/notes/attributes/material/thermal_properties.html

Heide, J. van der, Vreemann, H.L., & Haytink, T.G. (2016). Onderzoek innovatieve opties BENG (Bijna EnergieNeutrale Gebouwen). Retrieved 22 May 2019, from: https://www.rvo.nl/sites/default/files/2017/03/Onderzoek%20innovatieve%20opties%20BENG.pdf

Hexcel. (2000). Honeycomb sandwich design technology. Retrieved 22 May 2019, from: https://www.hexcel.com/content_media/raw/Honeycomb_Sandwich_Design_Technology.pdf

Jingglass. (n.d.) Energy saving low-e glass. Retrieved 22 May 2019, from: http://www.jingglass.com/product/Energy-Saving-Low-e-Glass.html

Kolb, K.E. (2016). Glass composition. Retrieved 22 May 2019, from: http://www.chemistryexplained.com/Ge-Hy/Glass.html

Mansour. (n.d.) Monolithic glass: Annealed float glass. Retrieved 22 May 2019, from: https://mansourglass.jo/index.php/monolithic-glass/

MonumentPlace. (2014). An energy efficient building. Retrieved 22 May 2019, from: http://www.monument-place.co.uk/2014/01/Monument_Place_energy_leaflet.pdf

Persistence Market Research. (2017). Global market study on flat glass: automotive and solar applications expected to remain lucrative segments during 2017-2025. Retrieved 22 May 2019, from: https://www.persistencemarketresearch.com/market-research/flat-glass-market.asp

PhysicsClassroom. (n.d.). Light absorption, reflection and transmission. Retrieved 22 May 2019, from: https://www.physicsclassroom.com/class/light/u12l2c.cfm

Pilkington. (2007). Student Information Pack. Retrieved 22 May 2019, from: https://www.pilkington.com/resources/studentpackversionmar2007.pdf

Pilkington. (2010). Glass Handbook. Retrieved 22 May 2019, from: http://www.pilkington.com/resources/glasshandbook2010english.pdf

RVO. (n.d.). MilieuPrestatie Gebouwen. Retrieved 22 May 2019, from: https://www.rvo.nl/onderwerpen/duurzaam-ondernemen/gebouwen/wetten-en-regels-gebouw-en/nieuwbouw/milieuprestatie-gebouwen

Sadeghi, G., Sani, R. M., & Wang, Y. (2015). Symbolic Meaning of Transparency in Contemporary Architecture: An Evaluation of Recent Public Buildings in Famagusta. Current Urban Studies, 3(4), 385-401.

Schott. (n.d.). Ultra-Thin Glass. Retrieved 22 May 2019, from: https://www.us.schott.com/advanced_optics/english/products/wafers-and-thin-glass/glass-wafer-and-substrates/ultra-thin-glass/index.html

Schott. (2014). Technical Glasses Physical and Chemical properties. Retrieved 22 May 2019 from: https://www.us.schott.com/d/tubing/1.0/schott-brochure-technical-glasses_us.pdf

Staib, G. (2012). From the origins to classical modernism. In C. Schittich (Ed.), Glass Construction Manual (pp. 10-29). Berlin: Walter de Gruyter.

Schittich, C. (2012). Glass architecture from the Modern Movement to the present day. In C. Schittich (Ed.), Glass Construction Manual (pp. 30-57). Berlin: Walter de Gruyter.

Trendmarine. (n.d.) Chemical Toughening. Retrieved 22 May 2019, from: http://www.trendmarine.com/glass-technology/chemical-toughening/

Rawn, E. (2014). Material Masters: Glass is more with Mies van der Rohe. Retrieved 22 May 2019, from: https://www.archdaily.com/material-masters-glass-is-more-with-mies-van-der-rohe

Valdevit, L., Hutchinson, J.W., & Evans, A.G. (2004). Structurally optimized sandwich panels with prismatic cores. International Journal of solids and structures, 41(18-19), 5105-5124.

Veer, F.A., Janssen, M.J.H.C., & Nägele, T. (2005) The possibilities of glass bond adhesives. Conference proceedings - Glass Processing Days, Tampere.

Wallender, L. (2019). How to tell if a window seal has failed. Retrieved 22 May 2019, from: https://www.thespruce.com/how-to-tell-if-a-window-seal-has-failed-1822894

Weller, B., Unnewehr, S., Tasche, S., & Härth, K. (2009).
Glass in building: principles, applications, examples. Berlin: Walter de Gruyter.

Wurm, J. (2007). Glass Structures. Design and construction of self-supporting skins.
Basel: Birkhäuser.

Zeegers, A. (2006). Warmte, warmtetransport, thermische isolatie. In A.C. van der Linden (Ed.), Bouwfysica (pp. 2-21). Utrecht/Zutphen: ThiemeMeulenhoff.

APPENDICES IX

9.1 DATASHEETS

Datasheet AGC Planibel Clearlite

LIGHT		ENERGY	
TRANSMISSION	81	SOLAR FACTOR	77
REFLECTION	14	REFLECTION	13

THERMAL PROPERTIES	EN 673
Ug [W/(m².K)] - Vertical	2.7

LIGHT PROPERTIES	EN 410
Light transmittance - τ_v (%)	81
Light reflectance - ρ_v (%)	14
Internal light reflection - ρ_{vi} (%)	14
Colour Rendering - RD65 - R_a (%)	98

ENERGY PROPERTIES	EN 410	ISO 9050
Solar factor (g-value) - g (%)	77	77
Energy Reflection - ρ_e (%)	13	13
Internal Energy Reflection - ρ_{ei} (%)	13	
Direct Energy Transmission - τ_e (%)	73	72
Solar abs. Glass 1 - α_e (%)	8	9
Solar abs. Glass 2 - α_e (%)	6	6
Total Energy absorption - α_e (%)	14	15
Shading coefficient - SC	0.89	0.88
UV Transmission - UV (%)	49	
Selectivity	1.05	1.05

OTHER PROPERTIES	
Resistance to fire - EN 13501-2	NPD
Reaction to fire - EN 13501-1	NPD
Bullet resistance - EN 1063	NPD
Burglar resistance - EN 356	NPD
Pendulum body impact resistance - EN 12600	NPD / NPD

ACOUSTIC PROPERTIES	
Direct airborne sound insulation (dB) (Rw (C;Ctr) - ESTIMATED) - dB	32 (-1; -3) (2)

THICKNESS AND WEIGHT	
Nominal thickness (mm)	28.00
Weight (kg/m²)	30

Source: www.yourglass.com

Datasheet AGC Falcon Glass

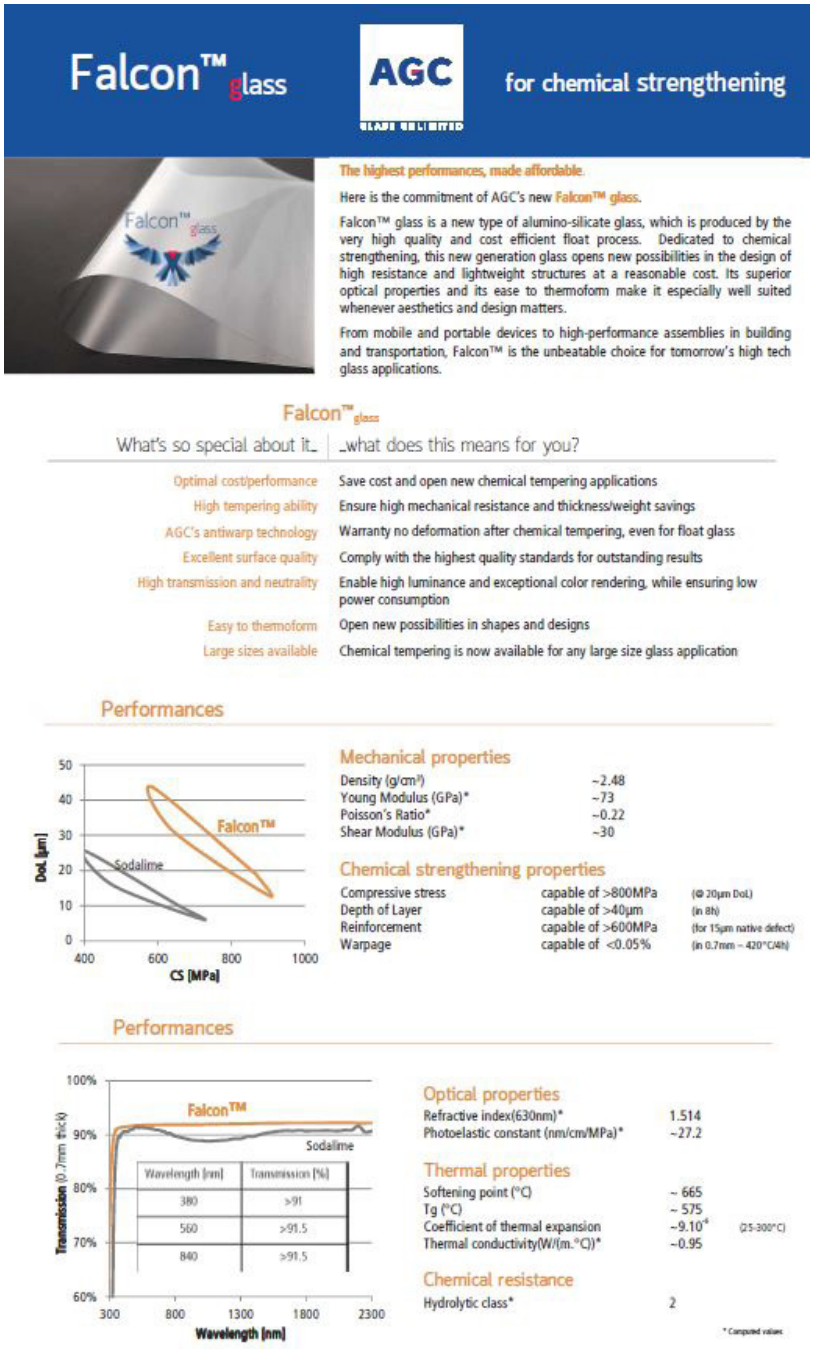

Source: www.agc-yourglass.com

Datasheet CORNING Gorilla Glass

CORNING
Gorilla® Glass

Corning® Gorilla® Glass 5 – Corning's latest glass design was formulated to address breakage – the greatest concern of consumers, according to Corning's research. The new glass is just as thin and light as previous versions, but has been formulated to deliver dramatically improved damage resistance allowing improved in-field performance. Corning® Gorilla® Glass 5 has been tested for performance when subjected to sharp contact damage.

Product Information

Benefits

- Improved drop performance
- High retained strength after use
- High resistance to scratch and sharp contact damage
- Superior surface quality

Applications

- Ideal protective cover for electronic displays in:
  - Smartphones
  - Laptop and tablet computer screens
  - Mobile devices
- Touchscreen devices
- Wearable devices

Dimensions

Available Thickness 0.4mm – 1.3mm

Viscosity

Softening Point ($10^{7.6}$ poises)	884 °C
Annealing Point ($10^{13.2}$ poises)	623 °C
Strain Point ($10^{14.7}$ poises)	571 °C

Properties

Density	2.43 g/cm³
Young's Modulus	76.7 GPa
Poisson's Ratio	0.21
Shear Modulus	31.7 GPa
Vickers Hardness (200g load)	
Unstrengthened	601 kgf/mm²
Strengthened	638 kgf/mm²
Fracture Toughness	0.69 MPa $m^{0.5}$
Coefficient of Expansion (0-300°C)	78.8 x 10^{-7}/°C

Chemical Strengthening

Compressive Stress Capability	≥ 850 MPa
Depth of Compression Capability	≥ 75 µm

Optical

Refractive Index (590 nm)

Core Glass*	1.50
Compression Layer	1.51
Photo-elastic constant	30.1 nm/cm/MPa

*Core index is used for FSM-based measurements since it is unaffected by ion-exchanged conditions.

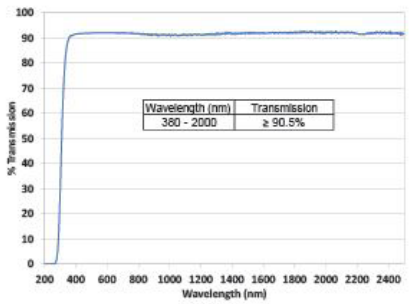

Chemical Durability

Durability is measured via weight loss per surface area after immersion in the solvents shown below. Values are highly dependent upon actual testing conditions. Data is reported for Corning® Gorilla® Glass 5.

Reagent	Time	Temperature (°C)	Weight Loss (mg/cm2)
HCl – 5%	24 hrs.	95	5.9
NH4F:HF – 10%	20 min.	20	1.0
HF – 10%	20 min.	20	25.2
NaOH – 5%	6 hrs.	95	2.7

Electrical

Frequency (MHz)	Dielectric Constant	Loss Tangent
54	7.08	0.009
163	7.01	0.010
272	7.01	0.011
381	7.00	0.010
490	6.99	0.010
599	6.97	0.011
912	7.01	0.012
1499	6.99	0.012
1977	6.97	0.014
2466	6.96	0.014
2986	6.96	0.014

Terminated coaxial line similar to that outlined in NIST Technical Notes 1520 and 1355-R.

Source: www.corning.com

Datasheet SCHOTT Xensation Cover

SCHOTT Xensation® Cover

SCHOTT's chemically strengthened alumino-silicate glass for innovative glazing solutions

Xensation® Cover is a floated alumino-silicate glass that offers an outstanding level of mechanical impact and bending strength, as well as high resistance to scratches. This specialty glass has been designed for highly efficient chemical strengthening (via an ion exchange treatment) to achieve strength performance levels ideally suited for cover glass protecting touch screen devices, as well as protective and ruggedized light-weight glazing solutions.

Key-Benefits of Xensation® Cover

- Extremely **high impact and bending strength** enables thinner, sleeker and more sensitive devices without compromising on strength
- **High scratch resistance and tolerance** for superior aesthetic appeal and durability
- Pristine, display grade cover glass for a clear, elegant **visual quality**
- Unique glass composition results in the most **robust and reliable** cover glass available
- **Easy to process** according to typical industry standards

Thermal Properties	
Thermal Conductivity $\lambda_{(25\,°C)}$	0.96 W/(m·K)
Specific Heat Capacity $C_{p(20\,°C;\,100\,°C)}$	0.84 KJ/(Kg·K)
Coefficient of Mean Linear Thermal Expansion $\alpha_{(20\,°C;\,300\,°C)}$	8.8 · 10^{-6} K^{-1}*
Transformation Point Tg	615 °C*
Annealing Point (10^{13} dPas)	635 °C
Softening Point ($10^{7.6}$ dPas)	880 °C
Working Point (10^{4} dPas)	1265 °C

cooled according to DIN

Chemical Properties		
Hydrolytic Resistance	DIN ISO 719	Class HGB 1
Acid Resistance	DIN 12116	Class S 4
Alkali Resistance	DIN ISO 695	Class A 1

Optical Properties			
Refractive Index at	**588 nm (n_d)**	**633 nm**	**780 nm**
Core Glass	1.508	1.506	1.502
Compression Layer			
KNO_3 pure	1.516	1.514	1.510
Transmittance τ (Glass Thickness 0.7 mm)			
840 nm			> 91.5 %
560 nm			> 91.5 %
380 nm			> 90 %
Photoelastic Constant			29.2 nm/cm/MPa

Sheet Dimensions	
Sheet Size*:	1150 x 950 mm
	475 x 575 mm
Thickness Range:	0.5 - 3.0 mm

* other sizes on request

Mechanical Properties	
Density	2.477 g/cm³*
Young's Modulus E	74 kN/mm²
Poisson's Ratio	0.215
Shear Modulus	30 kN/mm²
Knoop Hardness $HK_{0.1/20}$	
Non-strenghtened	534
Strengthened	639
Vickers Hardness $HV_{0.2/20}$	
Non-strengthened	617
Strengthened	681

* cooled according to DIN

Chemical Strengthening	
Compressive Stress	capable > 900 MPa
Depth of Layer	capable > 50 µm
4-Point Bending Strength	cap. > 800 MPa

Source: www.schott.com

Datasheet PETG

Tensile Properties ASTM D638 - Type V		
Property	**Imperial**	**Metric**
Toughness*	3.5 ft·lb/in2	7.3 KJ/m2
Tensile Modulus	304,579 psi	2.1 GPa
Ultimate Tensile Strength	6640 psi	45.8 MPa
Tensile Strength at Yield	7690 psi	53 MPa
Elongation at Yield	14%	14%
Elongation at Break	18%	18%
3D Printing Properties		
Property	**Imperial**	**Metric**
Expected Max Linear Print Speed	2.36 in/s	60 mm/s
Hardness, **ASTM D2240**	85D	85D
Solid Density, **ASTM D792**	4.66 x 10-2 lb/in3	1.29 g/cc
Impact Properties		
Property	**Imperial**	**Metric**
Notched Izod (machined), 23 C, **ASTM D256**	1.5 f·lb/in	80 J/m
Gardner Impact, 23 C, **ASTM D3029**	26.7 ft·lb	36 J
Thermal Properties		
Property	**Imperial**	**Metric**
Glass Transition by DSC, **ASTM E1356**	180 F	82 C
Glass Transition by DMA, **ASTM D792**	176 F	80 C
Heat Deflection Temperature, **ASTM D648**	163 F	73 C
Coefficient of Thermal Expansion, **ASTM E832**	38 x 10-6 in/in°F	68 x 10-6 m/m·K
Heat Capacity, **ASTM E1269**	0.29 Btu/lb·°F	1200 J/kg·K
Thermal Conductivity, **ASTM C518**	2.0 Btu·in/hr/ft²/°F	0.29 W/m·K
Available Colors		
Black, Blue, Clear, Green, Grey, Orange, Red, White		
Suggested Uses		
PETG is a great material for high impact mechanical parts that may be subjected to moderate heat loads. This material is more wear and impact resistant than ABS while still being very cost effective for production printing applications.		

*Toughness is not defined in ASTM D638 though can be calculated by taking the integral of the stress-strain curve collected by tensile data.

Source: www.sd3d.com

Datasheet DELO

Technical data

Color cured in a layer thickness of approx. 0.1 mm	colorless clear
Density [g/cm³] at room temperature (approx. 23 °C)	1.0
Viscosity [mPas] at 23 °C, Brookfield spindle/rpm 4/5	20000
Minimal curing time [s] DELO Standard 23, UVA intensity: 60 mW/cm², DELOLUXcontrol	7
Minimal curing time [s] DELO Standard 23, LED 400nm, intensity: 200 mW/cm², DELOLUXcontrol	3
Compression shear strength glass/glass [MPa] DELO Standard 5 UVA intensity: 55 - 60 mW/cm², DELOLUXcontrol, irradiation time: 60 s	28
Compression shear strength glass/Al [MPa] DELO Standard 5 UVA intensity: 55 - 60 mW/cm², DELOLUXcontrol, irradiation time: 60 s	25
Compression shear strength glass/PC [MPa] DELO Standard 5 UVA intensity: 55 - 60 mW/cm², DELOLUXcontrol, irradiation time: 60 s	15
Compression shear strength glass/PMMA [MPa] DELO Standard 5 UVA intensity: 55 - 60 mW/cm², DELOLUXcontrol, irradiation time: 60 s	4
Compression shear strength PC/Al [MPa] DELO Standard 5 UVA intensity: 55 - 60 mW/cm², DELOLUXcontrol, irradiation time: 60 s	5
Compression shear strength PC/PC [MPa] DELO Standard 5 UVA intensity: 55 - 60 mW/cm², DELOLUXcontrol, irradiation time: 60 s	18
Compression shear strength PMMA/PMMA [MPa] DELO Standard 5 UVA intensity: 55 - 60 mW/cm², DELOLUXcontrol, irradiation time: 60 s	10
Tensile strength [MPa] according to DIN EN ISO 527	20

Source: www.delo-adhesives.com

9.2 CALCULATION METHODOLOGY

In theory the last measured result from the half an hour readings is the most reliable one, because of a stable temperature. At the other hand heat flux from both sensors should be the nearly identical. Calibration for heat flux sensors: 60.76 V/(W/m^2) outside, 62.23 V/(W/m^2) inside.

Int. Box	Ext. Box	Inside	Outside	Inside	Outside	Inside	Outside	Average	Average
T (°C)	T (°C)	T (°C)	T (°C)	U (mV)	U (mV)	q (W/m^2)	q (W/m^2)	q (W/m^2)	U (W/m^{2}K)
48.6	23.4	39.2	27.7	3.28	3.85	54.05	61.93	57.99	5.04
48.6	23.4	41.3	32.5	3.62	3.77	59.61	60.52	60.06	6.83
48.2	23.4	39.8	32.6	3.80	3.60	62.48	57.88	60.18	8.36
48.6	23.3	40.5	32.9	3.96	3.58	65.21	57.50	61.35	8.07
48.8	23.3	40.7	32.4	4.06	3.57	66.82	57.40	62.11	7.48
49.0	23.3	40.9	32.6	4.17	3.57	68.63	57.30	62.97	7.59
49.1	23.3	41.1	32.6	4.26	3.56	70.05	57.24	63.64	7.49

Empty, last measurement

Int. Box	Ext. Box	Inside	Outside	Inside	Outside	Inside	Outside	Average	Average
T (°C)	T (°C)	T (°C)	T (°C)	U (mV)	U (mV)	q (W/m²)	q (W/m²)	q (W/m²)	U (W/m²K)
47.1	22.6	36.2	27.7	3.01	3.79	49.47	60.97	55.22	6.50
47.5	22.6	37.9	29.3	3.06	3.85	50.39	61.90	56.15	6.53
47.6	22.5	38.6	29.9	3.37	3.80	55.40	61.10	58.25	6.70
47.8	22.6	38.9	30.0	3.52	3.75	57.93	60.23	59.08	6.64
47.9	22.6	39.1	30.3	3.67	3.70	60.34	59.39	59.86	6.80
47.9	22.5	39.2	30.4	3.85	3.63	63.33	58.30	60.82	6.91
47.9	22.4	39.4	30.4	4.06	3.57	66.89	57.30	62.09	6.90

Hexagonal cell, measurement with small delta between heat flux sensors

Int. Box	Ext. Box	Inside	Outside	Inside	Outside	Inside	Outside	Average	Average
T (°C)	T (°C)	T (°C)	T (°C)	U (mV)	U (mV)	q (W/m²)	q (W/m²)	q (W/m²)	U (W/m²K)
46.2	22.1	38.1	29.7	3.94	4.28	64.91	68.78	66.84	7.96
46.5	22.4	38.7	29.6	3.99	3.98	65.60	63.92	64.76	7.12
47.0	22.4	39.5	29.7	3.98	4.11	65.50	66.11	65.81	6.71
47.3	22.4	40.2	29.8	3.99	4.15	65.73	66.72	66.23	6.37
47.4	22.4	40.5	29.8	4.07	4.16	66.92	66.85	66.88	6.25
47.4	22.4	40.7	29.8	4.09	4.17	67.38	67.01	67.19	6.16
47.5	22.4	40.7	29.8	4.08	4.17	67.22	66.95	67.08	6.15

Hexagonal knot, last measurement

Int. Box	Ext. Box	Inside	Outside	Inside	Outside	Inside	Outside	Average	Average
T (°C)	T (°C)	T (°C)	T (°C)	U (mV)	U (mV)	q (W/m²)	q (W/m²)	q (W/m²)	U (W/m²K)
47.3	22.5	36.9	28.7	3.18	4.08	52.37	65.60	58.98	7.19
47.5	22.6	39.0	30.5	3.41	4.21	56.16	67.62	61.89	7.28
47.6	22.5	39.4	30.8	3.56	4.17	58.53	67.01	62.77	7.30
47.6	22.5	39.5	30.8	3.63	4.13	59.78	66.37	63.07	7.25
47.6	22.5	39.7	31.0	3.69	4.10	60.76	65.95	63.36	7.28
47.6	22.5	39.8	31.2	3.78	4.07	62.24	65.34	63.79	7.42
47.6	22.5	39.8	31.2	3.83	4.05	63.03	65.02	64.03	7.44

Hexagonal element, last measurement

Int. Box	Ext. Box	Inside	Outside	Inside	Outside	Inside	Outside	Average	Average
T (°C)	T (°C)	T (°C)	T (°C)	U (mV)	U (mV)	q (W/m²)	q (W/m²)	q (W/m²)	U (W/m²K)
47.5	23.0	39.6	31.8	3.56	3.92	58.56	62.93	60.74	7.79
47.8	23.0	39.8	31.8	3.64	3.91	59.94	62.77	61.35	7.67
47.9	23.0	39.8	31.9	3.68	3.91	60.53	62.77	61.65	7.80
47.9	23.0	40.0	31.9	3.71	3.92	61.03	62.99	62.01	7.66
48.1	23.1	40.1	32.0	3.71	3.93	61.06	63.09	62.07	7.66
48.2	23.1	40.3	32.0	3.74	3.93	61.59	63.12	62.35	7.51
48.2	23.1	40.3	32.0	3.76	3.94	61.95	63.35	62.65	7.55

Square cell, last measurement

Int. Box	Ext. Box	Inside	Outside	Inside	Outside	Inside	Outside	Average	Average
T (°C)	T (°C)	T (°C)	T (°C)	U (mV)	U (mV)	q (W/m²)	q (W/m²)	q (W/m²)	U (W/m²K)
48.5	23.1	38.6	29.9	3.20	4.10	52.73	65.82	59.28	6.81
48.7	23.1	39.6	30.5	3.56	3.96	58.56	63.60	61.08	6.71
48.7	23.1	40.0	30.7	3.78	3.86	62.24	62.00	62.12	6.68
49.0	23.1	40.3	31.0	3.98	3.77	65.54	60.65	63.09	6.78
49.0	23.1	40.3	31.0	4.12	3.71	67.84	59.62	63.73	6.85
49.0	23.1	40.7	31.0	4.22	3.68	69.39	59.07	64.23	6.62
49.1	23.1	40.7	31.2	4.29	3.66	70.54	58.75	64.64	6.80

Square knot, average of all values, because of too much fluctuation: 62.50 W/m² and 6.75 W/m²K

Int. Box	Ext. Box	Inside	Outside	Inside	Outside	Inside	Outside	Average	Average
T (°C)	T (°C)	T (°C)	T (°C)	U (mV)	U (mV)	q (W/m²)	q (W/m²)	q (W/m²)	U (W/m²K)
48.6	23.1	38.9	31.2	3.60	3.67	59.32	58.97	59.15	7.68
48.7	23.3	40.2	32.7	3.76	3.70	61.95	59.39	60.67	8.09
48.8	23.3	40.7	33.0	3.92	3.65	64.48	58.72	61.60	8.00
48.8	23.3	40.8	32.6	3.89	3.61	63.99	58.04	61.02	7.44
48.8	23.4	40.9	32.1	4.16	3.59	68.43	57.62	63.03	7.16
48.8	23.3	41.1	33.4	4.13	3.56	67.94	57.21	62.57	8.13
48.7	23.5	41.1	33.4	4.21	3.54	69.32	56.95	63.14	8.20

Square element, average of selected values, because thermocouple came loose: 62.00 W/m² and 8.10 W/m²K

Int. Box	Ext. Box	Inside	Outside	Inside	Outside	Inside	Outside	Average	Average
T (°C)	T (°C)	T (°C)	T (°C)	U (mV)	U (mV)	q (W/m²)	q (W/m²)	q (W/m²)	U (W/m²K)
48.5	23.4	37.6	29.1	2.73	3.86	45.00	62.03	53.51	6.30
48.8	23.4	39.8	30.4	3.09	4.05	50.79	65.05	57.92	6.16
49.1	23.3	40.6	30.9	3.42	3.98	56.32	63.96	60.14	6.20
49.1	23.3	41.1	31.3	3.69	3.88	60.76	62.29	61.52	6.28
49.1	23.3	41.3	31.5	3.88	3.79	63.79	60.90	62.35	6.36
49.1	23.3	41.4	31.5	4.00	3.72	65.77	59.81	62.79	6.34
49.2	23.3	41.6	31.6	4.14	3.68	68.10	59.17	63.64	6.36

Triangular cell, measurement with small delta between heat flux sensors

Int. Box	Ext. Box	Inside	Outside	Inside	Outside	Inside	Outside	Average	Average
T (°C)	T (°C)	T (°C)	T (°C)	U (mV)	U (mV)	q (W/m²)	q (W/m²)	q (W/m²)	U (W/m²K)
48.7	22.6	38.7	29.4	3.59	4.27	59.05	68.68	63.87	6.87
48.7	22.6	39.4	29.9	3.64	4.31	59.91	69.29	64.60	6.80
48.8	22.4	40.1	30.7	3.84	4.22	63.20	67.78	65.49	6.97
48.8	22.8	40.3	30.8	4.02	4.15	66.10	66.72	66.41	6.99
48.8	22.6	40.5	31.0	4.04	4.08	66.46	65.50	65.98	6.95
49.0	22.6	40.7	31.4	4.15	3.99	68.33	64.15	66.24	7.12
49.0	22.6	40.8	31.5	4.21	3.94	69.29	63.25	66.27	7.13

Triangular knot, measurement with small delta between heat flux sensors while temperature is stable

Int. Box	Ext. Box	Inside	Outside	Inside	Outside	Inside	Outside	Average	Average
T (°C)	T (°C)	T (°C)	T (°C)	U (mV)	U (mV)	q (W/m²)	q (W/m²)	q (W/m²)	U (W/m²K)
49.1	22.6	33.7	28.0	3.46	3.46	56.91	55.60	56.26	9.87
48.8	22.8	38.6	29.8	2.95	4.34	48.58	69.68	59.13	6.72
48.6	22.6	39.6	30.7	2.87	4.37	47.17	70.19	58.68	6.59
48.4	22.8	40.9	31.8	3.75	4.42	61.72	70.99	66.36	7.29
49.0	22.6	41.4	32.1	3.98	4.27	65.54	68.68	67.11	7.22
49.0	22.5	41.6	32.4	4.20	4.15	69.06	66.69	67.87	7.38
49.0	22.6	41.7	32.5	4.32	4.04	71.17	64.98	68.07	7.40

Triangular element, measurement with small delta between heat flux sensors while sensor is attached

9.3 CORE MATERIAL DISTRIBUTION

	Width (m)	Avg. q (W/m^2)	Avg. Q (W)	Δ Q (W)	ψ (W/mK)	I (mm^4)	A (mm^2)
Rectangle 1	0.016	58.5577	8.7837	0.2702	0.0135	5461.33	256
Rectangle 2	0.008	57.6997	8.6550	0.1415	0.0071	2730.67	128
Rectangle 3	0.004	57.2441	8.5866	0.0732	0.0037	1365.33	64
Rectangle 4	0.016	57.5175	8.6276	0.1142	0.0057	3733.33	112
Rectangle 5	0.008	57.3423	8.6014	0.0879	0.0044	2154.67	80
Triangle 1	0.016	57.6317	8.6448	0.1313	0.0066	1820.44	128
Triangle 2	0.008	57.2165	8.5825	0.0690	0.0035	910.22	64
Triangle 3	0.004	56.9910	8.5486	0.0352	0.0018	455.11	32
Triangle 4	0.016	57.3176	8.5976	0.0842	0.0042	1589.79	82.6
Triangle 5	0.008	57.1579	8.5737	0.0603	0.0030	875.96	55.7
Circle 1	0.016	58.1353	8.7203	0.2069	0.0103	3216.99	201.1
Circle 2	0.008	57.4863	8.6230	0.1095	0.0055	1608.50	100.5
Circle 3	0.004	57.1341	8.5701	0.0567	0.0028	804.25	50.3
Circle 4	0.016	57.3441	8.6016	0.0882	0.0044	2199.12	88
Circle 5	0.008	57.2336	8.5850	0.0716	0.0036	1269.07	65
I-beam 1	0.016	57.3139	8.5971	0.0836	0.0042	3445.33	88
I-beam 2	0.008	57.1436	8.5715	0.0581	0.0029	1866.67	56
I-beam 3	0.004	57.0536	8.5580	0.0446	0.0022	1077.33	40
C-beam 1	0.016	57.3089	8.5963	0.0829	0.0041	3445.33	88
C-beam 2	0.008	57.1388	8.5708	0.0574	0.0029	1866.67	56
C-beam 3	0.004	57.0517	8.5578	0.0443	0.0022	1077.33	40
T-beam 1	0.016	57.1542	8.5731	0.0597	0.0030	1423.73	60
T-beam 2	0.008	57.0712	8.5607	0.0472	0.0024	1114.30	44
T-beam 3	0.004	57.0271	8.5541	0.0406	0.0020	858.22	36
L-beam 1	0.016	57.1518	8.5728	0.0593	0.0030	1423.73	60
L-beam 2	0.008	57.0689	8.5603	0.0469	0.0023	1114.30	44
L-beam 3	0.004	57.0262	8.5539	0.0405	0.0020	858.22	36
Rotation 1	0.002	57.0012	8.5502	0.0367	0.0018	682.67	32
Rotation 2	0.005	57.0027	8.5504	0.0370	0.0018	691.40	32.4
Rotation 3	0.007	57.0074	8.5511	0.0377	0.0019	718.89	33.6
Rotation 4	0.010	57.0107	8.5516	0.0382	0.0019	768.80	35.9
Rotation 5	0.014	57.0256	8.5538	0.0404	0.0020	848.75	39.6
Rotation 6	0.019	57.0459	8.5569	0.0434	0.0022	973.69	45.3

Cross-sections, average Q of the thermal bridge is compared to an average Q over the cavity of 8.5134 W

9.4 ENERGY CONSUMPTION EVALUATION

Benchmark

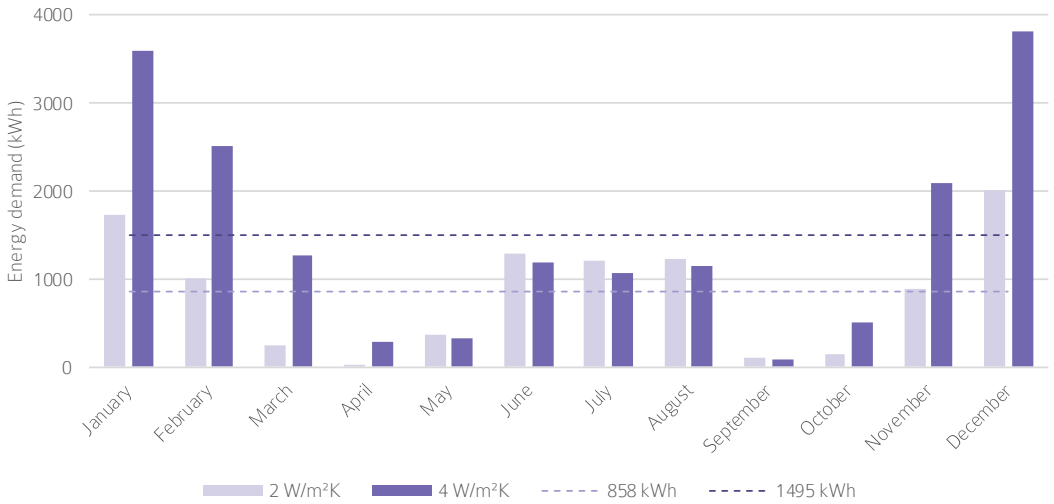

Glazing (%)	R-value (m²K/W)	Heat load (W/m²)	Heat capacity (cm)
50	7.0	30	10

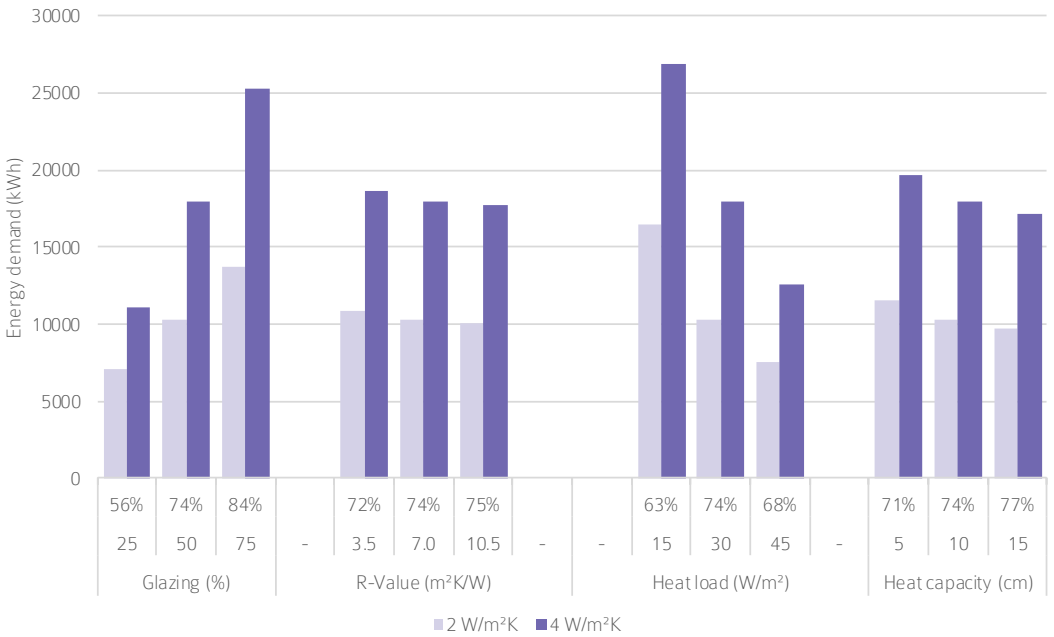

Annual comparison between different configurations

Glazing

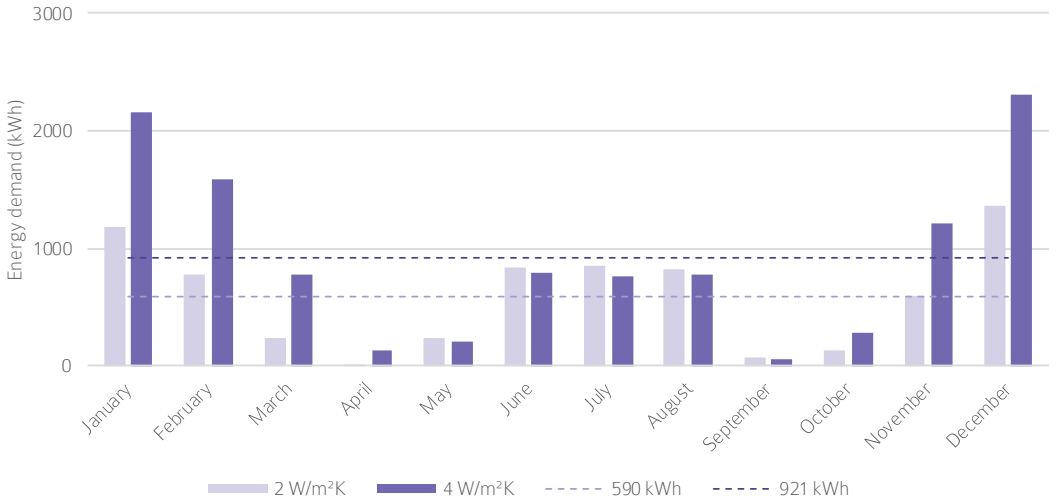

Glazing (%)	R-value (m²K/W)	Heat load (W/m²)	Heat capacity (cm)
25	7.0	30	10

Glazing (%)	R-value (m²K/W)	Heat load (W/m²)	Heat capacity (cm)
75	7.0	30	10

R-value

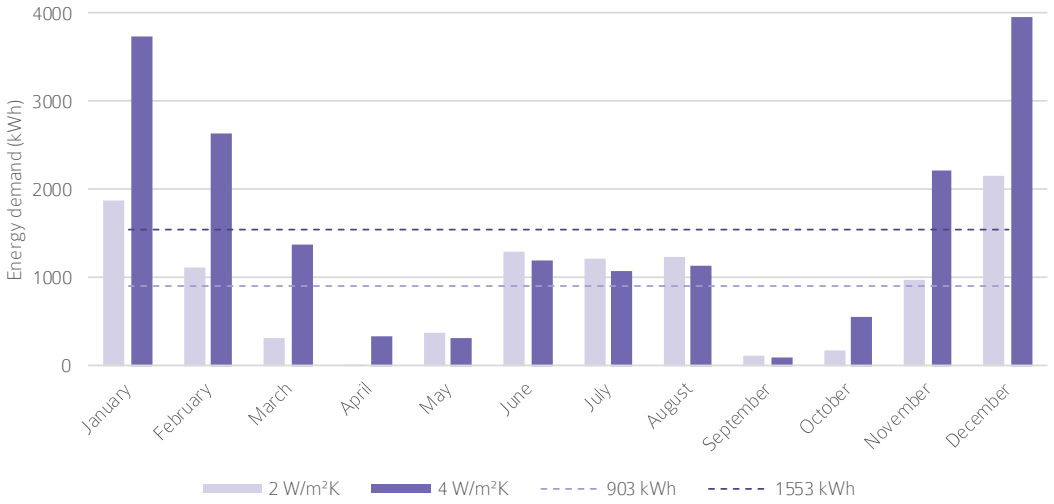

Glazing (%)	R-value (m²K/W)	Heat load (W/m²)	Heat capacity (cm)
50	3.5	30	10

Glazing (%)	R-value (m²K/W)	Heat load (W/m²)	Heat capacity (cm)
50	10.5	30	10

Heat load

Glazing (%)	R-value (m²K/W)	Heat load (W/m²)	Heat capacity (cm)
50	7.0	15	10

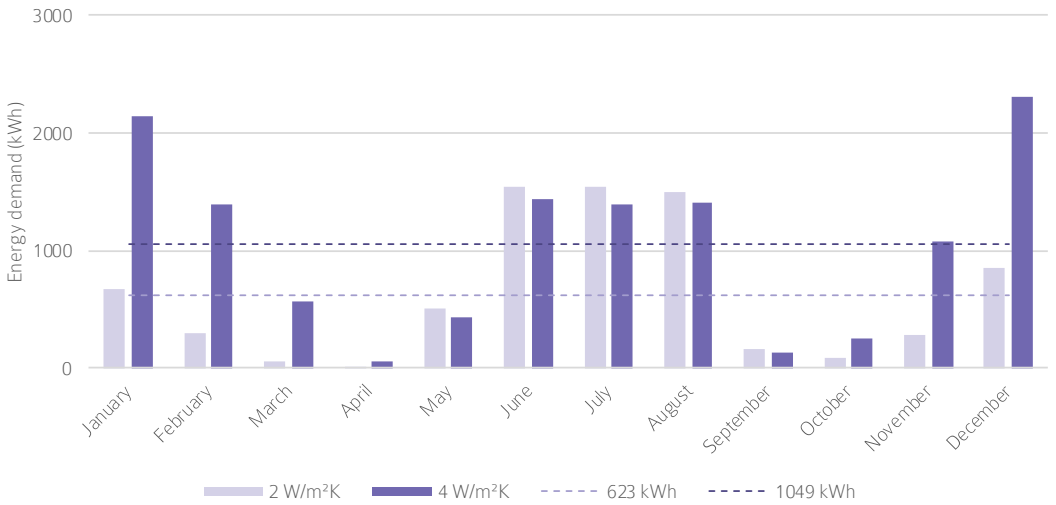

Glazing (%)	R-value (m²K/W)	Heat load (W/m²)	Heat capacity (cm)
50	7.0	45	10

Heat capacity

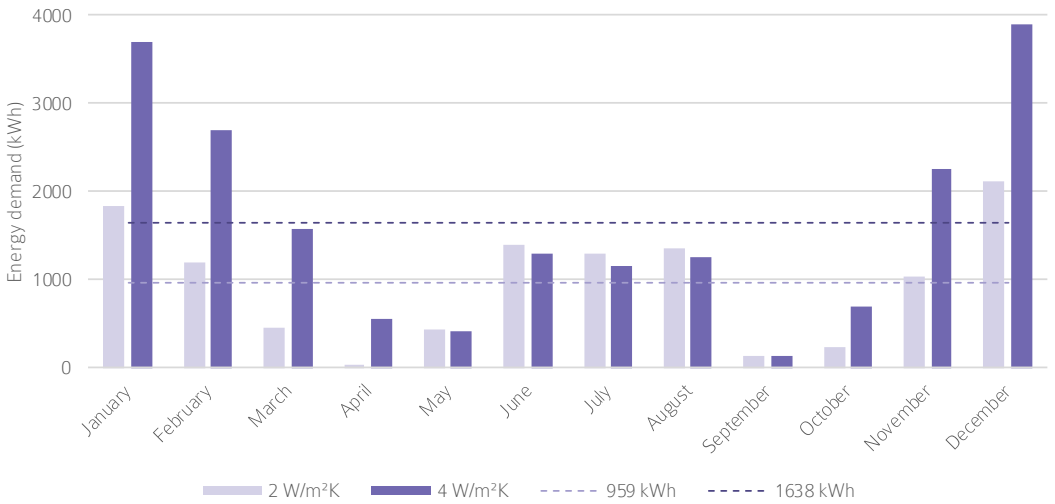

Glazing (%)	R-value (m²K/W)	Heat load (W/m²)	Heat capacity (cm)
50	7.0	30	5

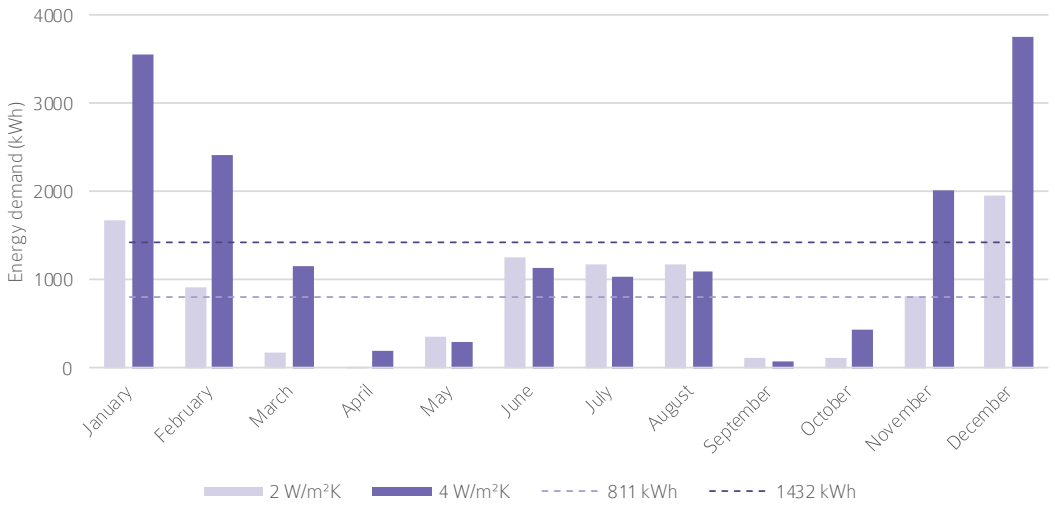

Glazing (%)	R-value (m²K/W)	Heat load (W/m²)	Heat capacity (cm)
50	7.0	30	15